MASTER IN BIOCHEMISTRY AND MOLECULAR AND CELL BIOLOGY RESEARCH FOCUS

Histidine metabolism and metal homeostasis in Brucella abortus

Focant, Charline

Award date:
2021

Awarding institution:
University of Namur

UNIVERSITÉ DE NAMUR

Faculté des Sciences

Histidine metabolism and metal homeostasis in *Brucella abortus*

Mémoire présenté pour l'obtention

du grade académique de master 120 en biochimie et biologie moléculaire et cellulaire

Charline Focant

Janvier 2021

Université de Namur
FACULTE DES SCIENCES
Secrétariat du Département de Biologie
Rue de Bruxelles 61 - 5000 NAMUR
Téléphone: + 32(0)81.72.44.18 - Téléfax: + 32(0)81.72.44.20
E-mail: joelle.jonet@unamur.be - http://www.unamur.be

Histidine metabolism and metal homeostasis in *Brucella abortus*

FOCANT Charline

Résumé

Le cuivre est un métal lourd jouant un rôle essentiel de co-facteur pour certaines protéines impliquées dans des processus biochimiques. Cependant, il peut devenir toxique pour la bactérie lorsque sa concentration augmente. Pour éviter des dommages, la bactérie doit mettre en place des mécanismes pour contrôler la concentration du cuivre et permettre l'homéostasie du métal. A l'heure actuelle, les mécanismes utilisés par *Brucella abortus* pour maintenir l'homéostasie du cuivre ne sont pas connus. Dans notre laboratoire, différents mutants de délétion pour certains gènes de la voie de synthèse de l'histidine ont montré une plus faible réplication dans deux modèles d'infection : les cellules HeLa et les macrophages RAW 264.7. L'histidine est un acide aminé qui possède la capacité de coordonner différents ions métalliques. Dans le présent travail, nous avons investigué l'impact de la délétion des gènes de synthèse de l'histidine sur l'homéostasie du cuivre chez *B. abortus.* Tout d'abord, une analyse bioinformatique a été réalisée afin d'identifier les protéines enrichies en histidine chez la bactérie, et cette analyse a confirmé le lien entre cet acide aminé et les métaux. Ensuite, nous avons montré que les mutants *his* présentaient une croissance plus faible lorsque le cuivre était présent dans le milieu, illustrant une sensibilité au cuivre. De plus, nous avons réussi à isoler des suppresseurs possédant diverses mutations dans l'opéron *opp*, suggérant que celui-ci serait une porte de secours pour la bactérie afin de tolérer le cuivre. Nous avons également constaté que *B. abortus* ne présente pas cette sensibilité lorsque des acteurs classiquement décrits comme étant impliqués dans la résistance au cuivre sont délétés. En conclusion, nos résultats suggèrent que *B. abortus* utiliserait l'histidine comme première ligne pour faire face à la toxicité du cuivre et non les systèmes habituellement décrits.

Mémoire de master 120 en biochimie et biologie moléculaire et cellulaire

Janvier 2021

Promoteur: Xavier De Bolle

Université de Namur
FACULTE DES SCIENCES
Secrétariat du Département de Biologie
Rue de Bruxelles 61 - 5000 NAMUR
Téléphone: + 32(0)81.72.44.18 - Téléfax: + 32(0)81.72.44.20
E-mail: joelle.jonet@unamur.be - http://www.unamur.be

Histidine metabolism and metal homeostasis in *Brucella abortus*

FOCANT Charline

Summary

Copper is a heavy metal that plays an essential role as a co-factor for several proteins involved in biochemical processes. However, it can become toxic to bacteria when its concentration increases. To avoid damage, the bacteria have to put in place mechanisms to control the concentration of copper and to allow the homeostasis of the metal. Currently, the mechanisms used by *Brucella abortus* to maintain copper homeostasis are unknown. In our laboratory, different mutants deleted for several genes of the histidine biosynthesis pathway showed lower replication in two infection models: HeLa cells and RAW 264.7 macrophages. Histidine is an amino acid that has the ability to coordinate different metal ions. In the present work, we investigated the impact of the deletion of histidine synthesis genes on Cu homeostasis in *B. abortus*. First of all, a bioinformatics analysis was carried out to identify histidine-enriched proteins in the bacterium, and confirmed the link between this amino acid and metals. Secondly, we demonstrated that *his* mutants showed lower growth when Cu was present in the medium, illustrating a sensitivity to copper. In addition, we were able to isolate suppressors with various mutations in the *opp* operon, suggesting that this could be a way for the bacteria to escape the toxicity of Cu. It was also found that *B. abortus* does not show this sensitivity when actors classically described as involved in copper resistance are deleted. In conclusion, our results suggest that *B. abortus* would use histidine as the first line of defence against Cu toxicity rather than the systems usually described.

Mémoire de master 120 en biochimie et biologie moléculaire et cellulaire

Janvier 2021

Promoteur: Xavier De Bolle

ACKNOLEDGMENTS

Tout d'abord j'aimerais remercier mon promoteur Xavier De Bolle. Merci pour votre soutien et votre enthousiasme tout au long de ce mémoire. Merci aussi pour votre bonne humeur et le partage de vos connaissances. Un remerciement particulier à Agnès. Merci pour ton encadrement et pour toutes les discussions que nous avons pu avoir. Je ne saurais comment te remercier pour la confiance que tu as eue en moi et je te souhaite beaucoup de réussite dans la suite de ta thèse. Merci à vous deux de m'avoir donné l'opportunité de travailler sur un tel projet, pour tout ce que vous avez pu m'apporté en connaissances et de m'avoir donné ce goût à la recherche.

Je tiens aussi à remercier la Xa team pour l'accueil et sa bonne humeur. Merci à Pierre, Caro, Aurore, Eme, Angy et Elodie pour votre aide, vos conseils et pour votre gentillesse. Merci à Caro pour ton aide lors de mes débuts en RTqPCR, ainsi qu'à Pierre pour tes conseils. Merci également à Angy pour ton aide et pour les casse-têtes qu'on a eus autour de ces fameuses PCR ratées.

Un grand merci également à tous les membres de l'URBM pour l'accueil, la bonne ambiance, votre gentillesse et pour le partage de connaissance que ça soit autour d'une bière ou non. Un merci particulier à Elie pour son temps et son aide dans l'analyse des SNP.

Un remerciement spécial à Marty Roop et Clayton Caswell, pour leur enthousiasme et leur feed-back sur mon travail. Je suis reconnaissante d'avoir pu faire leur connaissance et je les remercie d'avoir partagé de leur expérience sur un sujet qu'ils connaissent par cœur.

Evidemment je ne peux ne pas remercier Hala, Madeline, Audrey, Max et Elisabeth pour avoir passé ces onze derniers mois, un peu particulier, tous ensemble. Merci Elisabeth pour toutes nos pauses café/croissants le matin, les pauses bonbons et surtout, pour tous ces diners frites de chez Gabi. Cela va me manquer de ne plus t'entendre nous demander « Vous n'avez pas envie de frites ? ». Merci à tous pour les bons moments passés ensembles, les soirées d'été au rosé, pour le soutien reçus face à mes PCR foirées, pour le soutien lors du confinement et pour le partage d'une quarantaine. A tous nos fous rires, les mentals break down et les pauses ragots qu'on a pu avoir dans ce bureau mémos. Merci également à mes cokoteurs, avec qui j'ai pu passer six belles années remplies de fous rire, de soirées et de longues conversations. Mention spécial à Margot et Ariane, qui ont toujours été à mes côtés et à m'encourager depuis plus de douze ans maintenant.

Damien, je ne saurais comment te remercier, de me supporter depuis ces huit années. Merci d'avoir toujours cru en moi, de m'avoir toujours poussée vers le haut et d'être fier de moi. Merci pour ta patience et ton courage face à toutes les sautes d'humeur subies en période de blocus.

Enfin, merci aux membres de mon jury, Madame Pasty Renard et Messieurs Michel Jadot, Jean-Yves Matroule et Alex Quintero pour votre temps et votre attention consacrés à la lecture de ce travail.

“The value of a man should be seen in what he gives and not in what he is able to receive.”

Albert Einstein

TABLE OF CONTENTS

ABBREVIATIONS

ABC transporter	ATP-binding cassette transporter
AICAR	Amino-imidazole carboxamide riboside 5'-phosphate
αKG	α-keto-glutarate
ATP	Adenosine triphosphate
BBM-II	*N'*-[(5'-phosphoribosyl)-formimino]-5 aminoimiazole-4 carboxamide ribonucleotide
BBM-III	*N'*-[(5'-phosphoribulosyl)-formimino]-5 aminoimiazole-4 carboxamide-ribonucleotide
BCV	*Brucella*-containing vacuole
BmcO	*Brucella* multi-copper oxidase
CAS	Chrome azurol S
CM	Cytoplasmic membrane
Co	Cobalt
Ctr1	Cu^{+} transport protein 1
Cu	Copper
DC	Dendritic cell
EE	Early endosome
ER	Endoplasmic reticulum
Fe	Iron
Gln	Glutamine
Glu	Glutamate
GSH	Glutathione
HAL	$_{L}$-histidinal
HALY-1	Histidine ammonia lyase
His	Histidine
HOL	$_{L}$-histidinol
HOL-P	$_{L}$-histidinol-phosphate
Hut	Histidine utilisation
ICP-OES	Inductively coupled plasma-optical emission spectrometry
IGP	Imidazole glycerol-phosphate
IMAC	Immobilized metal ion affinity chromatography
LAP	Imidazole acetol-phosphate
LE	Late endosome
LPS	Lipopolysaccharide
Lys	Lysosome
Mg	Magnesium
Mn	Manganese
NAD	Nicotinamide adenine dinucleotide
Ni	Nickel
NRAMP1	Natural resistance-associated membrane protein
OM	Outer membrane
OPT	Oligopeptide transporter
PPi	Pyrophosphate
PRAMP	*N'*-5'-phosphoribosyl-AMP
PR-ATP	Phosphorybosyl-ATP
PRPP	Phosphoribosylpyrophosphate
PT	Oligopeptide transporter
PTR	Peptide transporter

ROS	Reactive oxygen species
RP	Ribosyl phosphate,
RPPP	Ribosyl triphosphate,
SBP	Substrate-binding protein
SNP	Single-nucleotide polymorphism
YSL	Yellow Stripe-like
WT	Wild-type
Zn	Zn

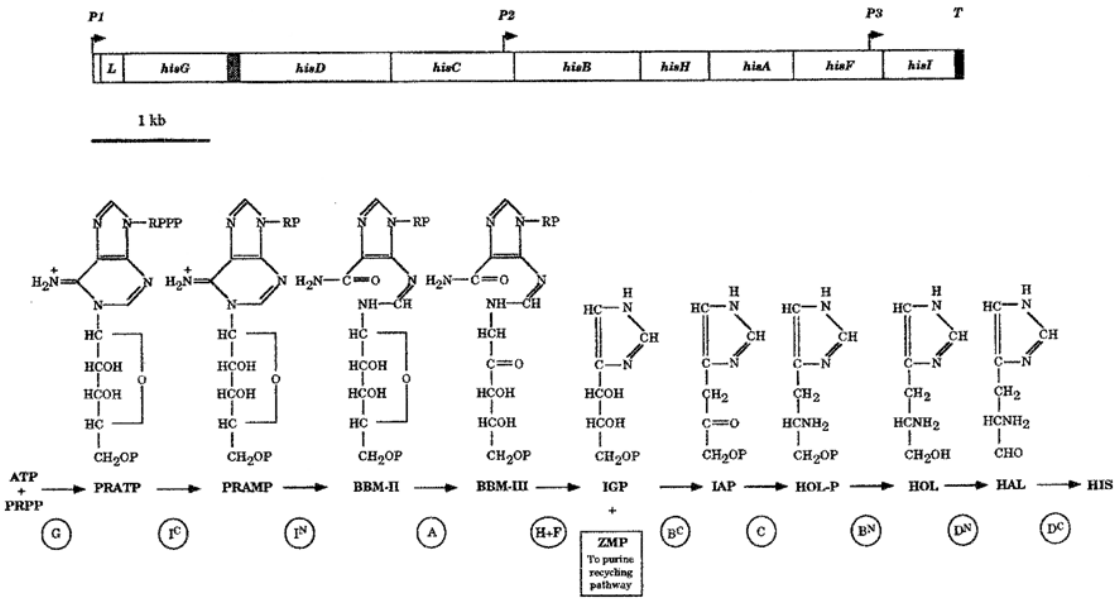

Figure 1**. Genes organisation in the *his* operon and biosynthetic pathway of histidine of *S.* Typhimurium.** Top: Structural genes are represented to scale. The relative position of primary promoter (*P1*) and internal promoters (*P2* and *P3*) are indicated by arrows. *T* represents the transcriptional terminator and *L* the leader region. Bottom: Schematic representation of biosynthetic pathway of L-histidine. In order: ATP; adenosine triphosphate, PRPP; phosphoribosylpyrophosphate, RPPP; ribosyl triphosphate, PRATP; *N'*-5'-phosphoribosyl-ATP, RP; ribosyl phosphate, PRAMP; *N'*-5'-phosphoribosyl-AMP, BBM-II (5'-ProFAR); *N'*-[(5'-phosphoribosyl)-formimino]-5 aminoimiazole-4 carboxamide ribonucleotide, BBM-III (5'-PRFAR); *N'*-[(5'-phosphoribulosyl)-formimino]-5 aminoimiazole-4 carboxamide-ribonucleotide, IGP; imidazole glycerol-phosphate, ZMP (AICAR); 5'-phosphoribosyl-4-carboxamide-5-aminoimiazole, LAP; imidazole acetol-phosphate, HOL-P; L-histidinol-phosphate, HOL; L-histidinol, HAL; L-histidinal, HIS; L-histidine. Below the arrows, enzymes are indicated in the circles. N and C are referencing to amino or carboxyl terminal respectively representing domain performing the reaction when enzyme is bifunctional (adapted from [1]).

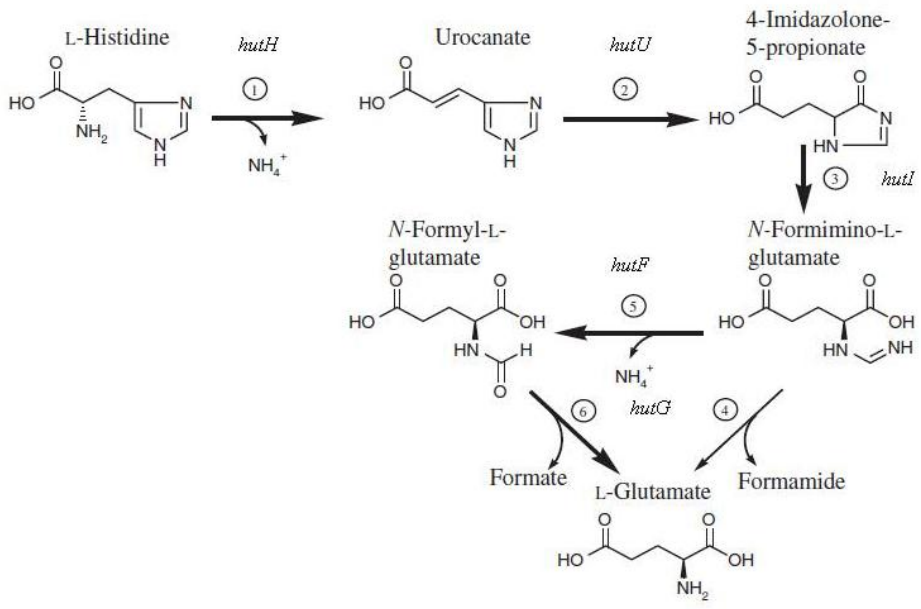

Figure 2**. Catabolic pathway of histidine. Each reaction is catalized by an enzyme:** (1) HutH is a histidine ammonia-lyase, called histidinase; (2) HutU is urocanase, an urocanate hydratase; (3) HutI is an imidazolone propionase; (4) the fourth step is catalyzed by hutG, a formimidoylglutamase; (5) HutF is a *N*-formiminoglutamate deiminase and (6) the sixth step is also catalyzed by HutG, a *N*-formyl-L-glutamate amidohydrolase (adapted from [2]).

INTRODUCTION

1 Histidine, an interesting amino acid

1.1 Biosynthesis and regulation

Histidine is an amino acid formed at the end of a ten steps enzymatic reaction. In *Escherichia coli* and *Salmonella enterica* serovar Typhimurium, each step is catalysed by an enzyme and all the 8 genes are organised in one operon on the single chromosome (Figure 1) [3,4]. Histidine operon is formed by an operator region followed by genes coding the biosynthetic enzymes of the pathway [3]. Gene homology indicates the conservation of this metabolic pathway among many species [1]. The histidine biosynthesis pathway intersects with purine biosynthesis pathway via AICAR, amino-imidazole carboxamide riboside 5'-phosphate (Figure 1), a by-product of histidine synthesis which is also a precursor for the purine biosynthesis pathway [5]. Bacteria such as *E. coli* and *S.* Typhimurium are using two different ways to regulate histidine biosynthesis. The first is feedback inhibition where histidine itself is acting as an allosteric inhibitor of the activity of the first enzyme in the pathway, the phosphorybosyl-ATP (PR-ATP) syntethase, which is sensitive to histidine. This inhibition is leading to a conformational change of the enzyme and an adjustment of the biosynthetic activity to histidine concentration [3,6]. The biosynthesis pathway is allosterically repressed when histidine rates are sufficient and derepressed when cell needs this amino acid [3]. The second way to regulate histidine biosynthesis is transcriptional repression which allows the control of the intracellular concentration of the enzymes themselves [3]. Several regulatory genes were identified, *hisR, hisT, hisU, hisS* and *hisW.* The maturation process of histidine tRNA involve *hisT*, *hisU,* and *hisW*. *HisR* is the structural gene for histidyl-tRNA and its amount dec reasing when mutations occurs in *hisR* gene and *hisS* is linked to the histidyl-tRNA synthetase, which is defective when *hisS* is mutated [3]. Other regulatory mechanisms exist at different levels to control the pathway [1,7]. The metabolic cost of histidine biosynthesis is expensive for the cell, costing 41 ATP equivalents for each molecule produced. The regulation of the biosynthesis pathway is complex and histidine formation needs to be in coordination with the cell's needs [3].

1.2 Catabolism and regulation

Histidine degradation, a very common pathway, is leading to the formation of ammonia, glutamate and one-carbon compound [2,8]. It is not a simple reversion of the biosynthetic pathway [8]. The histidine utilization (hut) system is responsible for histidine catabolism, comprising five enzymatic steps where the three first seem to be universal among bacteria (Figure 2) [2,8]. Depending on the organism, the *hut* genes are organised differently. They are clustered and form 1 to 4 operons [8]. Despite the high frequency of the pathway among bacteria, it is imperative to note that the *hut* genes are lacking in *E. coli.* In eukaryotes, the presence of hut pathway is spotty. However, it is present is the entire vertebrate branch [8].The first enzyme of hut system is histidinase which catalyses the reaction leading to urocanate, the first intermediate in the pathway, by the release of the amino group [9]. Histidinases in bacteria and mammalian are identical with more than 40% amino acid identity, making this enzyme highly conserved [10]. Histidine and urocanate are two physiological inducer of the hut system in bacteria leading to the *hut* genes expression [8,11–13]. In opposite to the induction, *hutC* is coding for HutC which has a role of repressor of de Hut system [14]. As histidine is an "expensive" amino acid to synthesize, the degradation needs to be highly regulated [3,8]. This regulation differs between bacteria, however certain characteristics are common. The Hut

enzymes are not synthesized at maximal rates unless the cells are in essential need which can only be compensated by the degradation of histidine. Cells are degrading histidine to use it as carbon source or protein synthesis [8]. Moreover, *hut* genes are not expressed unless the concentration of exogenous histidine exceeds the concentration of synthesized histidine [8]. Finally, histidine level has to be enough for protein synthesis process [8].

1.3 Transport

Structural and genetic studies did not uncover a histidine or urocanate transporter [8]. However, bacteria have a diversity of permeases involved in histidine transport and these differ in regulation, capacity and affinity [15]. Nevertheless, at least one transporter for uroconate or histidine appears to be present in most clusters of *hut* genes [8]. In *Pseudomonas fluorescens*, the hut system contains a gene annotated as *hutT*. This gene, coding for a hypothetical histidine transporter, appeared to be essential for *P. fluorescens* growth when histidine is the only carbon source [16]. In the Gram-positive bacterium *Bacillus subtilis*, the *hutM* gene is located at the end of the *hut* operon and it is similar to *hutT* present in *P. fluorescens*. It is hypothesized that HutT could be a histidine transporter [8].

1.4 Coordination with metal ions

Through its imidazole ring, histidine is capable of binding transition metal ions (elements whose last electronic layer is incomplete allowing them to have multiple valencies; they are located in groups 3 to 12 of the periodic table [17]) within a variety of biologically important molecules such as metalloproteins or iron-heme systems [18]. The histidine molecule contains three possible coordination sites in aqueous solution; the carboxyl group (pKa = 1.9), the imidazole nitrogen (pKa = 6.1) and the amino nitrogen (pKa = 9.1) [18,19]. Based on immobilized metal ion affinity chromatography (IMAC) principle, a study investigated contribution of histidine residues in proteins to coordinate metal ions. With a set of model proteins comprising cytochrome c or ubiquitin for example, the presence of electron donors such as histidyl residues within proteins allows the coordination of transition metal ions copper (Cu), nickel (Ni), cobalt (Co) or zinc (Zn). Whether in peptides or proteins, histidyl residues have an important function in the binding of metal ions process [18]. The affinity is the most important when the number of histidine residues is high. Nevertheless, this coordination depends in part on the steric accessibility of these residues [20]. Results of titration experiments indicate that Cu is usually bound by one or two histidine molecules through the imidazole nitrogen and the carboxyl oxygen [19]. Dietl and her team conducted a study on the crucial role of histidine biosynthesis in metal homeostasis in *Aspergillus fumigates*, a fungal pathogen [21]. Indeed, an increase in histidine content during Fe starvation was highlighted in *A. fumigates*, illustrating the potential role of histidine in metal homeostasis in this pathogen. A decreased in metal resistance to Cu, Zn, Ni, Co, iron (Fe) and manganese (Mn) was observed when *hisB* gene is deleted. The metal resistance was enhanced when higher concentration of histidine was added to the medium. To further understand the role of histidine in Fe homeostasis, the siderophore production in the WT was investigated when histidine is supplemented to the medium. The results illustrated a decrease in siderophore production when histidine is supplemented due to its metal-chelating capacity [21].

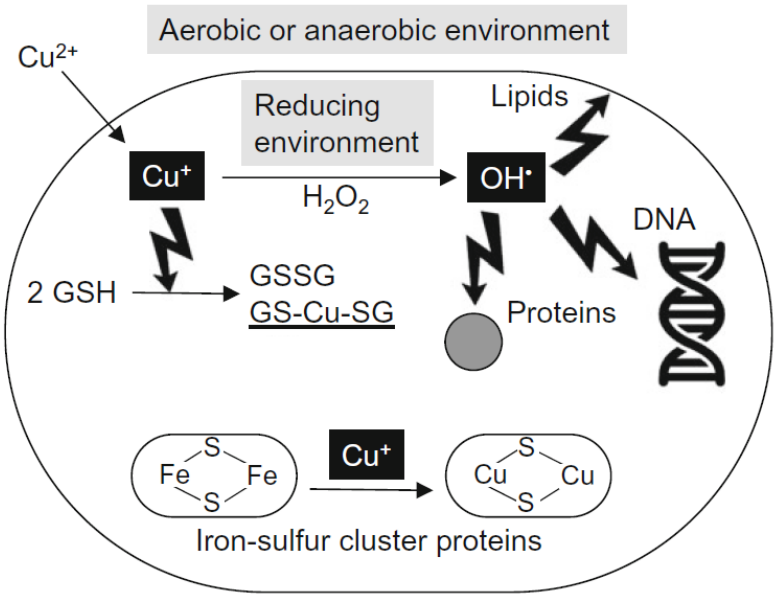

Figure 3. **Mechanisms of Cu toxicity.** Mechanisms by which Cu enters in the cell are uncharacterized. Inside cytoplasm, the reducing conditions are converting Cu^{2+} (oxidized form) into Cu^{+} (reduced form). Then Fenton reactions can occur and lead to reactive oxygen species (ROS) production. These can then affect DNA, proteins and lipids. Within glutathione (GSH) pool, thiol depletion can be induced by Cu^{+}. Cu can also displace Fe from iron-sulfur cluster proteins (adapted from [22]).

2 Copper

Cu is an essential structural and catalytic cofactor for important biochemical processes. Actually, over 30 types of proteins are holding Cu [23]. The arrival of dioxygen in the atmosphere allowed the selection of respiratory enzymes which used Cu as cofactor [22,24,25]. Most of the bacteria are using Cu as redox catayst and an electron carrier [24–26]. To keep a non-toxic cytoplasmic Cu level, at least one Cu export ATPase gene is found in all microorganisms [22]. Irwing-Williams series represent the general order of preference for donor ligands: $Mn^{2+} < Fe^{2+} < Co^{2+} < Ni^{2+} < Cu^{2+} > Zn^{2+}$ [22,27]. However it does not take into account the difference of properties between Cu^{2+} and Cu^{+} [22]. Cu^{+} is classified as a soft acid and prefers to bind to cysteines, imidazole nitrogens or methionines [22]. A key of Cu toxicity is the ability of Cu to compete with other metal ions for the same binding site [22,26,27]. Cu possesses two oxidation states; Cu^{+} and Cu^{2+}. Cu^{+} is the intracellular cytoplasmic form of Cu ion [22,26]. The concentration of free cytoplasmic Cu was estimated to be around one zeptomolar [22].

Cu toxicity is generally ascribed to its redox properties. However, it is possible that the most toxic action of Cu is the substitution of Fe cofactor in iron-sulfur clusters proteins leading to their destruction [22,27]. Indeed, in *E. coli*, Fe^{2+} replacement in iron-sulfur clusters by Cu was identified as the primary cause of Cu toxicity [28]. This mismetallation is due the Pearson concept where Cu^{+} has a higher affinity for the ligand than Fe^{2+} [22]. Moreover, Cu can generate reactive oxygen species (ROS) by the Fenton reaction [22]. Cell damages induced by this heavy metal are due to ROS production, oxidative damages of DNA, proteins and lipids and thiol depletion (Figure 3) [22]. Glutathione (GSH) is acting against heavy metal toxicity and can also be depleted by Cu [22]. Cu^{+} is more toxic than Cu^{2+} due its higher permeability trough cytoplasmic membrane and higher thiophilicity [22].

2.1 Cu biochemistry in bacteria

Cu penetrates bacterial cell through passive diffusion according to its chemical gradient. Even though membranes are rather impermeable to Cu, most of bacterial cytoplasms are poor in Cu [26]. The periplasm is the place where Cu homeostasis is taking place in gram-negative bacteria [29]. In Enterobacteria, all the enzymes that necessitate Cu (terminal respiratory oxidases, superoxide dismutases, amine oxidases and multi-Cu oxidases) are localized in periplasm [26]. Bacteria limit the levels of available Cu by different strategies: excreting Cu in excess, regulating Cu import, oxidizing Cu^{+} to Cu^{2+} and boosting the cell's buffering capacity through Cu sequestration by high-affinity ligands [24,26]. Once inside the periplasm, Cu availability can be reduced by active export, sequestration by high-affinity ligands and oxidation to Cu^{2+} [26]. Cu^{2+} is biologically inert and no protein bind it exclusively [26,30]. Then, bioavailable Cu is lower than the total Cu amount. As explained above, Cu can be toxic for cells by entering in the cytoplasmic compartment, displace cofactors in metalloenzyme and conducting to oxidative damage. Free Cu in the periplasm can be inserted in cuproproteins by three different ways: ; it is directly captured by an apo-protein; it enters in the cytoplasmic space and is then exported by a P-type ATPase to be bound by a cuprochaperone; or it is bound by a cuprochaperone and delivered by protein-protein interaction to a target enzyme [26].

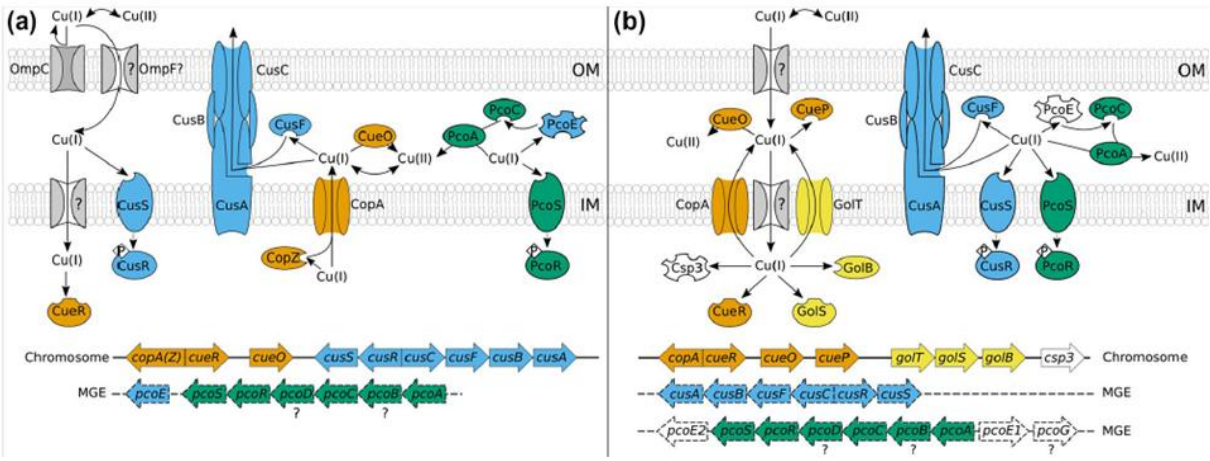

Figure 4. **Copper homeostasis in *E. coli* and *S. enterica*.** (a) In *E. coli*, three systems, Cue (orange), Cus (blue) and Pco (green), control Cu^{+} levels in the cytoplasm and periplasm. These systems are containing sensory elements: CueR, CusSR and PcoSR respectively. Cu is actively secreted from cytoplasm and periplasm by two efflux pumps, CopA and CusCBA respectively. In addition, high-affinity cuprochaperone bind Cu in the cytoplasm; CopZ and in the periplasm; CusF. In the periplasm, Cu detoxification is carried out by a multi-copper oxidase, CueO. The Pco system includes one multicopper oxidase, PcoA and periplasmic chelators, PcoC and PcoE. (b) In *S. enterica*, the homologous *gol* regulon (yellow) is a duplicate of the *cue* regulon and contains the efflux pump Gol, a chaperone GolB in the cytoplasm and the transcriptional regulator GolS. The *cus* system is not present on the chromosome but can be supplied by mobile genetic elements (MGE) (adapted from [26]).

2.2 Cu homeostasis

In the cytoplasm, less than one atom of Cu per cell is available in *E. coli* and *S. enteric* [26]. Among species living in Cu-rich environments, Cu homeostasis is quite dynamic at the evolutionary level, due to horizontal gene transfer that can occur [26]. Metal ions are indispensable for metabolism and for life in general [31]. However metals cannot be synthesized or degraded [32]. Therefore, metal homeostasis is based on transport into and out of the cell [32]. The expression of specific sets of genes will be activated by the bacteria when they face metal ions limitation or excess. Bacterial adaptation to excess or limitation is complex [32]. Metal homeostasis in bacteria is based on three main concepts, (1) the labile metal pool, (2) the metal quota and (3) the thermodynamically 'free' concentration of metals in the bacterial cell at equilibrium [32].

Among bacteria, the core *cue* (Cu efflux) regulon function is conserved (Figure 4) [30,33]. This efflux system is regulated by CueR (Cu efflux regulator) which is a transcriptional regulator belonging to the MerR-family and allowing the control of cytosolic Cu concentration [34]. CueR upregulates two genes from the regulon, *copA* and *cueO* [17,33,34]. CopA is a P-type ATPase inducible by Cu and represents the main component in Cu efflux in *E. coli* [17,33,34]. CueO (Cu efflux oxidase) is the periplasmic multi-copper oxidase which oxidizes Cu^{+} to Cu^{2+} using O_2 as an electron acceptor [17,33,34]. The oxidase activity is inducible by Cu through the binding [24,33]. Since this activity requires oxygen, it is possible that Cu homeostasis is perturbed when oxygen is lacking. In *E. coli* WT strains, Cu sensitivity is not affected by *cueO* deletion, even if it is leading to a potential increase in Cu^{+}, but Cu sensitivity is impacted by *copA* deletion. Under stress induced by Cu, *copA* and *cueO* are up-regulated indicating that these two proteins are forming the primary system used in *E. coli* to face Cu. However when Cu concentration is high, CopA and CueO are overwhelmed and Cu^{+} level is increasing in the periplasm [33]. The *cue* regulon also includes the CopZ cuprochaperone which is co-expressed with CopA [17,26]. In most of *S. enterica* serotype, *cue* regulon is present but a duplicated homologous regulon was identified, the *gol* regulon (Figure 4) [35]. In these strains, GolS is a CueR homogue that regulates GolT, an additional CopA and GolB, a putative CopZ-like cuprochaperone found in the cytoplasm, at the transcriptional level [26].

In addition to the *cue* regulon, some other adaptations specific to the bacterial niche can be observed in different species [26]. Indeed, to avoid being killed by macrophages, *S. enterica* presents additional weapons to fight Cu [36]. In its periplasm, a supplementary cuprochaperone was identified, CueP. Homologous sequences were also found in other bacterial pathogens for example *Yersinia sp.* suggesting that it is an adaptation to a pathogenic lifestyle [17,35].

To better adapt to its biofilm- and surface-associated lifestyle, *E. coli* possesses a second Cu efflux system; the *cus* system (Cu-sensing) (Figure 4). This Cu-sensing system is controlled by *cusR* and *cusS*, a two-component signal transduction [26,33]. CusRS is activating the expression of the *cusCFBA* operon when Cu levels are elevated [33]. In opposite to *cue* system, *cus* system could play an essential role for Cu efflux under anaerobic conditions. A high level of Cu is required for *cus* transcription [33]. The *cusCBA* genes are under CusRS control and form a proton-cation antiporter [17,26,34]. Within this system, a periplasmic cuprochaperone is encoded by *cusF* [26].

The genomic island *pco* is spread among *E. coli* and *S. enterica* strains (Figure 4). As in the two previous systems, the *pco* locus presents a Cu-sensing system named PcoSR, a periplasmic chaperone PcoC and a multi-copper oxidase PcoA [26].

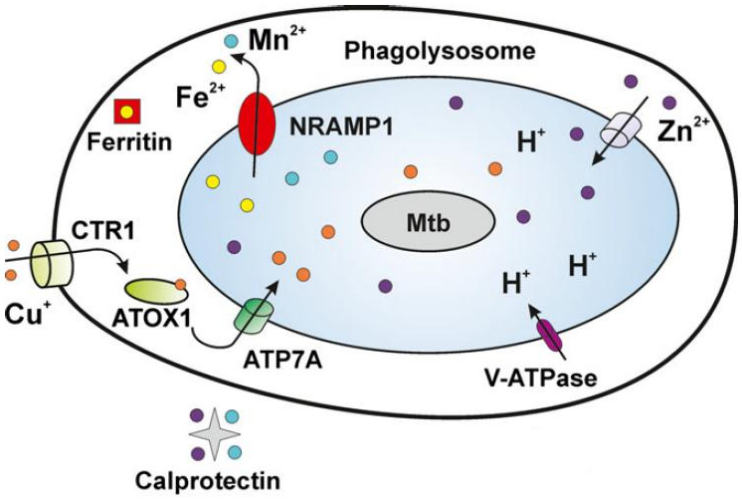

Figure 5. **Nutritional immunity process during *Mycobacterium tuberculosis* infection.** Extracellular Cu^{+} is transported into the cytoplasm of infected macrophages by CTR1. Then, the chaperon ATOX1 is binding Cu^{+} and delivers it to the ATP7A pump, leading to Cu^{+} accumulation inside the phagosome. Fe^{2+} and Mn^{2+} are pumped out of the phagosome *via* NRAMP1. Zn^{2+} is uptaken into the phagosome by an unknown transporter. Neutrophils are secreting calprotectin at infectious sites to sequester Zn^{2+} and Mn^{2+} (adapted from [37]).

2.3 Nutritional immunity

Transition metal ions are important to ensure a range of cellular processes and to ensure a proper vertebrate immune function. These elements are required for a variety of processes such as bacterial metabolism or virulence factor function [32,38]. Several strategies are established in host cells in the arms race of host-pathogen co-evolution [39]. Nutrient immunity is a concept, part of host immune response, used by vertebrates and invertebrates during which transition metals are sequestered in order to prevent pathogens from acquiring these essential elements for their virulence [17,32,38]. Fe sequestration by host cells is the most well studied example of nutritional immunity. During infection, the host also sequester Zn and Mn trough the calprotectin release by neutrophils at infection sites to prevent microbial replication [32,38]. Zn was identified as an important co-factor for bacterial proteins [40]. In addition to metal sequestration, metal intoxication is also used as an antibacterial strategy to strengthen microbial invaders inhibition [32,41]. Different studies have illustrated that immune cells are using metals to poison microbes [39].

To face metal limitation, different responses are adopted by bacteria. First, high-affinity uptake systems are derepressed to enhance metal import. A second response is to substitute a protein or an enzyme that is dependent on the limited metal with one that can function without this metal. And thirdly, the bacterial proteome is remodelled: non-essential enzymes are repressed and the synthesis of enzymes essential for survival and growth is promoted, and limiting metal ions are mobilised from the cell reservoirs [32].

As described above, Cu has important roles in metalloproteins and metalloenzymes and due to Cu toxicity, Cu homeostasis is high regulated [22,26]. X-ray microprobe analysis showed that Cu^{+} and Zn^{2+} concentrations were increasing within phagosomes enclosing mycobacteria [42]. Consistent with this, a Zn augmentation was highlighted in phagosome containing avirulent and virulent bacteria [43]. Therefore, host cells are using Zn starvation and Zn intoxication [17,32]. However the balance between these two mechanisms is not determinate and is probably depending on different criteria such as pathogen intracellular trafficking, cell type or infectious cycle [17]. Cu is used as antimicrobial agent for a very long time. However, its role in innate defence was only investigated recently [17,44]. Hosts cells are expressing two different pumping systems: the first one pumps in Cu^{+} and Zn^{2+} to reach toxic levels and the second one, NRAMP1 (natural resistance-associated membrane protein), pumps out important metals for persistent pathogens growth [39]. It is within phagolysosomes in mammalian hosts that bacteria encounter Cu^{+} [17,23,44]. Inside phagocytic cells, Cu^{+} transport protein 1 (Ctr1) is localized in the plasma membrane and has a high affinity for Cu. Besides, the expression of Ctr1 is induced by proinflammatory signals and it actively pumps in Cu^{+} from extracellular environment [17,23,44]. It results in an increase in Cu uptake [39]. These proinflammatory signals also induce ATP7A localization into phagolysosome membrane [39,44]. Then, the metal ion is transported by ATP7A *via* ATOX1, a copper chaperone, facilitating the metal accumulation within the phagolysosome (Figure 5) [17,23,39,44]. ATP7A is a P-type ATPase transporting Cu into subcellular vesicles [39]. The expression of the ATP7A Cu transporter is required for macrophage-mediated pathogen killing [44]. The Cu influx into phagosomes appears to raise the bactericidal activity. The study of metal poisoning strategies used by mammalian phagocytes as antimicrobial show the importance of metal as Cu and Zn for immunity. Within macrophage, Zn accumulation also occurs, however the transporter is unknown [39].

Table 1. **Different species of *Brucella* and their host specificity [45].**

Species	Host preference
Brucella abortus	Cattle
Brucella melitensis	Goat, sheep and camel
Brucella suis	Swine
Brucella canis	Dog
Brucella ovis	Sheep
Brucella microti	Common vole and foxes
Brucella ceti	Cetaceans
Brucella pinnipedialis	Seals
Brucella neotomae	Desert wood rats
Brucella inopinata	(unknown)
Brucella papionis	Baboons

3 *Brucella abortus*

3.1 An overview of the pathogen

Brucella is the pathogen that is responsible for the brucellosis discovered by Sir David Bruce in 1887 [45–47]. Brucellosis, also known as Malta fever or undulant fever, remains a main health issue in countries where health services are scarce or inexistent causing disease in humans and domesticated animals worldwide [45,46,48]. *Brucella spp.* are Gram-negative bacteria belonging to second subclass of α-proteobacteria [49]. Other bacteria that co-evolved with plant or animal hosts as *Agrobacterium, Rhizobium, Bartonella* and *Rickettsia* are also included in this subclass [45,48–50]. *Brucella* genome is 3.2 Mb long and it is divided in two circular chromosomes [51]. These bacteria are characterized by a coccobacilli shape (0.6-0.8 μm) and they are non-motile and non-sporulating [47,48,52]. Genome analyses have identified 11 species genetically very close, related to the host infected and their pathogenicity (Table 1) [53]. Only three of them are pathogenic for humans: *B. melitensis*, *B. abortus* and *B. suis* [45]. *Brucella abortus* is the disease-causing agent in bovine animals [51]. The *Brucella* genus is highly homogeneous with >95% homology among all species [54]. The other *Brucella* species are less relevant for human health. The mammalian host range is very wide for this pathogen and illustrates the complexity of *Brucella* [45]. It enters by digestive, respiratory or genital mucosa [45,47,52]. The particular tropism of *Brucella* in primary host is the reproductive system leading to abortion and thus bacterial colonization of the placenta and sterility in male [47,48,50]. Humans are accidental hosts and they are infected by ingesting contaminated food or by direct contact with animals [45,46,48]. Brucellosis is a flu-like illness, with periodic fever combined with joint and muscle pain that can lead to complication with arthritis. However mortality is rare [45]. Nevertheless, the incidence of brucellosis in human is unknown and varies from country to country. The diagnosis is complicated because symptoms are not specific. The treatment by antibiotics is long and debilitating [46,55]. There is no vaccine in humans yet [46].

Originally characterized as a facultative intracellular pathogen, it would be more correct to define *Brucella spp.* as intracellular facultatively extracellular parasite since they almost exclusively replicate inside cells in their host [56]. However, these bacteria can easily replicate in classical laboratory medium [48]. *Brucella* pathogens can infect phagocytic and nonphagocytic cells [46]. They are able to multiply successfully inside macrophages and dendritic cells (DC) [45,57]. Phagocytosis is killing about 90% of bacteria, however the 10% remaining proliferate and interfere with macrophage function [45]. Inside cells, *Brucella* is reducing the immune response and remains hidden [45,57]. On the other hand, macrophages and DCs serve as safe haven for the bacteria and protect them from immune response in the host [58]. Non-professional phagocytes such as placental trophoblasts are also host cells where *Brucella* can replicate intracellularly. During pregnancy in animals, bacteria can infect and multiply within the placenta leading to its disruption followed by abortion [59]. The transmission of *Brucella* between animals is mostly due to placenta ejection in the environment [58]. Different cellular models were developed to study *Brucella* infection such as macrophages, HeLa cells or trophoblasts as well as an *in vivo* model with mouse infection [48].

3.1 Trafficking

The mechanism through which bacteria enter inside macrophages and DCs is still uncharacterized [45]. Nevertheless, interactions between lipid rafts present on the macrophage surface and the O-chain of the smooth lipopolysaccharide (LPS) of *Brucella* have been recognized to be required for bacteria entrance and survival by inhibiting early phagosome-lysosome fusion inside host cells [60,61]. In contrast, the lack of O-chain in rough mutants

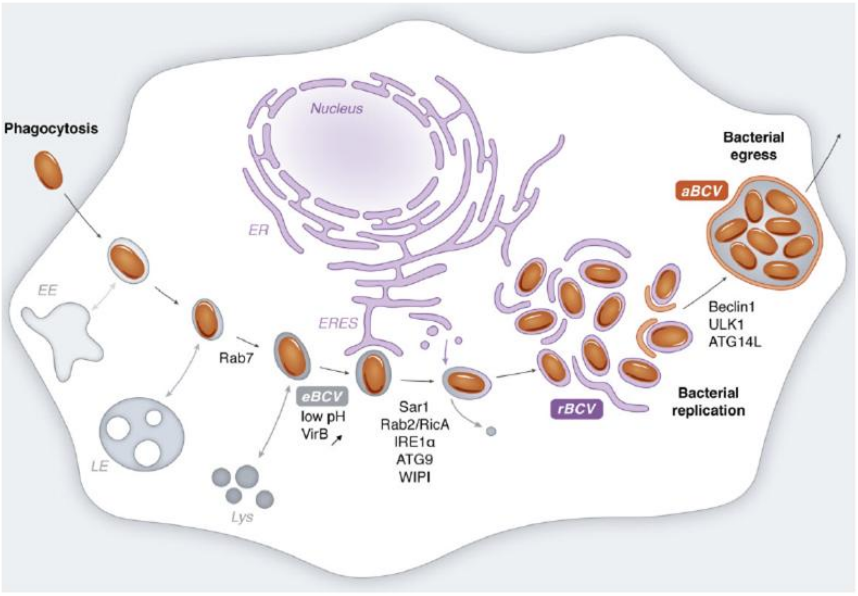

Figure 6. ***Brucella*** **intracellular trafficking in host cells.** Inside phagocytotic cells, *Brucella* lives within the *Brucella*-containing vacuole (BCV). At their endosomal stage (eBCV), BCV undergoes interactions with early endosomes (EE) and late endosomes (LE). Then, eBCV partially fuse with lysosomes (Lys). During the early stages of maturation, eBCV undergoes acidification, and the decrease in pH is inducing the *virB* operon, which encodes the Type IV secretion system. Following acidification step, the BCV is interacting with endoplasmic reticulum (ER), which is leading to ER-derived vacuole formation (rBCV). rBCV is the replicative niche of *Brucella*. After proliferation, BCV acquire non-canonical autophagy marker to become aBCV, which allow their egress from the host cell (adapted from [62]).

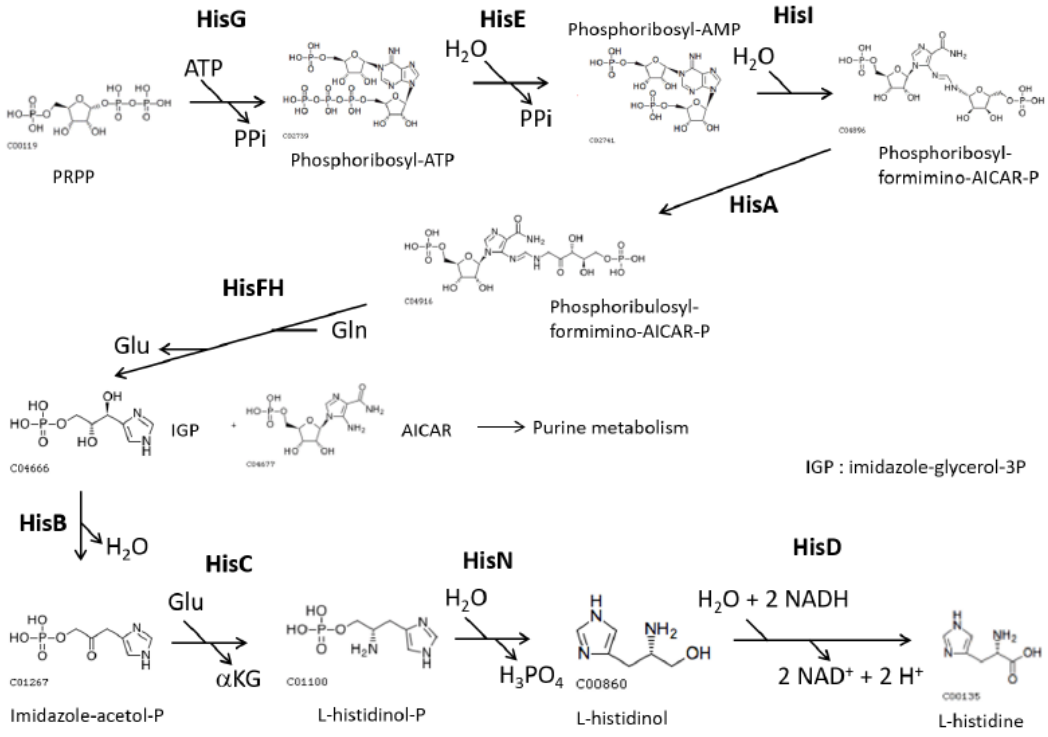

Figure 7. **Schematic representation of biosynthetic pathway of L-histidine.** HisA is an isomerase involved in the fourth step of the pathway. Cyclisation of the imidazole ring is catalysed by the HisFH complex. HisB is an imidazoleglycerol-phosphate dehydratase catalysing the sixth step of the pathway. The seventh step is catalysed by HisC, an aminotransferase. HisD performs the last two steps of the pathway with an aldehyde intermediate. We have mutants in *B. abortus* 544 for *hisA*, *hisB*, *hisC*, *hisD* and *hisFH*. Abbreviations are PRPP; phosphoribosylpyrophosphate, ATP; adenosine triphosphate PPi; pyrophosphate, Gln; glutamine, Glu; glutamate, αKG; α-keto-glutarate, NAD; nicotinamide adenine dinucleotide.

prevent the entry via lipids rafts and lead to degradation by the phagosome-lysosome fusion [60]. Once inside the cell, *B. abortus* is enclosed in a membrane-bound compartment, the *Brucella*-containing vacuole (BCV)(Figure 6) [63,64]. Most of phagocytosed *Brucella* are rapidly killed in cells but some bacteria do survive [45,65]. BCV enters into an endocytosis pathway and transiently undergo interactions with early and late compartments of the endocytic pathway, illustrated by the acquisition of early and late endosomes markers [63]. During the early stages of maturation, BCV undergoes acidification. This pH reduction is important for the induction of the *virB* operon which encodes the Type IV secretion system, a major virulence factor. In addition, BCV acidification is necessary for bacterial replication and survival [63]. Following BCV acidification and *Brucella virB* expression, the BCV is interacting with endoplasmic reticulum (ER) in the secretory pathway leading to their fusion. This fusion gives to ER-derived vacuole in which bacteria can replicate. Therefore, VirB allows *Brucella* to reach a safe replicative niche [63,65]. The mechanism behind recruitment and interaction with ER used by *Brucella* is unknown [65].

3.2 About histidine

As described above, histidine biosynthesis genes are organised in operons in *S.* Typhimurium and *E. coli* but in *Brucella* (Figure 7), the *his* genes are spread out on the two chromosomes. On the first chromosome *hisB*, *hisH*, *hisA*, *hisF* and *hisE* are at the same locus. The *hisD*, *hisC* and *hisI* genes are dispersed elsewhere on the first chromosome. The *hisN* gene is located on the second chromosome as well as *hisZ* and *hisG* genes that are organized in operon with *hisS*, a gene potentially coding for the essential the histidyl-tRNA synthetase. To identify essential genes for *B. abortus* during infection, a Tn-seq analysis was previously carried out in the lab, on RAW 264.7 macrophages (24 hours post-infection) [66] and intra-nasally infected mice (2 and 5 days post-infection). The results indicated that the histidine biosynthesis pathway is required for infection by *B. abortus*. In the lab, deletion mutants for several genes (*hisA, hisB, hisC, hisD*) of the pathway have been constructed in the *B. abortus* 544 strain to confirm the Tn-seq data. These *his* mutants demonstrate histidine auxotrophy and replicate less efficiently inside HeLa cells and RAW 264.7 macrophages (Roba Agnès, unpublished data). Surprisingly, some mutants of these mutants show an aberrant morphology. In particular, mutants for *hisB* gene have a chain-like morphology. This unusual morphology was observed in a fraction of the bacteria cultured in rich culture medium but at a higher frequency in a HeLa cell infection model.

3.3 About Cu

The mechanisms by which *Brucella* faces Cu are still unknown. In Brucellae, like in most other bacteria, genes involved in Cu import are not present in the genome. But homologs of several genes linked to Cu resistance, e.g. *copA*, *cueO*, *cueR*, *copZ*, *pcuC*, *senC* and *fixI* are identified in the *Brucella* genome (Figure 8). However, only *cueO* has been investigated functionally [53]. Wu and his team studied a CueO homog in *Brucella melitensis* named BmcO for *Brucella* multi-copper Oxidase and showed its multi-copper oxidase activity. *BmcO* deletion mutant appeared to be more sensitive to $CuCl_2$, indicating that *bmcO* contributes to Cu tolerance. Interestingly, BmcO displayed a ferroxidase activity. A *Brucella bmcO* mutant was not attenuated in murine macrophages [67].

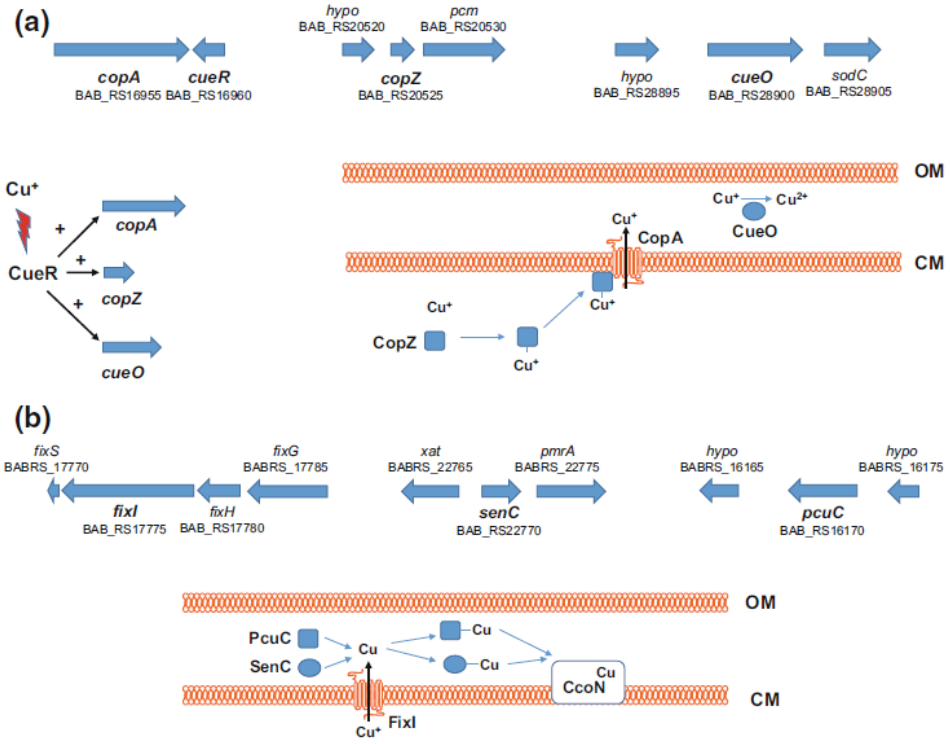

Figure 8. **Putative roles of different *Brucella* proteins involved in the response to Cu toxicity**. (a) CopA, CueO, CopZ and CueR. (b) PcuC, FixI and SenC. CM: cytoplasmic membrane; OM: outer membrane; CcoN: subunit N of cbb_3-type cytochrome *c* oxidase (adapted from [53]).

OBJECTIVES

As described previously, copper is a heavy metal that can cause various types of damage in bacteria due to its toxicity. Therefore, different mechanisms are put in place to control the concentration within the cells and to avoid Cu toxicity. These different systems are not identified in *B. abortus.* In this work, we will specifically be interested in the toxicity induced by Cu on the growth of different auxotrophic mutants for histidine. Indeed histidine is able to bind different metal ions and it has been shown in the lab that the biosynthetic pathway of this amino acid is important for the replication of *B. abortus* within host cells. This work first aims to investigate histidine-enriched proteins by a bioinformatic analysis. Then, we will study the impact of incomplete biosynthesis pathway of histidine on Cu homeostasis by carrying out different growth experiments in the presence of Cu. Through these experiments, we will also try to characterize potential mechanisms used by *B. abortus* to face the toxicity of this heavy metal.

Box 1 | Zn^{2+} import by ZnuABC system

ZnuABC (Zinc uptake) system is a high affinity Zn import system encoded at *znuABC* locus [69,72]. First identified in *Escherichia coli*, Znu is part of the ATP-binding cassette (ABC) transporter family [68]. The *znuA* gene is coding for a periplasmic zinc-binding protein of the ABC-type transporter [69,71,72]. The domains binding Zn^{2+} are H-, E- and D-rich [69]. The *znuB* gene is producing the cytoplasmic permease responsible for Zn^{2+} transport across inner membrane and *znuC* codes for the ATPase component of the transporter coupling the transport process to ATP hydrolysis [69,71,72]. Growth defect on Zn^{2+}-depleted medium are observed when *znuA* and *znuB* are mutated and mutants are no able to pump Zn^{2+} into the cell [71]. In Brucellacae, it is the only Zn^{2+} import system found [53]. The system is expressed under low extracellular Zn concentration [71]. This import system allows the bacteria to survive in Zn-poor environment like animal or human serum. This low Zn^{2+} concentration is inducing *znuABC* expression [69].

The Znu system is regulated at the transcriptional level by a zinc uptake regulator, named Zur. Zur is a metal-sensing regulator, a metalloregulatory protein, binding directly metal and modulating gene transcription in response to direct metal-binding [73]. It is a zinc-dependent repressor [71]. It is a dimer comprising 2 zinc-binding sites; a structural one and a sensing one [32]. The binding site of Zur on DNA is 31 base-paired long and is located in the *znuABC* promoter. The binding is inhibited by the presence of Zn^{2+}-chelator and needs the presence of Zn^{2+} to be occur [70].

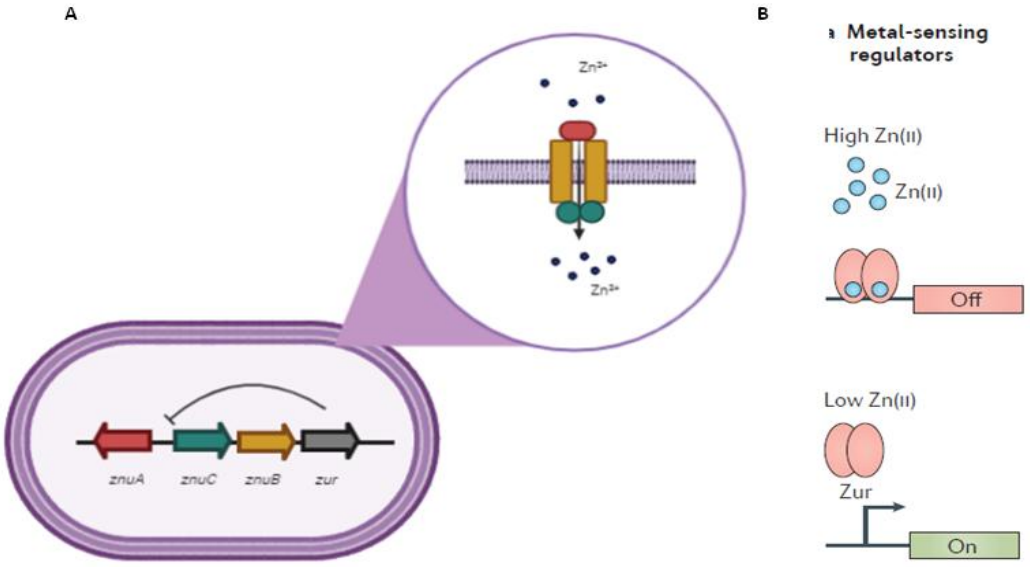

The **ZnuABC zinc import system.** A| The zinc uptake system is composed by ZnuA a periplasmic zinc-binding protein, ZnuB, an inner membrane permease, and ZnuC, the ATPase protein facilitating Zn import. Zur is the metal-sensing regulator (adapted [53]). B| Metal-sensing regulator Zur. Zur repressed *znuABC* genes when Zn^{2+} is present (adapted from [32]).

RESULTS

1 Bioinformatic analysis

As explained in the Introduction, histidine biosynthesis pathway is incomplete in our different histidine mutants, meaning that they are histidine auxotrophs. This lack of endogen histidine production could have a significant impact on protein synthesis. In order to identify the proteins most affected by the reduced histidine availability, a bioinformatic analysis on the *B. abortus* strain 2308 predicted proteome was carried out. With the help of Damien Devos (CABD, Sevilla, Spain), a bioinformatic program able to calculate the percentage of histidine enrichment in the proteome of *Brucella* was created. For each protein sequence, the proportion of histidyl residues was computed. A threshold value was defined at 5% due to the low proportion of proteins (2.8%) above this percentage (Figure S1). The results showed that several of the proteins with a percentage beyond 5% were proteins having a role in metal homeostasis or using metals as a cofactor (Table S1) These results are consistent with the fact that histidine has a role in coordination of metal ions as explained briefly in the Introduction (see Introduction, 1.4 Coordination with metal ions). From this analysis, it is conclude that histidine metabolism could impact metal homeostasis in this bacterium. However the link between histidine biosynthesis and metal homeostasis remains not fully characterized, even in model bacteria. Given that metals availability and/or toxicity is at the heart of host-pathogens interactions (see Introduction, 2.3 Nutritional immunity), it was justified to take an interest in this aspect of histidine metabolism. Thanks to our enrichment list, a lot of protein candidates could be interesting to test for metal homeostasis in *Brucella*. Indeed our hypothesis is that in the absence of a full histidine biosynthesis pathway, even if there is histidine available in the medium, histidine level is limiting and thus proteins that are particularly rich in histidine residues would be less efficiently generated by translation. Since testing the abundance of His-tRNA is quite complex, we propose to first concentrate on specific phenotypes related to metal acquisition or resistance in our mutants.

Interestingly, three main proteins involved in Zn^{2+} import system (Box 1) are found in the list with a high histidine enrichment rate (Table S1); ZnuC (7.2%), ZnuA (6.29%) and Zur (6.21%). Proteome analyses have shown that about 5% of bacterial proteins bind Zn^{2+}, making this ion an important metal for proteins [40]. Zn^{2+} are linked in the active center or in a structural site of many bacterial enzymes [69]. In addition, it is shown that mammals deprive phagosomes of Zn^{2+} to fight bacterial infection (see Introduction, 2.3 Nutritional immunity) [38]. ZnuA is predicted to be the periplasmic binding component of a transport system in which it would bring Zn^{2+} to the ZnuABC transporter (ZnuB being the permease and ZnuC being the ATPase) [70–73]. In order to study the impact of histidine auxotrophy on zinc homeostasis in the *his* mutants, *znuABC* overexpression mutant in a WT and *hisB* backround were constructed.

2 Zinc experimentation

As explained above, Zn^{2+} is a metal ion which has an important role as co-factor in bacterial proteins. In 2003, a first study on the Zn^{2+} import system (*znu* locus) showed that in the presence of EDTA (a well-known chelating agent), *B. abortus* mutants for *znuA* stop their growth after 24 hours and are unable to replicate in HeLa cells and macrophages [74]. Another study carried out by Caswell and Roop on Zn^{2+} homeostasis in *Brucella* demonstrated that Zn^{2+} depletion in the medium induces an increase in the expression of *znuA* and indicates that *znuA* expression is sensitive to Zn^{2+} levels [75]. Assuming that ZnuA could be non-functional or

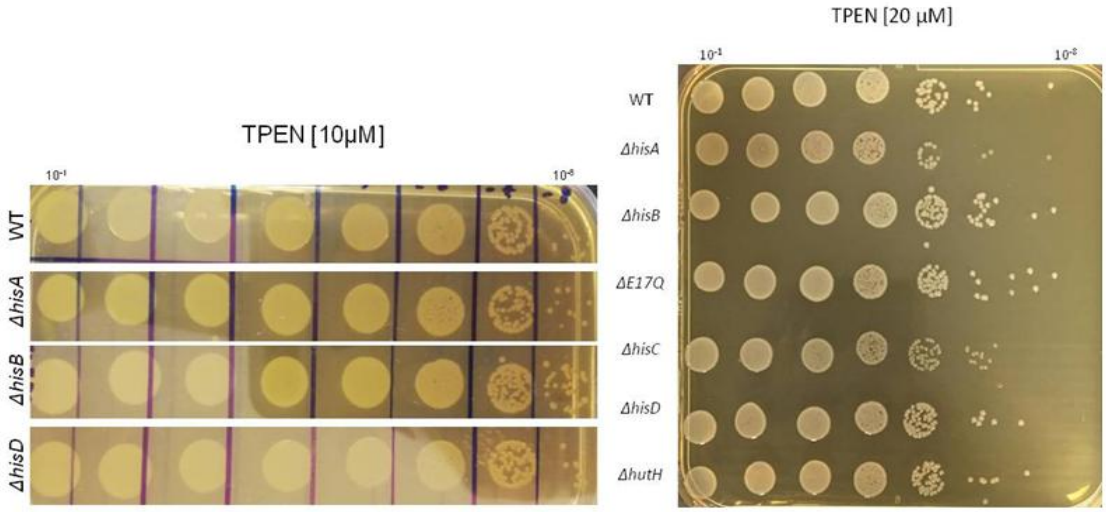

Figure 9. **TPEN at a final concentration of 10 and 20 µM is not affecting Δ*hisA*, Δ*hisB*, Δ*E17Q*, Δ*hisC*, Δ*hisD*, Δ*hutH* and WT growth.** Overnight liquid cultures of *B. abortus* 544, Δ*hisA*, Δ*hisB* and Δ*hisD* were normalized at OD 0.1 and serially diluted and spotted on TSB agar plate containing 10 µM TPEN (left) and 20 µM (right). The pictures were taken after 4-5 days at 37°C.

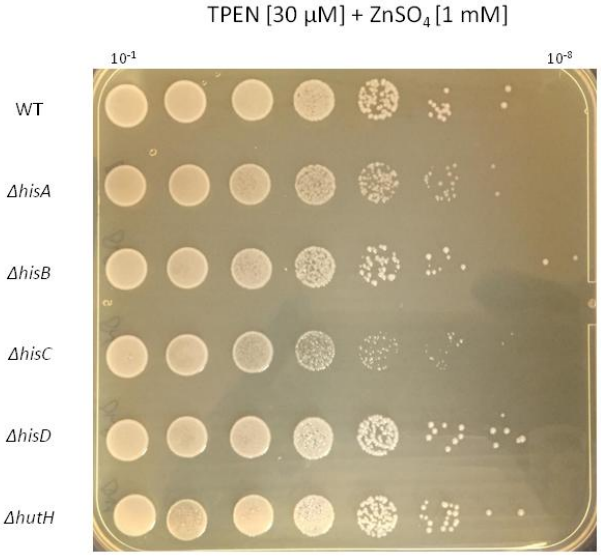

Figure 10. **$ZnSO_4$ repletion restores Δ*hisA*, Δ*hisB*, Δ*E17Q*, Δ*hisC*, Δ*hisD*, Δ*hutH* and WT growth.** Overnight liquid cultures were normalized at OD 0.1 and serially diluted and spotted on TSB agar plate containing 30 µM TPEN and 1 mM $ZnSO_4$. The picture was taken after 4-5 days at 37°C.

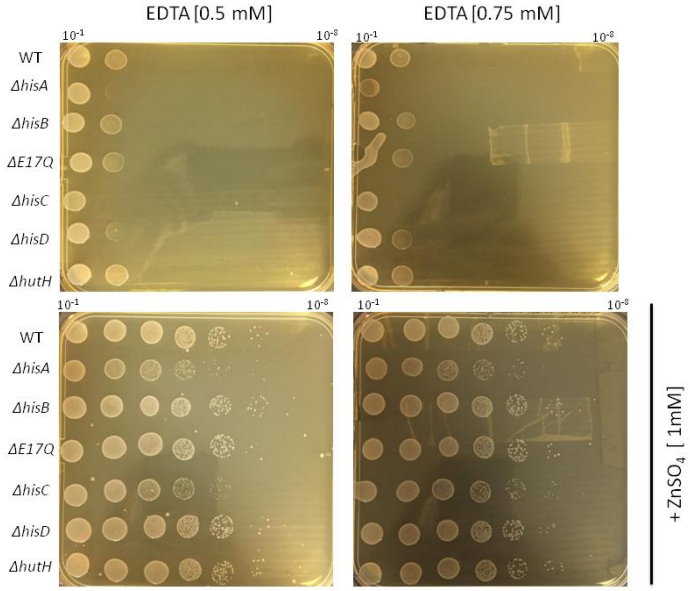

Figure 11. **EDTA at a final concentration of 0.5 and 0.75 mM inhibits Δ*hisA*, Δ*hisB*, Δ*E17Q*, Δ*hisC*, Δ*hisD*, Δ*hutH* and WT growth and $ZnSO_4$ repletion restores bacterial growth.** Overnight liquid cultures were normalized at OD 0.1 and serially diluted and spotted on TSB agar plate containing 0.5 (top left) or 0.75 mM (top right) EDTA and 1 mM $ZnSO_4$ (bottom). The pictures were taken after 4-5 days at 37°C.

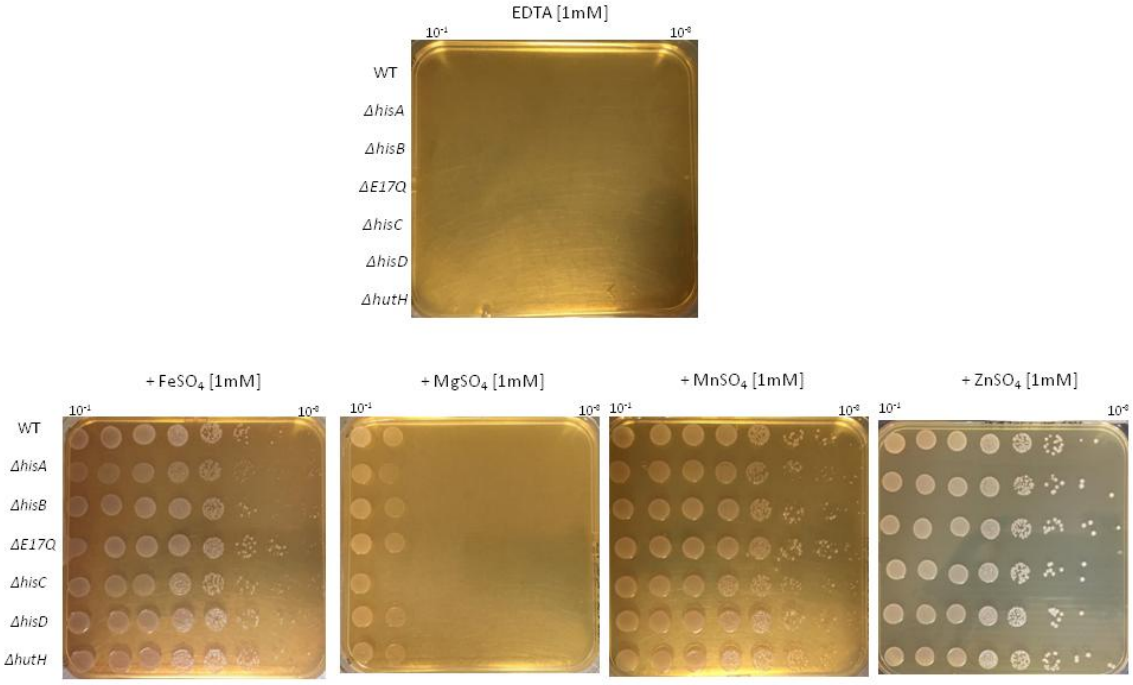

Figure12. **EDTA at a final concentration of 1 mM inhibits Δ*hisA*, Δ*hisB*, Δ*E17Q*, Δ*hisC*, Δ*hisD*, Δ*hutH* and WT growth and metals repletion restores bacterial growth.** Overnight liquid cultures were normalized at OD 0.1 and serially diluted and spotted on TSB agar plate containing 1 mM EDTA (top). Different metals were added at a final concentration of 1 mM. Bottom, in order; $FeSO_4$, $MgSO_4$, $MnSO_4$ and $ZnSO_4$. The pictures were taken after 4-5 days at 37°C.

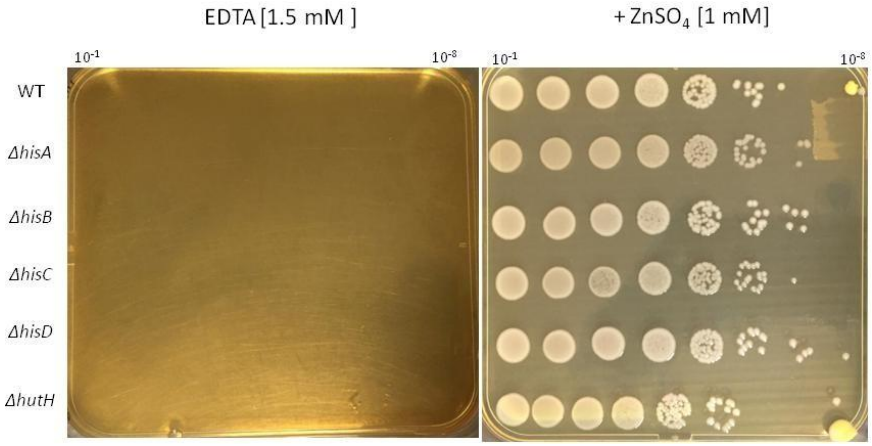

Figure 13. **EDTA at a final concentration of 1.5 mM inhibits Δ*hisA*, Δ*hisB*, Δ*hisC*, Δ*hisD*, Δ*hutH* and WT growth and $ZnSO_4$ repletion restores bacterial growth.** Overnight liquid cultures were normalized at OD 0.1 and serially diluted and spotted on TSB agar plate containing 1.5 mM EDTA (left) and 1 mM $ZnSO_4$ (right). The pictures were taken after 4-5 days at 37°C.

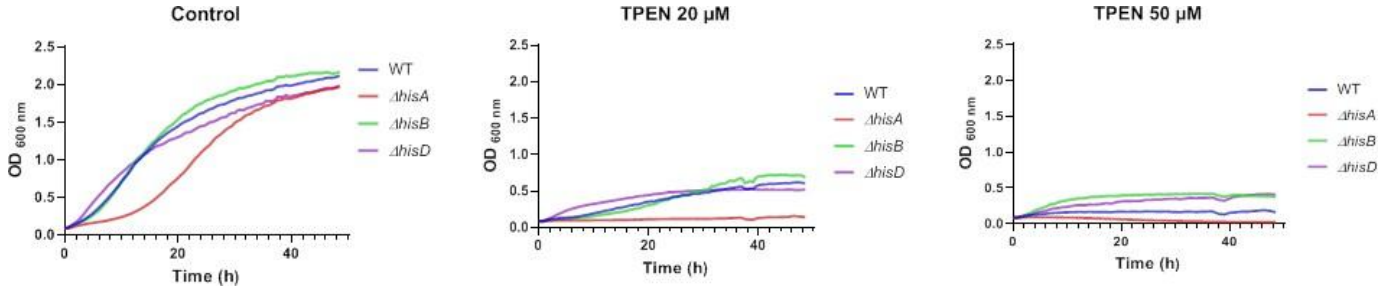

Figure 14. **Growth curves of *B. abortus* 544 in control condition (top) and in presence of TPEN 20 µM (middle) and 50 µM (bottom).** WT and *his* mutants were grown in TSB medium. Overnight cultures of strains grown in TSB were diluted to optical density (OD) of 0.1. During growth, OD at 600 nm was measured every 30 minutes for 48 hours.

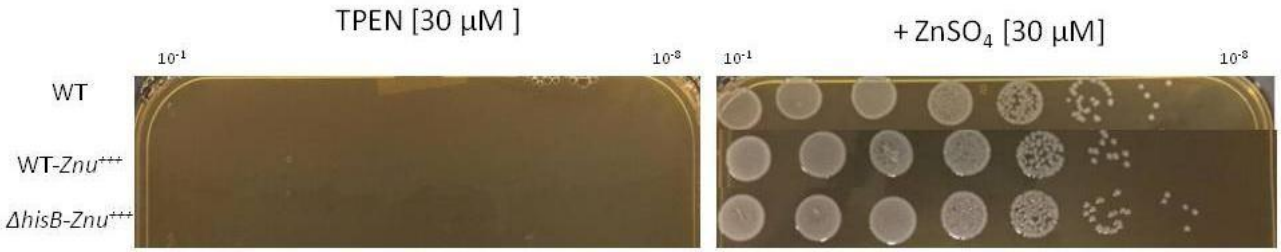

Figure 15. **TPEN at a final concentration of 30 µM inhibits WT-*Znu*$^{+++}$, Δ*hisB*-*Znu*$^{+++}$ and WT growth and $ZnSO_4$ repletion restores bacterial growth.** Overnight liquid cultures were normalized at OD 0.1 and serially diluted and spotted on TSB agar plate containing 30 µM TPEN (left) and 30 µM $ZnSO_4$(right). The pictures were taken after 4-5 days at 37°C.

less produced in our mutants, the same experiment, i.e. grow our *his* and *znuABC* mutants on a Zn^{2+}-depleted medium by adding a Zn^{2+}-specific chelator (TPEN) and a non-specific chelator (EDTA) was conducted, to compare their growth to the WT when Zn^{2+} is depleted.

Different concentrations of TPEN were added to TSB Agar; 10, 20 and 30 µM. Twenty µl drops of serial 10-fold dilutions of the different strains were spotted on the plate. At the 10 µM final concentration of TPEN, tree mutants were tested besides the WT; *ΔhisA*, *ΔhisB,* and *ΔhisD* (Figure 9). The results indicated that the presence of this chelator at such a low concentration did not affect the growth of the bacteria, since no difference between the strains was observed. When the concentration was doubled, 20 µM final, again bacterial growth was not impacted by the chelator presence. Here *ΔhisC* and *ΔhutH* were added to the experiment, as well as the catalytically dead mutant *hisB*E17Q (Figure 9). Certainly the growth was not as important as with 10 µM of TPEN but a difference in growth inhibition due to chelator present could not be demonstrated between strains. When the concentration was tripled, all the strains were unable to grow. These different results indicate that the variation in TPEN concentration is tricky since growth of the strain goes from everything to nothing. As none of the strains were able to grow in the presence of 30 µM of TPEN, medium was repleted with Zn^{2+} to try to restore the growth in our histidine mutants. $ZnSO_4$ was added at a final concentration of 1 mM in the medium and the bacterial growth was restored (Figure 10). This is indicating that the chelating action of TPEN is bypassed by the addition of Zn^{2+}. However, the different strains do not present any significant growth differences.

In addition to TPEN, EDTA, a non-zinc-specific chelator was also used for this experiment. Different concentrations were tested: 0.5, 0.75, 1 and 1.5 mM. When a low concentration was used (0.5 or 0.75 mM), bacteria were able to grow but for the two first 10-fold dilutions (Figure 11). *ΔhisA* and *ΔhisC* showed a difference of growth; however our *ΔhisA* mutant presents already slight growth defect on TSB agar plate and in liquid culture medium (Figure S2Figure **S3**). EDTA action was also suppressed by $ZnSO_4$ addition to the medium (Figure 11). When 1 mM of $ZnSO_4$ was added, bacterial growth was restored for all the strains, without any significant difference between them. When EDTA is added at higher concentrations such as 1 or 1.5 mM, bacterial replication was completely inhibited (Figure 12-13). EDTA is known to be a non-specific chelator, being able to chelate different metal ions. Medium repletion in addition of Zn^{2+} was also done with other metal ions such as magnesium (Mg), Mn and Fe. These ions were added at 1 mM concentration to a medium containing 1 mM of EDTA (Figure 12). Medium repletion was conclusive with Fe and Mn but surprisingly addition of Mg did not allow the growth restoration of bacterial strains.

Growth in liquid medium was also studied in the presence of the chelator. The *ΔhisA*, *ΔhisB* and *ΔhisD* grew in liquid culture in the presence of two different concentrations of TPEN. Unlike growth on solid medium, in the presence of 20 µM of TPEN, bacteria are not able to proliferate properly and a strong growth inhibition could be highlighted. At 50 µM of the chelator agent, bacterial strains do not growth at all (Figure 14).

In a second step, WT and Δ*hisB* strains transformed with a medium-copy plasmid carrying the *znuACB* genes were constructed. These strains potentially overexpress *znuABC* and were thus called Znu^{+++}, they were constructed to study Zn^{2+} homeostasis, as explained above. Some of the chelation experiments were repeated with these strains. In the presence of TPEN at a final concentration of 30 µM, WT and *ΔhisB* overexpressing the Zn^{2+}-import system are not able to grow, like all the strains tested before. Their growth was restored when 30 µM of $ZnSO_4$ was added to the medium, similarly to *his* mutants (Figure 15). Less $ZnSO_4$ was added than for the previous experiment to try to see at which concentration TPEN can be saturated and if less

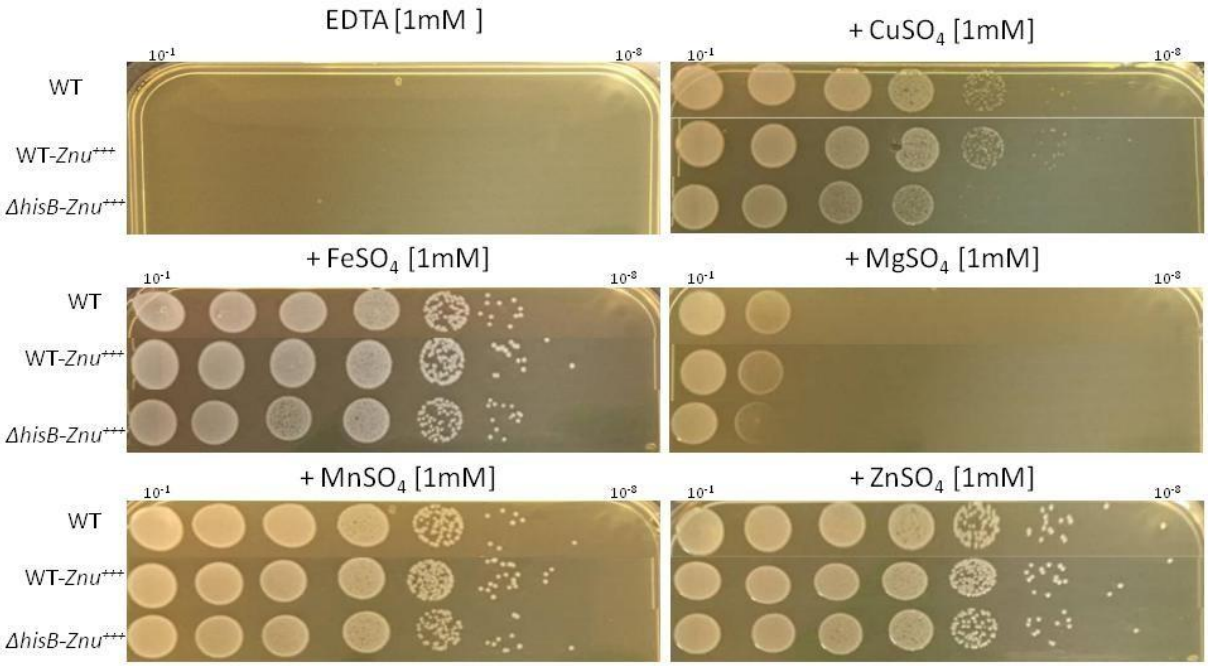

Figure 16. **EDTA at a final concentration of 1 mM inhibits WT-*Znu*$^{+++}$, Δ*hisB-Znu*$^{+++}$ and WT growth and metals repletion restores bacterial growth.** Overnight liquid cultures were normalized at OD 0.1 and serially diluted and spotted on TSB agar plate containing 1 mM EDTA (top left). Different metals at 1 mM were added. In order; $CuSO_4$, $FeSO_4$, $MgSO_4$, $MnSO_4$ and $ZnSO_4$. The pictures were taken after 4-5 days at 37°C.

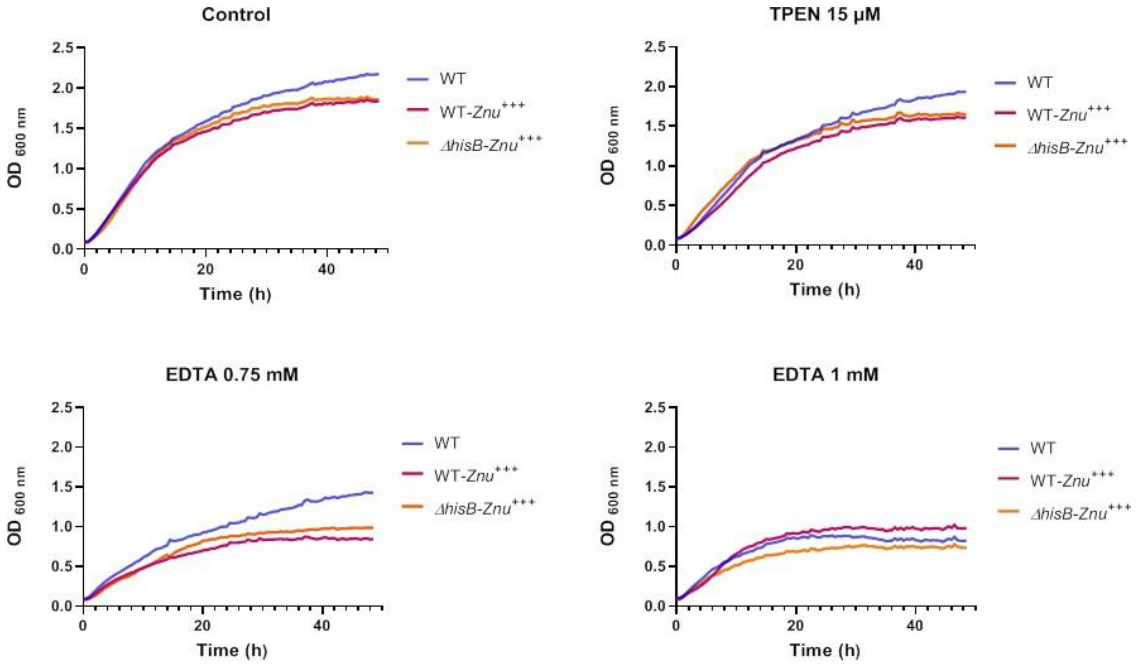

Figure 17. **Growth curves of *B. abortus* 544 in control condition (top left) and in presence of TPEN 15 µM (top right) and EDTA 0.75 and 1 mM (bottom).** WT and *Znu*$^{+++}$ strains were grown in TSB medium. Overnight cultures of strains grown in TSB were diluted to optical density (OD) of 0.1. During growth, OD at 600 nm was measured every 30 minutes for 48 hours.

Zn^{2+} could also rescue the growth. The two *Znu*$^{+++}$ strains were spotted on a plate containing 1 mM of EDTA, and again a growth inhibition was observed for both strains. The medium was then repleted with Zn^{2+} but also Cu^{2+}, Fe^{2+}, Mn^{2+} and Mg^{2+}. Replication was totally rescued by manganese, Zn^{2+}, Mn^{2+} and Fe^{2+} addition (Figure 16). There is no difference between the three strains excepted when $CuSO_4$ is added, *ΔhisB-Znu*$^{+++}$ presents a clear replication defect compared to WT-*Znu*$^{+++}$. As observed with *his* mutants, Mg^{2+} addition did not restore growth in the presence of EDTA (Figure 16).

As with *Δhis* mutants, growth in liquid medium was analysed in the presence of 15 µM of TPEN or 0.75 mM of EDTA (Figure 17). The presence of TPEN at 15 µM concentration did not impact the growth of all the three strains. On the contrary, EDTA at 0.75 or 1 mM did inhibit the replication of the WT, WT-*Znu*$^{+++}$ and *ΔhisB-Znu*$^{+++}$ strains. Here, the repletion with Zn^{2+} or other metals was not performed.

All the results together indicated that the presence of a chelator (TPEN or EDTA) could inhibit bacterial growth. This inhibition could be rescued by metal ions addition and there are differences in repletion depending on the metal ion, such as Mg which rescued only partially the growth. However, any difference of growth could be highlighted between all the strains on depletion medium and on repleted medium with different metals ions. The dose-response relationship between the presence of chelator and growth inhibition seems very difficult to determine. In addition, TPEN action can be bypassed by other metal ions than Zn^{2+}. Indeed, medium containing 30 µM of TPEN was also repleted with equimolar concentration of $MnSO_4$ and $CuSO_4$. Cu or Mn addition can rescue WT, WT-*Znu*$^{+++}$and *ΔhisB-Znu*$^{+++}$ growth (Figure S4) suggesting that TPEN specificity might be not only for Zn^{2+}. Moreover, the right concentration to allow saturation of the chelator without inducing an excess of the ion is complex to determine and requires further adjustments. Given the absence of an effect of the *his* mutations, biological triplicates were not achieved.

3 Copper sensitivity

Cu^{2+} is a heavy metal toxic for cells and can lead to damage (see Introduction, 2. Copper). According to the hypothesis where metal homeostasis is impacted by mutations in the histidine biosynthesis pathway, Cu homeostasis was also studied. For this purpose, bacterial growth in presence of Cu has been studied with different experiments and Cu sensitivity or potential resistance of our *his* mutants was explored.

Firstly, a disk diffusion test was used to evaluate Cu sensitivity (Figure 18). As the Cu^{2+} concentration for which *Brucella* would be sensitive was unknown to us, an initial experiment was done in which a disk of Whatman paper was soaked with 10 µl of 37.3 mM $CuCl_2$ solution which is placed on TSB plates where 100 µl of overnight culture of wild-type (WT), *ΔhisA, ΔhisB, hisB*E17Q, *ΔhisC* and *ΔhutH* strains were just plated. However, any inhibition zone in WT or mutant strains could be observed (Figure S5). This experiment was thus repeated with higher concentrations; 2 M and 4 M of $CuCl_2$ solution and with WT, *ΔhisA, ΔhisB, ΔhisC* and *ΔhisD* strains. Diameters of growth inhibition zones were measured around the disk in millimetres, for three biological replicates (Figure 19). Results indicate that the diameters of inhibition zone are increasing in *his* mutants compared to WT, especially for *ΔhisA*. When the deleted gene is expressed *in trans* (complemented strains), inhibition zones become smaller, similar to WT, suggesting that Cu sensitivity is increased when the histidine biosynthesis pathway is incomplete. Statistical analyses *via* ANOVA with Dunnett's test were carried out. Differences observed between WT and *ΔhisA* were statistically significant for both concentrations: 2 and 4 M (**, $P<0.0016$ and **, $P<0.0025$ respectively), indicating that

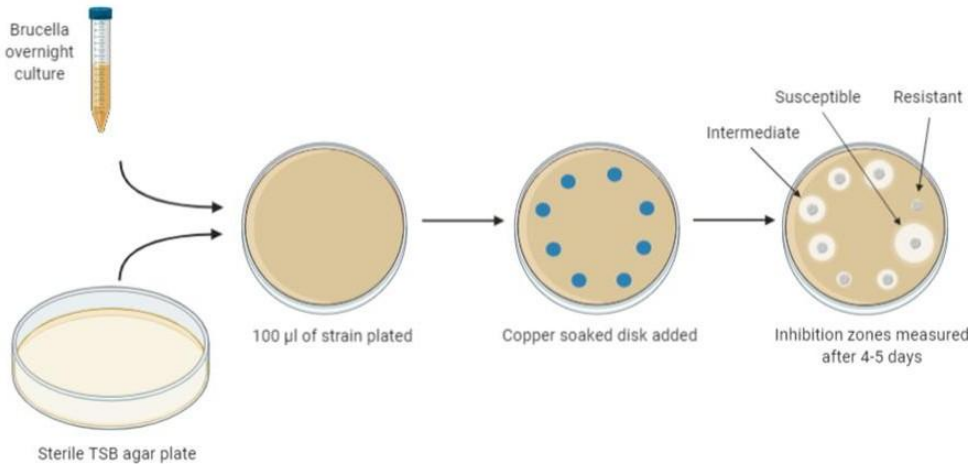

Figure 18. **Schematic illustration of disk diffusion assay.** Hundred µl of an overnight culture of *Brucella* are spread out on a sterile TSB Agar. After cultures had dried, a sterile Whatman disk was placed in the center of the plate. Each disk was previously soaked with 2 or 4 M solution of $CuCl_2$ for one hour, and the plates were incubated at 37°C for 4 days. The diameter of the inhibition zones around each disk was measured in three different ways and the mean was indicated in millimetres.

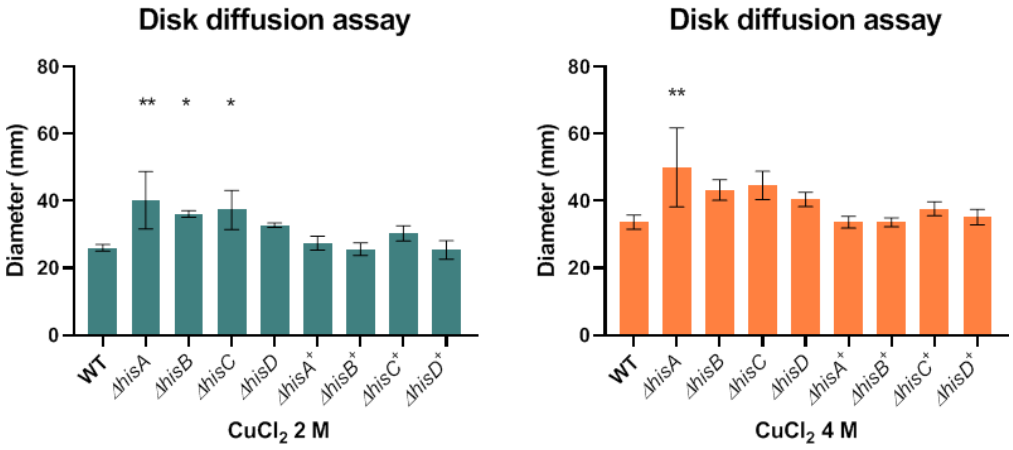

Figure 19. **Cu sensitivity of WT and *Δhis* strains**. Hundred µl of an overnight culture of each *B. abortus* strain was spread out on TSB plates where a disk soaked with 2 (left) or 4 M (right) of $CuCl_2$ was placed in the middle solution. Inhibition zones were measured (mm) and reported in a histogram. Statistical analysis were carried out by an ANOVA with Dunnett's test (*, $P < 0.05$, **, $P < 0.005$).

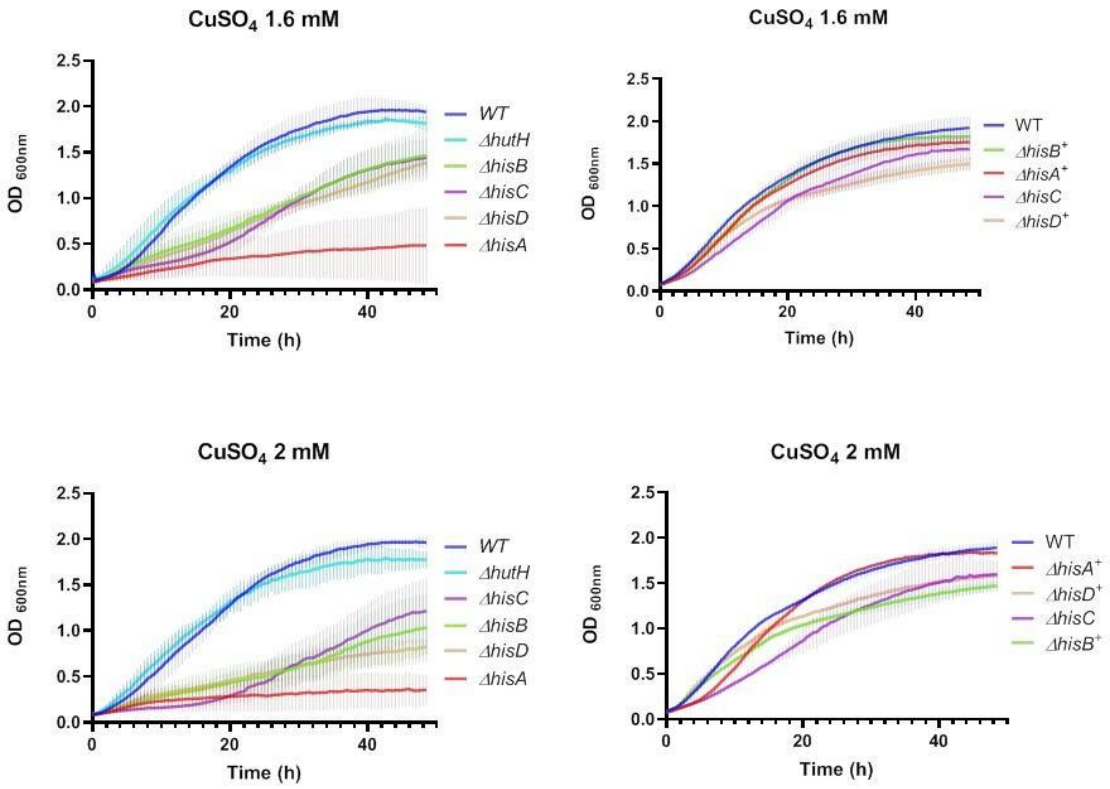

Figure 20. **Growth curves of *B. abortus* 544 in the presence of Cu.** WT, *his* mutants and complemented strains were grown in TSB medium containing 1.6 or 2 mM of $CuSO_4$. Overnight cultures of strains grown in TSB were diluted to optical density (OD) of 0.1. During growth, OD at 600 nm was measured every 30 minutes for 48 hours. Data are representative of results of biological triplicates.

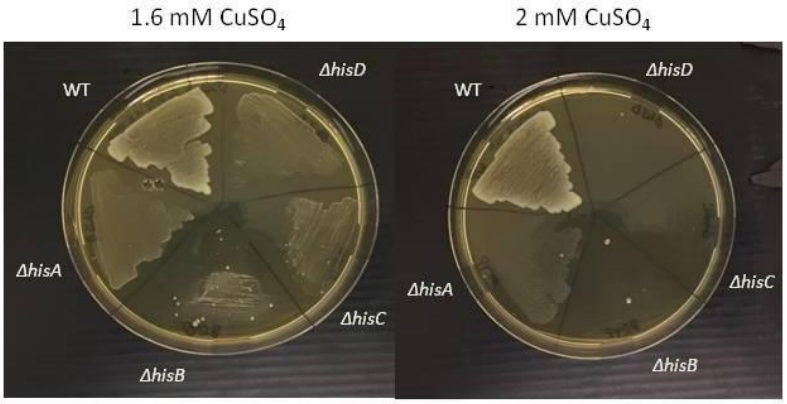

Figure 21**. *B. abortus* WT and mutant strains $CuSO_4$ sensitivity on plates.** Cu sensitivity of WT and *ΔhisA*, *ΔhisB* and *ΔhisD* mutant strains (in this clockwise order) was tested on TSB medium containing 1.6 mM (left) or 2 mM (right) of $CuSO_4$. Both plates were divided in five parts where 20 µl of each culture were deposited and spread after their OD was normalized to 0.1. Pictures were taken after a four-day incubation at 37°C. Data are representative of results of biological triplicates. It is interesting to note the presence of individual colonies for *ΔhisA*, *ΔhisB* and *ΔhisD*, suggesting that suppressors mutants may be easily obtained for this phenotype.

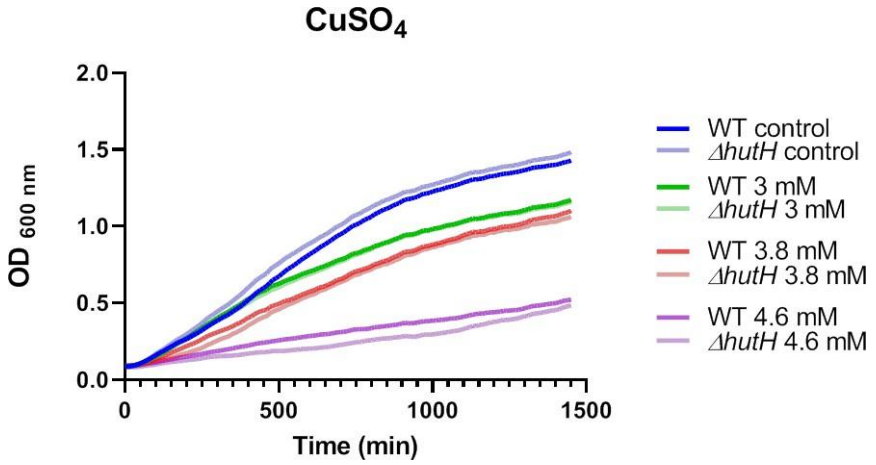

Figure 22. **Growth curves of *B. abortus* 544 in the presence of Cu.** WT and *ΔhutH* mutants strains were grown in TSB medium containing increasing concentration (from 3 to 4.6 mM) of $CuSO_4$. Overnight cultures of strains grown in TSB were diluted to optical density (OD) of 0.1. During growth, OD at 600 nm was measured every 30 minutes for 24 hours. Data are representative of results of biological triplicates.

ΔhisA is sensitive to Cu compared to the WT. The *ΔhisB* and *ΔhisC* strains also present a Cu sensitivity that is significant (*, $P<0.02$ and *, $P<0.01$ respectively) at 2 M concentration. However, *ΔhisD* does not show a significant sensibility to Cu compared to the WT for both concentrations.

Secondly, growth in the presence of Cu solution in liquid culture was measured during 48h. Mutants (*ΔhisA, ΔhisB, ΔhisC, ΔhisD* and *ΔhutH*) and WT strains were placed in 96-well plate in the presence of $CuSO_4$ solution at a final concentration of 1.6 and 2 mM. Growth curves showed a clear growth inhibition with 1.6 mM concentration for the Δ*hisA* mutant compared to WT and an intermediate inhibition for *ΔhisB, ΔhisC* and *ΔhisD* strains. The growth inhibition was present in all four *his* mutants when the $CuSO_4$ concentration is increased to 2 mM (Figure 20). In addition, *ΔhutH* mutant did not show any growth inhibition and seemed to tolerate Cu as well as WT. This experiment was done with the complemented strains and bacterial replication was restored, without showing a higher Cu sensitivity compared to the WT. The same concentration of $CuCl_2$ solution was also tested instead of $CuSO_4$, and growth inhibition for all mutants was similar (data not shown). The results indicate that the growth inhibition observed in our mutant strains is due to Cu and not to sulfate. This second experiment is along in the same line as the first experience, showing a higher Cu sensitivity when histidine could be not produced.

Thirdly, a last experiment was conducted, the growth of our mutants was measured on solid medium supplemented with Cu. $CuSO_4$ was added to TSB agar at a final concentration of 1.6 and 2 mM and poured into a Petri dish on which WT, *ΔhisA, ΔhisB,ΔhisC, ΔhisD* and *ΔhutH* strains were smeared. Results showed a clear growth inhibition for each *his* mutant, with only a few colonies formed but not for WT that grew massively (Figure 21). This correlated to the results obtained with the disk diffusion test as well as growth in liquid medium in the presence of Cu. Altogether; results showed that *ΔhisA, ΔhisB, ΔhisC* and *ΔhisD* are more sensitive to Cu toxicity. It is possible that the absence of *ΔhisD* growth defect around the $CuCl_2$ disk (Figure 19) is due to a small effect of the mutation that is not significative with only three replicates.

Despite the Cu sensitivity in our mutants, the results highlighted a surprisingly good Cu tolerance of *Brucella abortus* 544 WT and *ΔhutH*. As the toxic concentration for the growth of *Brucella* was unknown, bacterial growth in liquid medium in the presence of Cu was conducted again but with higher concentrations than 1.6 and 2 mM only for 24 h. A panel of concentrations from 3 to 5 mM of $CuSO_4$ allowed us to determine a concentration range where growth inhibition can be observed (data not shown). *B. abortus* started struggling to grow over 4.8 mM of $CuSO_4$. The concentration used for biological triplicates were 3, 3.8 and 4.6 mM. The growth curves demonstrated a gradual growth inhibition for both strains. No significant difference between WT and *hutH* mutant was observed (Figure 22).

The most interesting result with growth experiment on solid medium is the presence of a few colonies among the mutants that were not able to grow properly (Figure 21). The appearance of mutations in these bacteria could possibly allow them to tolerate the presence of Cu. In this case, these colonies could correspond to suppressors, i.e. clones in which a second mutation removes the phenotypic effect of a first mutation (Δ*hisA*, Δ*hisB*, Δ*hisC* or Δ*hisD*). This identification of the second mutation could be very informative to understand the effect of the first mutation. To confirm the genetic basis of the phenotype of these colonies, the experiment was repeated and for each mutant, isolated colonies were streaked on new TSB agar dishes and on both Cu plates at 1.6 and 2 mM final concentration. For most of them, largest colonies were selected when it was possible. In total, 29 potential suppressors were streaked, all mutants combined, and only eight of them were unable to grow in the presence of Cu. These

Table 2. **Table of suppressors SNPs.**

Suppressors						
Suppressors[a]	Position[b]	Type[c]	Ref.[d]	Alt.[e]	Gene[f]	
A1, A2	chr2. 696738	snp	T	C	BAB2_0700 & 0701	Opp operon
B7, B8, B12, D7	chr2. 694270	complex	ATG	CTC	BAB2_0699	OppA1
	chr2. 695907	complex	TCT	CCG	BAB2_0700	OppA2
B7, B8, B9, B10, B12, C8, D7	chr2. 695019	deletion TA -> T missing			BAB2_0699	OppA1
C3, C4, C5, C6, C8	chr1. 1419703	del	TA	T	BAB1_1460 & 2215	Intergenic region
C4, D5	chr1. 1122459	del	GCGCCGT	G	BAB1_1150	AceF
B4, C6	chr2. 766953	complexe mutation missing			BAB2_0775	Hypothetical protein

The SNP analysis program used was usegalaxy.org, using Snippy tool. The program aligns the reads given by the sequencing to a reference genome, here *Brucella abortus* 544. The output given is a table showing the different SNPs appearing in the suppressors.

[a] The name of the repressor with the letter of the his mutant to which it refers as well as a number related to the colony streaked.

[b] Refers to the position on the chromosome.

[c] SNP type. Del: deletion.

[d] Ref. Nucleic acids found in the genome of the reference mutant for the suppressor: *ΔhisA*, *ΔhisB*, *ΔhisC* and *ΔhisD*.

[e] Alt. Nucleic acids found in the genome of the suppressor.

[f] Gene tag where SNP is occurring.

mutants were putted aside. The remaining 21 that were resistant to copper were sent for sequencing in order to identify any potential SNP present in these bacteria that could allow Cu tolerance. The genome of the parental Δ*hisA*, Δ*hisB*, Δ*hisC* and Δ*hisD* strains was also sequenced. Sequencing reads were analysed with the Snippy tool available on usegalaxy.org website. Each reference mutant (*ΔhisA*, *ΔhisB*, *ΔhisC* and *ΔhisD*) genome was compared to the reference *B. abortus* 544 genome. Then, each suppressor genome was compared to the reference genome. The list of SNPs obtained for each suppressor and reference mutant were compared. Only the SNPs present in our suppressors were selected from the analysis. A total of 29 mutations were identified among the suppressors. Seven of them were recurring in different suppressors (Table 2), suggesting that they have not been acquired independently but were already present in the parental strains. For reasons of time and interest, only the mutations appearing once in suppressors were retained. Then, 22 mutations were retained (Table 3). The first mutation identified was on the first chromosome, inside *lysK21* gene. LysR21 is a transcriptional regulator which is binding upstream a gene encoding a thioredoxine reductase [50]. This mutation is leading to an amino acid change; glutamine to a glycine. The second mutation was on the second chromosome, replacing a lysine for asparagine in the *lysK* sequence. LysK is a lysine–tRNA ligase. The *lysK* gene was previously found to be essential [66]. Two mutations are appearing in *pdhA* and *pdhB,* which are forming the enzymatic components E1 of the pyruvate dehydrogenase complex which represents the metabolic link glycolysis and the Krebs cycle [76]. In *pdhA*, a 1 pb deletion was found and a mutation generating a stop codon was identified in *pdhB.* In addition to these mutations, 15 others have been identified. Surprisingly and unexpectedly, these mutations appear **all within the same operon, the *opp* operon** (Table3). Opp, for oligopeptide transport, is composed of 5 genes. The first two; $oppA_1$ and $oppA_2$ are two periplasmic proteins. The two genes following *oppB* and *oppC* are permeases and the last *oppD/F* is the ABC transporter. Strikingly, only the two first genes are touched by SNP (Figure 23). Among all these SNPs within the *opp* operon (in Table 3), some lead to amino acid changes (in green) while others do not, described as silent mutations (in grey). In the case of the B10 suppressor, the first mutation generates a stop codon (in red), thus qualifying the 3 following mutations as silent, since the translation reading frame is interrupted. It is thus likely that in the B10 suppressor, $OppA_1$ lost its function compared to the parental strain. Among all these mutations, one appeared particularly interesting for the expression of the operon. The mutation is located in the C6 suppressor, upstream of the operon and located in a potential distal promoter region, 70 pb upstream of the operon (Table 3,Figure 23). The mutation was investigated as it is likely to influence the expression of the first two proteins of the operon. To do this, mRNA abundance for the $OppA_1$ and $OppA_2$ proteins were analysed in WT, *ΔhisC* and C6 strains. The change in mRNA abundance for the two proteins can be compared between the suppressor and its reference mutant. The mRNA abundance of *ΔhisC* compared to the WT. To evaluate the mRNA abundance, an RT-qPCR was carried out. It has to be noted that, due to the lack of time, biological triplicates were not done. In order to highlight the fold expression change in the *ΔhisC* strain, the mRNA abundance for both proteins in the WT is defined as 1. The results illustrate a very slight increase of $oppA_1$ and $oppA_2$ mRNA abundance in the Δ*hisC* strain compared to the WT (Figure 24). The fold change of the two genes expression of C6 strain was evaluated against *ΔhisC* strain, where mRNA abundances were defined as 1. Interestingly, the $oppA_1$ and $oppA_2$ mRNAs appeared to be 5 fold more abundant compared to the *ΔhisC* strain (Figure 24). However, since this experiment could only be carried out once, the statistical analysis could not be performed.

In the lab, *Δopp* mutant was previously constructed in the *B. abortus* 544 background (P. Godessart, master thesis, 2017). To investigate Opp role and how it is helping suppressor growth when Cu is present in the medium, the same experiments performed before were

Table 3. **Table of suppressors SNPs.**

Suppressors					
Mutant[a]	Suppr.[b]	Position[c]	Amino acid change[d]	Gene[e]	
ΔhisA	**A1**	chr1. 1472668	Gln -> Lys	BAB1_1517	LysR21
	A2	chr1. 936216		BAB1_0955 & 0956	Intergenic region
ΔhisB	**B1**	chr2. 695058	60 pb deletion	BAB2_0699	OppA1
	B4	chr1. 460842		BAB2_0464 & 0465	Intergenic region
	B9	chr2. 695451	Glu -> Gln	BAB2_0700	OppA2
		chr2. 695457	Ser -> Thr		
		chr2. 695468	Arg-Ile -> Arg-leu		
		chr2. 695483			
		chr2. 695489			
	B10	chr2. 694185	Stop	BAB2_0699	OppA1
		chr2. 694191	Glu -> Lys		
		chr2. 694200	Asp->Tyr		
		chr2. 694219	Ser-Gly -> Phe-Cys		
ΔhisC	**C5**	chr2. 444440	Lys->Asn	BAB2_0447	LysK
		chr2. 745096		BAB2_0748 & 0749	Intergenic region
	C6	chr2. 693379	Potential promoter region	BAB2_0698 & 0699	OppA1
	C8	chr2. 693942		BAB2_0699	OppA1
		chr2. 693957			
		chr2. 693966			
		chr2. 695612	Lys -> Asn	BAB2_0700	OppA2
ΔhisD	**D4**	chr1. 1124993	1 pb deletion	BAB1_1152	PdhA
	D6	chr1. 1124208	Stop	BAB1_1151	PdhB

The SNP analysis program used was usegalaxy.org, using Snippy tool. The program aligns the reads given by the sequencing to a reference genome, here *Brucella abortus* 544. The output given is a table showing the different SNPs appearing in the suppressors.

[a] There are the different *his* mutants constructed in the lab.

[b] The name of the repressor with the letter of the his mutant to which it refers as well as a number related to the colony streaked.

[c] Refers to the position on the chromosome

[d] Green: SNP leading to an amino acid change, Grey: silent SNP and Red: SNP leading to codon stop.

[e] Gene tag where SNP is occurring.

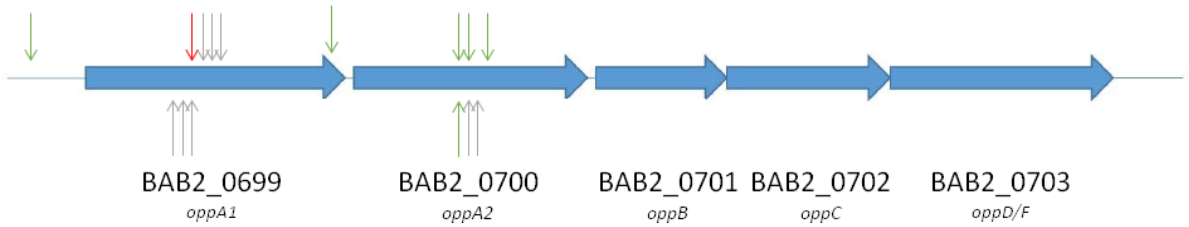

Figure 23. **Localisation of SNP on the *opp* operon.** Each arrow represents SNP position. Green arrows represent SNP leading to amino acid changes, grey arrows represent SNP silent and red arrow represents STOP codon. The 60 pb deletion is represented by a green arrow at the end of BAB2_0699.

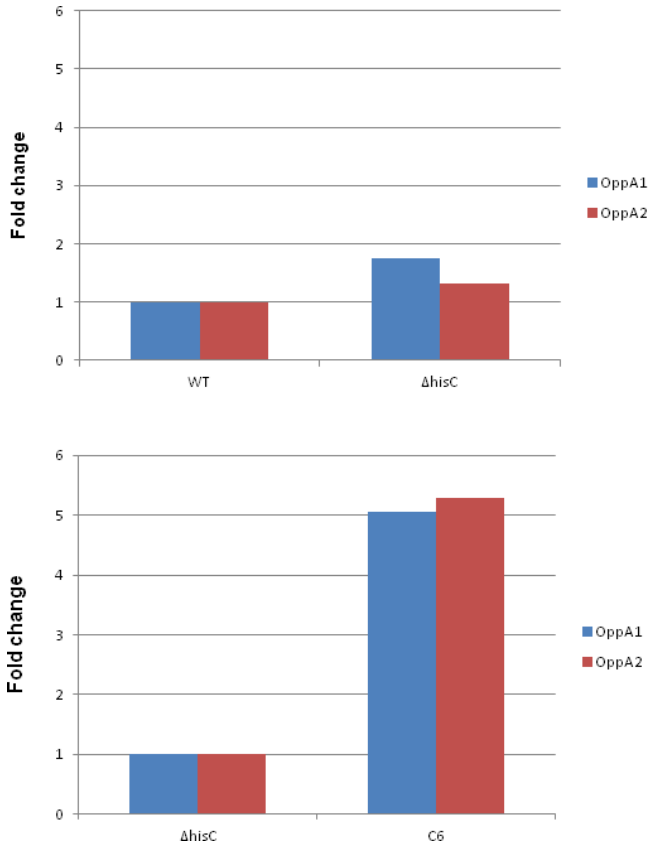

Figure 24. **Expression relative of *oppA*$_1$ and *oppA*$_2$ in WT, *ΔhisC* and C6 strains.** Quantitative RT-PCR was performed to estimate the fold change compared to the WT for *ΔhisC* and to *ΔhisC* for C6. RT-qPCR was performed on exponential phase of *B. abortus* cultured in TSB overnight. Biological triplicates were not achieved.

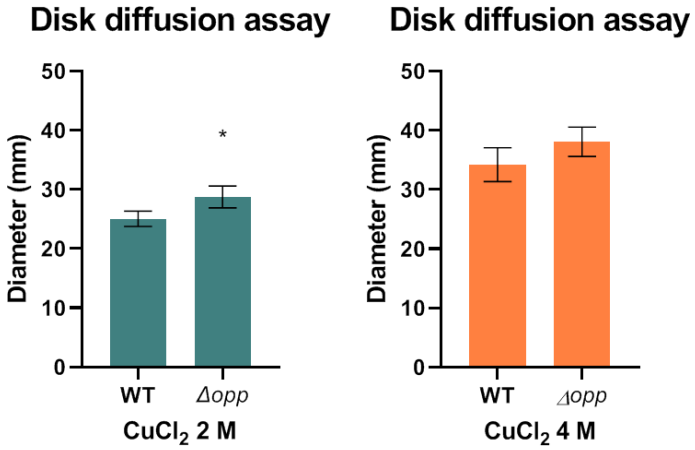

Figure 25. **Cu sensitivity of WTand *Δopp* strains**. Hundred µl of an overnight culture of each *B. abortus* strain was spread out on TSB plates where a disk soaked with 2 (left) or 4 M (right) of $CuCl_2$ was placed in the middle solution. Inhibition zones were measured (mm) and reported in a histogram. Statistical analysis was carried out by a *t* test (*, *P;* 0.05).

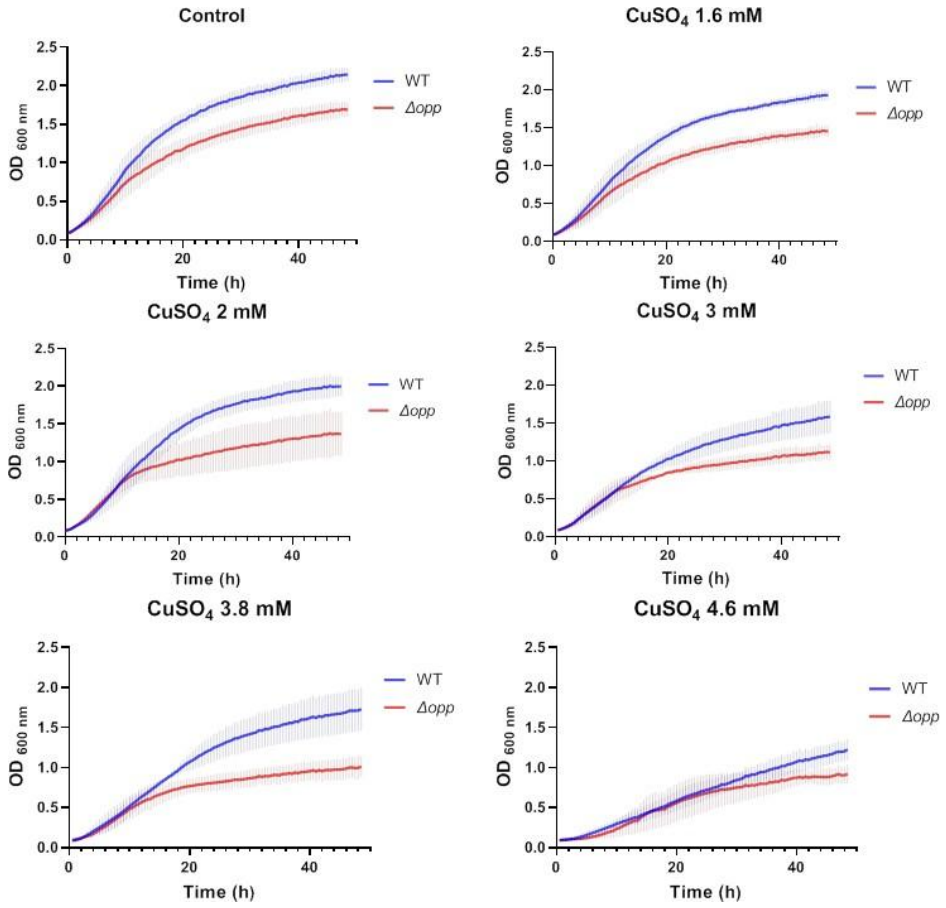

Figure 26. **Effect of *opp* deletion on the growth curves of *B. abortus* 544 in the presence of Cu.** WT and *Δopp* strains were grown in TSB medium containing 1.6, 2, 3, 3.8 or 4.6 mM of $CuSO_4$. Overnight cultures of strains grown in TSB were diluted to optical density (OD) of 0.1. During growth, OD at 600 nm was measured every 30 minutes for 48 hours. Data are representative of results of biological triplicates.

applied with the *Δopp* mutant. Disk diffusion assay with 2 and 4 M of $CuCl_2$ did not illustrate a clear Cu sensitivity in *Δopp* compared to the WT (Figure 25). Concerning 2 M, inhibition zone difference between WT and *Δopp* is qualified as statistically different *via* a *t* test analysis (*, $P<0.05$) but at 4 M a *t* test is qualifying the difference between WT and *Δopp* as non-significant (ns, *P*; 0.15). On solid medium, *Δopp* mutant growth is not impacted by Cu presence at 1.6 and 2 mM (data not shown). To confirm this Cu insensibility growth curves were measured during 48 hours in the presence of 1.6 and 2 Mm of $CuSO_4$. Compared to WT, *Δopp* growth is slightly lower. However, its growth in control condition (TSB medium) is already inferior to that of the WT (Figure 26). Cu sensitivity cannot be spotlighted. Then higher concentrations were added; 3, 3.8 and 4.6 mM, as the ones used for WT Cu resistance (Figure 26). The increase in copper concentration does not seem to affect the growth of the bacteria *Δopp* compared to the WT. These results indicate that this mutant is not sensitive to Cu as the *his* mutants were.

At the end of our histidine enrichment list, a multicopper oxidase, called CueO was found. As described below (see Introduction, 3.3 About Cu), few proteins involved in Cu homeostasis have been identified in *Brucella spp.*, and these include CueO. To study Cu homeostasis in our mutants deeper and to learn more how *B. abortus* deals with this heavy metal, *ΔcueO* but also *ΔcopA*, the inner membrane ATPase were constructed. As the experiments highlighted a Cu sensitivity in our auxotroph mutants for histidine, the same experiments with the same conditions were repeated with the two new mutants. In the same order than in the beginning of this point, disk diffusion assay was done with *ΔcopA* and *ΔcueO* mutants. The disks were soaked with 2 and 4 M of $CuCl_2$ for at least 1 hour before being placed in the center of dishes where strains were plated. As for the first time, diameters of inhibition zone were measured and reported in a graph. In contrast with the *his* mutants, results did not illustrate any clear difference between WT and *ΔcueO* and *ΔcopA* and a Cu sensitivity could not be observed (Figure 27). ANOVA with Dunnett's test were carried out and confirmed the absence of Cu sensitivity in the two mutants tested by a non-significant difference compared to the WT.

The second experiment was growth curves in the presence of 1.6 and 2 mM. Again, opposite to results obtained with *his* mutants, no Cu sensitivity was illustrated in these two mutants. It could be possible that the loss of these two genes is only illustrated when the bacterium is faced with a high concentration of Cu, such as the one used to illustrate the tolerance of the WT and the *ΔhutH* mutant. Then 3, 3.8 and 4.6 mM of copper were added to liquid medium (Figure 28). Even with higher copper concentrations, *copA* and *cueO* mutants did not present Cu sensitivity. The variation between biological triplicates was large.

The last experiment carried out was the growth on solid medium containing copper. AT 1.6 and 2 mM concentration, no difference between WT and mutants growth was observed. Then higher concentration were added; 3 and 3.5 mM (data not shown). Even there, no significative difference was observed. These results and the ones from the two first experiments are indicating that *copA* and *cueO* deletion do not cause any detectable Cu sensitivity compared to the one observed with our histidine mutants.

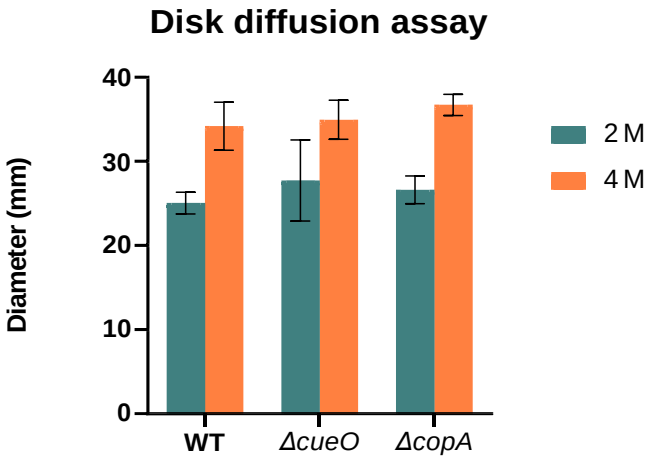

Figure 27. **Cu sensitivity of WT, *ΔcueO* and *ΔcopA* strains**. Hundred µl of an overnight culture of each *B. abortus* strain was spread out on TSB plates where a disk soaked with 2 or 4 M of $CuCl_2$ solution was placed in the middle. Inhibition zones were measured (mm) and reported in a histogram. Statistical analysis was carried out by an ANOVA with Scheffe Post Hoc test (*, $P<0.05$). No statistical significance was determined.

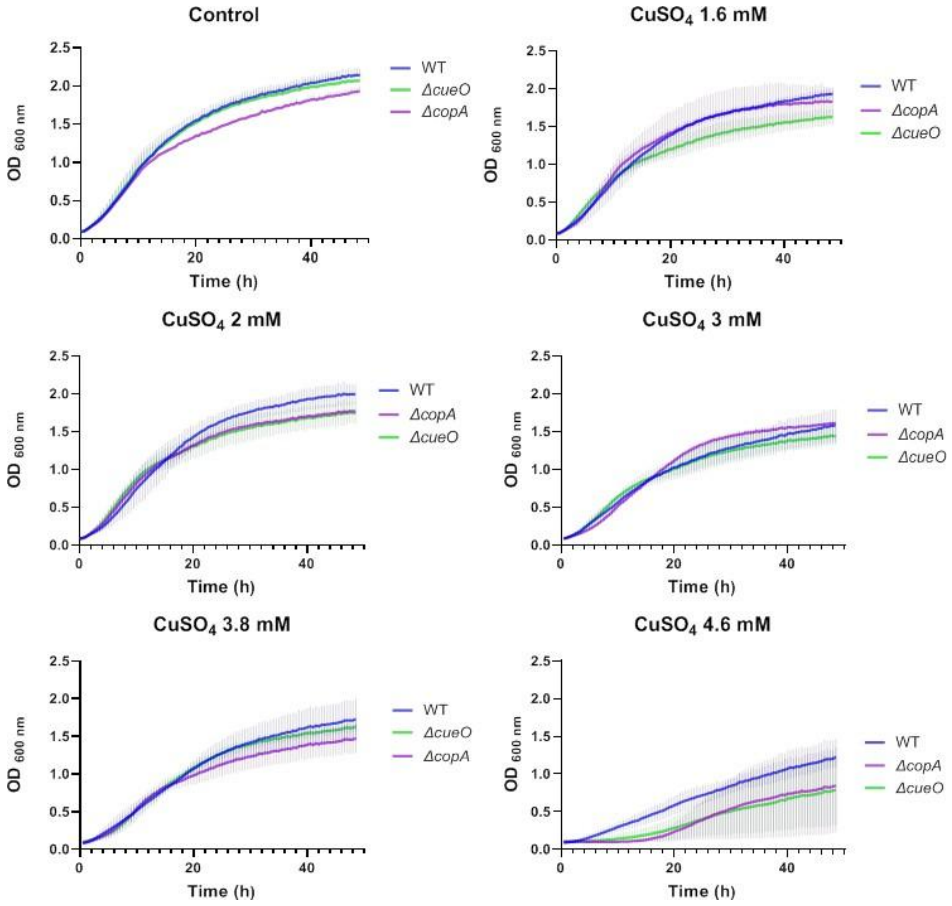

Figure 28. **Effect of *cueO* and *copA* deletion on the growth curves of *B. abortus* 544 in the presence of Cu.** WT, *ΔcueO* and *ΔcopA* strains were grown in TSB medium containing 1.6 or 2 mM of $CuSO_4$. Overnight cultures of strains grown in TSB were diluted to optical density (OD) of 0.1. During growth, OD at 600 nm was measured every 30 minutes for 48 hours. Data are representative of results of biological triplicates.

DISCUSSION

1 The role of histidine in metal homeostasis

Metal ions are important for the various mechanisms taking place in every organism. In particular, during intracellular infection, host cells will use various mechanisms to deprive or intoxicate the pathogen with metal ions [17,38,39]. It is therefore interesting to study the homeostasis of certain metals in *Brucella* in order to better understand how the pathogen deals with them.

The results of our bioinformatics analysis of the *B. abortus* proteome and growth experiments showed that histidine is a frequent residue in proteins involved in metal homeostasis but also in proteins requiring metal ions for their proper function (Table S1, see Results, 3 Copper sensitivity). In addition, free histidine is also able to coordinate various metal ions [18].

As explained in the Introduction, our *his* mutants are histidine auxotrophs. To cultivate our *his* mutants, it is imperative to have histidine in the medium to allow their growth. The medium used in each experiment is TSB, a rich medium for which the exact composition is unknown, meaning that histidine concentration (either free histidine or peptides containing histidine) is not quantified. Therefore it seems to be necessary to measure histidine concentration in the extracellular environment but also free histidine concentration in the WT which present an intact His biosynthetic pathway. The quantification would allow the determination of histidine produced in the cell and to what extent the histidine present in the environment influences the results obtained in our different mutants through the different experiments. This quantification can be performed by mass spectrometry. On the other hand, it would be interesting to establish a minimal medium, containing the minimal concentration of histidine allowing the WT-like growth of our mutants. In this way, the results would be more accurate, unbiased by the presence of histidine in the medium and the Cu sensitivity observed could be exacerbated. Similarly to histidine, it is important to quantify the intracellular concentration of free Cu in our mutants, suppressors and WT and to compare the concentrations with each other to explore the ability of each strain to detoxify copper. This Cu quantification can be performed using ICP-OES (Inductively Coupled Plasma-Optical Emission Spectrometry).

1.1 Do histidine levels protect against metal toxicity?

The role of histidine in protecting against the toxicity of Zn and Ni was investigated in *Caenorhabditis elegans*. Unlike *B. abortus*, *C. elegans* is not able to synthesize histidine and must find it in its food, in other words it is a histidine auxotroph. Mutations affecting negatively the histidine ammonia lyase (HALY-1), the enzyme that degrades histidine, appeared to confer a strong resistance to Zn. The metal tolerance was not caused by an increase in the excretion or a decrease in the absorption of Zn, but rather because of an improved tolerance to the metal ion. The decrease in the function of the protein HALY-1, or even a total absence of it, results in a high level of histidine. The hypothesis is that the high concentration of $_{L}$-Histidine is responsible for Zn resistance in the worm. It was proved by an increase in metal tolerance as the proportion of histidine in the organism's diet increased. As with Zn, WT worms showed improved Ni resistance when histidine is supplemented in the medium. Histidine appears to confer a metal resistance by its ability to bind metal ions [77]. This hypothesis is perfectly consistent with the higher Cu sensibility in *ΔhisA*, *ΔhisB*, *ΔhisC* and *ΔhisD*, compared to the WT. Indeed, these mutants have shown a significant sensitivity to

Cu in both solid and liquid media (see Results, section 3,Figure 19-21). This Cu sensitivity is not present in the complemented strains, indicating that the deletion of genes involved in the histidine biosynthesis pathway is responsible for Cu sensitivity. Contrary to what has been done in *C. elegans*, here different enzymes of the histidine biosynthesis pathway have been deleted. These results support the hypothesis that histidine plays an important role in the resistance to metal ions. In addition, a strain deleted for ammonia lyase, HutH in *Brucella,* demonstrated a lack of sensitivity to Cu and a Cu tolerance similar to the one observed in WT. However, an increase in resistance compared to WT was not demonstrated in this present work. To go even further, a strain overexpressing *hutH* has been built in a WT and *ΔhisB* background. In view of the results obtained in *C. elegans*, where the mutation of the *hutH* homolog (HALY-1) confers a better tolerance to metals, it would have been expected to observe an increased Cu sensitivity in the WT and in the *ΔhisB* mutant overexpressing the enzyme. However, no growth defect was observed in both mutants in presence of Cu in liquid medium (Figure S6). Because histidine degradation is highly controlled due to the high energy cost of its biosynthesis, it is possible that the bacteria prevent this overexpression or inactivate the overproduced enzyme. The *hutH* overexpression has not been checked here and it has to be noted that this experiment was performed only once. Thus the confirmation of *hutH* overexpression is needed and can be done through a reverse transcription followed by quantitative PCR to evaluate the mRNA abundance and through a Western Blot to identify HutH quantity in the mutant. Furthermore, biological triplicates have to be carried out to confirm the results obtained with *hutH* overexpression strains.

In addition to the sensitivity to Cu in our *his* mutants, the results also showed that *B. abortus* is able to tolerate large amounts of Cu. The growth of the WT and the *ΔhutH* mutant showed tolerance to Cu until 4.6 mM before showing a strong inability to replicate (Figure 22). Compared to *Caulobacter crescentus*, where WT shows growth defects at 225 µM (P. Cherry, personal communication), *B. abortus* is therefore 20-fold more resistant to Cu. This Cu resistance could be linked to the pathogenic lifestyle of *Brucella.* As described in the Introduction (see Introduction, 2.3 Nutritional immunity), one of the strategies of host cells is to intoxicate the phagolysosome with high Cu concentrations through ATP7A relocalisation into the phagolysosome membrane [39,44]. Due to the pathogenic nature, testing the impact of Cu sensitivity *in vivo* in macrophages and mice would be judicious. Moreover, initial data have shown that *his* mutants replicate less in a HeLa or RAW 264.7 cell model. Because of its key role in Cu transport within the phagolysosome [39,44], the infection of macrophages that do not express the *ATP7A* gene by *his* mutants could be interesting. This infection experiment would allow to study the *his* mutants replication inside cells and to potentially observe an improved replication when ATP7A is not expressed, confirming that the replication defect in the *his* mutants in macrophage in normal condition is due to Cu sensitivity. In addition, a Cu-specific fluorescent probe could be used to visualize a potential co-localisation between bacteria and Cu within phagolysosome. One thing that has not yet been tested is infection in mice and study the virulence of the different *his* mutants, this model of infection would complement the potential results of an infection in a cellular model.

The present work was only interested in Cu toxicity, however some questions remain about the toxicity of other metals and if the *his* mutants present a sensitivity similar to that observed for Cu. Various studies have highlighted the ability of histidine to bind to other metals such as Zn or Ni [18]. In *C. elegans*, histidine confers tolerance to Zn and Ni in the presence of high His concentrations [77]. To test the hypothesis that histidine has a major role in the homeostasis of other metals in general in *B. abortus*, the same experiments performed with Cu could be carried out with metals similar to Cu in terms of structure and redox potential but also with

metals characterised as non-redox such as Zn. Therefore, this would specify whether the sensitivity of *his* mutants is Cu specific, redox potential specific or general to transition metals.

1.2 Histidine, a possible metallophore?

Enteric bacteria have to face environment perturbations inside the host, including anaerobiosis and amino acid limitation. In *E. coli*, it was demonstrated that under these stresses, Cus system and CopA were induced. Individual amino acids were added to the growth medium and results highlighted the Cu^+-chelator function of methionine. Indeed, periplasmic Cu^+ concentration increased when methionine was absent and Cu sensitivity in *E. coli* when methionine biosynthesis is impaired, illustrating the importance that methionine and its biosynthesis could have to deal with Cu toxicity in *E. coli* [78].

For some human pathogens, Ni acquisition is critical for the colonization of the host [79,80]. Indeed, Ni is the co-factor of urease, which allow the pathogen to survive in acidic environment [79–81]. In bacteria, the Ni ABC-type importer is a high-affinity uptake system composed of an extracytoplasmic solute-binding protein (SBP) presents in the periplasm in Gram-negative bacteria and anchored to the membrane in Gram-positive bacteria, two nucleotide-binding proteins and two channel-forming transmembrane proteins [79–81]. SBP are able to bind a diversity of ligands and are the main determinant of the transport specificity [80].
A previous study showed an increased of Ni uptake in *E. coli* when $_L$-Histidine is added in minimal growth medium [82]. Similar results were obtained in *Staphylococcus aureus* [79]. The crystal structure of Ni-BP in *E. coli*, *Ec*NikA was investigated and the results demonstrated that Ni ion coordinated by two free $_L$-Histidines can be bound in the Ni-binding site of NikA. The bond between $Ni(_L\text{-His})_2$ and NikA happens through the Ni coordination by the imidazole ring of one histidine residue in the binding-site [83]. Therefore, Ni-BP from several bacteria have been studied, NikZ from *Campylobacter jejuni* (*Cj*NikZ), NikA from *Brucella suis* (*Bs*NikA), YntA from *Yersiniae pestis* (*Yp*YntA) and NikA from *S. aureus* (*Sa*NikA) [80]. As *Ec*NikA, *Bs*NikA and *Yp*YntA bound chelated Ni through a single protein-based histidine residue, while three histidine residues are required to bind Ni in *Cj*NikZ [80]. In *Sa*NikA, there is no direct contact with Ni ions. It is only interacting with the chelator agent, as the protein shows a high binding affinity for $Ni(_L\text{-His})_2$ [79,80]. The Ni-BP, *Bs*NikA, *Yp*YntA, *Cj*NikZ and *Sa*NikA appeared to be able to bind Ni-histidine complexes *in vitro* [80]. In *Helicobacter pylori*, it appeared that the Ni-BP CeuE present also an affinity to $Ni(_L\text{-His})_2$ [84]. Notwithstanding, the physiological function of Ni-histidine complexes as nickelophore has to be demonstrated in these bacteria [79,80,84]. In most bacteria, no putative gene coding for a nickelophore have been identified in the region of the Ni ABC-importer operon, suggesting that some bacteria may use nickelophores already present in the environment, such as free histidine [79].

According to the potential role of histidine as a metal chelator, it could be possible that histidine is excreted in the medium as Cu-chelator. The absence of a His biosynthesis pathway in our *his* mutants would explain the observed Cu sensitivity, by a defect in the ability to excrete free histidine. To investigate the potential role of histidine as a Cu-chelator agent, a chrome azurol S (CAS) agar plate assay, usually used for iron could be adapted in order to detect Cu-chelator production in *Brucella* strains. Indeed this test is based on competition principle between a chelator produced by bacteria and the ferric complex CAS, an indicator dye. The iron removal from CAS by the chelator lead to in a color change of CAS [85].

1.3 Histidine, a buffer for metals ions?

In the majority of living systems, Zn is the second most abundant transition metal and it is bound to structural or active sites in 5% of the bacterial proteome [17,40,69]. Transition metal ions, such as Zn, are crucial for a diversity of mechanisms and virulence factor among bacteria [32,38]. During infection, host cells use Zn sequestration by calprotectin protein (nutritional immunity), or Zn intoxication inside the phagolysosome *via* a yet uncharacterized pump to fight pathogen infection [17,32]. In response to Zn limitation, bacteria are modulating the expression of their ZnuABC import system [32,69,71,75,86]

In response to Zn limitation, *Acinetobacter baumannii* upregulates its high-affinity Zn importer ZnuABC and survival when Zn is limiting is impaired when *ZnuB* is deleted [87]. *A. baumannii* is a Gram-negative opportunistic pathogen responsible for ventilator-associated pneumonia [88]. Zur is a regulator not only of *znuABC* genes (see Introduction, box 1) but also other proteins involved in Zn homeostasis, including *zigA.* ZigA (Zur-induced GTPase A) is a Zn metallochaperone and appeared to be the most upregulated gene upon Zn limitation or loss of *zur* [89]. Interestingly, *zigA* is localized next to the *hut* operon, coding for the enzymes of the histidine degradation pathway. Therefore, a model in which the intracellular labile Zn pool could be buffered by free histidine has been proposed in *A. baumannii*. During Zn sequestration, the Hut system is upregulated, indicating that the Hut system is influenced by Zn levels in the cell. It appeared that HutH is binding Zn and under Zn starvation *ΔhutH* present growth defect, illustrating the link between HutH activity and Zn homeostasis. The model proposed in *A. baumannii* is such that when Zn levels are low, HutH is degrading histidine, allowing Zn release from histidine, giving access to the Zn pool for Zn-dependent proteins. $_{L}$-histidine levels increased in *ΔzigA*, indicating that ZigA could activate HutH. This way, *A. baumannii* is able to replicate under low Zn conditions. The *hutT* gene, coding for the main histidine transporter HutT, is localized in the *hut* operon. When HutT is defective, *A. baumannii* appeared to be less resistant to Zn toxicity. HutT is also able to transport Zn-complexed histidine, meaning that HutT can impact *A. baumannii* adaptation to Zn starvation. In this model, Zn toxicity is prevented by histidine buffer action inside the cells [90]. Metal homeostasis is impacted by the coordination of Zn into exchange-labile complexes by free histidine [77].

In *B. abortus, znuA* is upregulated in Zn-limiting environment, indicating that *znuA* expression is sensitive to Zn^{2+} levels [75]. Previous studies reported a growth defect of *B. abortus ΔznuA* in Zn-low condition and the inability of this mutant to replicate inside HeLa cells, macrophages and BALB/c mice [86,91]. This decreased replication illustrates the role of Zn import system for *B. abortus* virulence [53,86,91]. The growth defects observed were rescued by Zn addition in the medium [86,91]. Actually, the role of ZnuB and ZnuC in Zn import are not described empirically, nevertheless they are necessary for Zn uptake in *Brucella* [53]. One of our hypotheses is that the ZnuABC uptake system was defective in our *his* mutants due to the interrupted histidine biosynthesis pathway. As a reminder, ZnuA and ZnuC were some of the most histidine-enriched proteins of *B. abortus* based on the bioinformatic analysis (Table S1). With the results of previous studies [75,86,89,91], the histidine buffering Zn model [90] and the presence of a ZigA homologue in *Brucella* (the *zigA* gene is also located near the *hut* operon in *Brucella*), we proposed the hypothesis that our *his* mutants could possibly present a growth defect when Zn levels are low in the environment. However, when TPEN, a zinc specific chelator, was added to the medium at final concentration of 10 and 20 µM, our mutants did not present any growth defect and any difference with the WT strain (Figure 9). When TPEN concentration reached 30 µM, none of the strains (WT or *his* mutants) were able to growth unless $ZnSO_4$ was supplemented to the medium (Figure 10). In addition, when EDTA was

added at final concentration of 0.5 and 0.75 mM, intermediate growth of our *his* mutants were observed (Figure 11). When the concentration is increased to 1 and 1.5 mM, again complete growth inhibition was observed in the mutant strains (Figure 12-13). Similarly with TPEN, strain growth was rescued when ion metal was supplemented to the medium (Fe, Mg, Mn or Zn) (Figure 12-13). This sensitivity of WT, *ΔhisA*, *ΔhisB* and *ΔhisD* to TPEN was also observed in liquid medium (Figure 14), as well as EDTA sensitivity for WT (Figure 17). This replication defect in WT is not correlated to the results were WT was described as slightly or no sensitive to EDTA [91]. Our results demonstrated that WT and mutants strains are not able to grow when medium is metal depleted and showed that bacterial replication can be rescued when metal ions are added to the medium by bypassing chelator action. However, at this stage, it is not possible to determine if the ZnuA, ZnuC and Zur are defective in our mutants.

To further investigate the hypothesis where the Zn uptake system is faulty in our *his* mutants, mutants overexpressing *znuABC* genes have been constructed in a WT and *ΔhisB* background. WT-*Znu*$^{+++}$ and *ΔhisB*-*Znu*$^{+++}$ presented a total growth inhibition in presence of 30 µM of TPEN (Figure 15) and 1 mM of EDTA (Figure 16) on solid medium. Growth was rescued by the addition of different metals, Zn, Cu, Fe, and Mn, at equivalent concentration as the chelating agent (Figure 15-16, Figure S4). Surprisingly, Mg addition did not rescue completely bacterial replication (Figure 16). The *ΔhisB*-*Znu*$^{+++}$ strain presented a lower replication when Cu is added (Figure S4), maybe due to the toxic nature of Cu since *ΔhisB* is more sensitive to Cu than the WT. In addition to solid medium, the growth defect in these three strains was also displayed in liquid medium when the chelator is present (Figure 17). The overexpression attempt of the *znuABC* genes did not bypass the action of the chelator to rescue the growth of bacteria. However, the overproduction of the system has not been proven, it may be not occurring.

Before going any further, biological triplicates need to be carried out to confirm these preliminary results. Then, the concentration range tested for TPEN or EDTA showed that growth is quickly inhibited by the chelator, even for the WT strain. This drastic change indicates that the effect of chelators is not gradual and thus it could be that the concentrations were overestimated, and would require more precise calibration in future experiments. The growth rescues for the different strains when adding different metal ions illustrate the necessity of metals for the survival and growth of the bacteria. Moreover, it would be interesting to directly investigate if the production of ZnuA, ZnuC and Zur is impaired in our *his* mutants and if the *znuABC* expression is raised in our *ZnuABC* "overexpression" mutants. To test the overexpression in our *Znu*$^{+++}$ mutants, a reverse transcription followed by quantitative PCR could be carried out, giving a quantification of the mRNA levels. In addition, proteins levels can be estimated by doing Western Blots. Then, mRNA levels should be higher and the bands in Western Blot more intense than in the WT. Since the hypothesis is that *znuA*, *znuC* and *zur* are defective in our mutants, the band in Western Blot would be less intense than in the WT, used as control.

In the histidine buffer model, the importance of HutT is also pointed, suggesting that the transport is part of the metal tolerance process of the histidine [90]. Another way to illustrate the importance of histidine in the Cu homeostasis is to prevent it from entering the cell. In *Brucella*, *hutT* gene is not localized in the *hut* operon but near to VirB system. By deleting the histidine transporter in the WT, it would allow to determinate if the intracellular histidine pool is enough to counteract Cu toxicity or if bacteria need to import histidine from the environment to face this metal. In order words, *hutT* deletion in our *his* mutants should be lethal since they would no longer have access to histidine, unless unless other transporters exist bringing in free histidine or peptides containing histidine residues.

2 Histidine: first-line for Cu homeostasis in *Brucella*?

In bacteria such as *E. coli* and *S. enterica*, CueO with its multicopper oxidase activity is involved in Cu tolerance by oxidizing Cu^{+} into Cu^{2+}. Cu tolerance mechanisms used by *Brucella* are not characterized yet [53]. Only one study investigated experimentally the role of CueO, designated as *Brucella* multicopper oxidase (BmcO) in *Brucella melitensis* 16M [67]. BmcO was identified in our histidine enrichment list (Table S1), suggesting that it could be impacted in our *his* mutants. The Cu-binding sites in BmcO are histidine-rich and are common among different bacteria such as *E. coli, S.* Typhimurium, or *M. tuberculosis* [67]. This observation could explain the presence of CueO in our histidine enrichment list and link the structure of the Cu-binding sites with the ability of histidine to coordinate with Cu ions. In the presence of Cu, BmcO expression is upregulated in a dose-dependent manner [67]. To confirm BmcO function in Cu tolerance in *B. melitensis*, *Δbmco* mutant growth was studied by serial dilution on TSB medium containing $CuCl_2$ at different concentrations. *ΔbmcO* appears to be highly sensitive to Cu compared to WT and complemented strain [67]. Nevertheless, Bmco was recognized as not essential for intracellular growth of the bacteria [67].

In contrast to the study carried out with *B. melitensis*, the *ΔcueO* mutant constructed in *B. abortus* in the present work did not show a higher Cu sensitivity compared to the WT, whether in liquid medium (Figure 28), with disk diffusion assays (Figure 27) or growth on Cu-containing plates. Similar results were obtained for a *ΔcopA* deletion mutant (Figure 27-28), which was also as tolerant to Cu as the WT. The results obtained with these two mutants, *ΔcueO* and *ΔcopA,* also are in contradiction to what was shown in *E. coli* and *S.* Typhimurium. Indeed, the deletion of *copA* and *cueO* leads to a higher Cu sensitivity compared to WT in *E. coli*. This sensitivity was increased for *ΔcopA* under anaerobic conditions [24,33,92]. This sensitivity to Cu due to the loss of *copA* is also observed in *S.* Typhimurium [35,92]. Similarly, the loss of *cueO* increases the sensitivity to copper and this sensitivity is exacerbated in anaerobic conditions [36,92]. Where CopA and CueO seem to be the first system involved in Cu homeostasis in *E. coli* and *S.* Typhimurium, this system seems not to be used by *Brucella* as a first strategy to deal with Cu toxicity. Indeed, our *his* mutants have demonstrated to be more sensitive to Cu than the WT, opposite to *ΔcueO* and *ΔcopA*. These results suggest that, at least in our laboratory conditions, it is more advantageous for *Brucella* to have a sufficient histidine pool rather than a detoxification system as in *E. coli* and *S.* Typhimurium. This hypothesis can be supported by the previously mentioned studies where the role of histidine in the resistance to metal ions is highlighted whether it is within a protein allowing metal coordination, by a chelating function in the environment or an intracellular buffering action [21,77,79,80,83,90]. Therefore, measuring the intracellular concentration of free histidine would be interesting.

3 Opp, a solution to face Cu toxicity?

Opp is an ATP-binding cassette (ABC) transporter and is involved in the transport of oligopeptides into the cell. Opp is composed of 5 subunits; a substrate-binding protein, two transmembrane proteins constituting the pore through which transport occurs and the substrate is shuttled across the membrane *via* two nucleotide binding proteins that provide the energy by binding and hydrolysis of ATP [93,94]. ABC transporters possess a huge variety of substrates [94,95]. The *opp* genes are generally organised in operon, *oppABCDF* [96,97].

The growth experiments on Cu-containing plates unexpectedly led to the generation of suppressors, mutant bacteria that have acquired compensatory mutations to tolerate Cu and

that allow them to grow despite their initial mutation. Among all these mutations, a dozen appeared in the *opp* operon, and more particularly in the two periplasmic substrate-binding proteins $OppA_1$ and $OppA_2$ (Table 3). A preliminary study of the expression of $oppA_1$ and $oppA_2$ was carried out in C6, the suppressor showing a mutation in the potential promoter region. The abundance of mRNA in C6 for both genes was compared to the mRNA abundance in *ΔhisC*, the reference mutant in this case. The results have indicated a 5-fold increase of $oppA_1$ and $oppA_2$ mRNA in C6 compared to *ΔhisC* (Figure 24). The mRNA abundance of $oppA_1$ and $oppA_2$ in *ΔhisC* was also compared to the mRNA abundance in WT. The results showed a slight increase in the mRNA abundance in *ΔhisC*, which could be a compensation for *hisC* mutation (Figure 24). Before going further, these preliminary results need to be confirmed by performing biological triplicates. Nevertheless, the question remains, how do the mutations in $oppA_1$ and $oppA_2$ lead to a phenotype of Cu tolerance in our suppressors?

In plants, peptide transport can be mediated by three different transporter families: the oligopeptide transporters (OPT) family, the peptide transporter (PTR) superfamily and ABC family. The OPTs are divided into two classes, the oligopeptide transporter (PT) and the Yellow Stripe-like (YSL) clades. OPTs are able to transport three categories of substrates, small peptides (three to five residues), metal-complexed secondary amino acids, as phytosiderophores, and glutathione [95,98]. These two clades are involved in metal-chelate transport, heavy metal sequestration, nitrogen mobilization, *etc* [98]. In *Arabidopsis thaliana*, *At*OPT3 was identified as Fe transporter where its expression is induced by Fe deficit. If histidine is present in growth medium, Fe-histidine complexes can be transported *via* OPT3 [98]. In addition, *At*YSL2 is able to shuttle Cu-complexed chelator. Its expression is repressed by Cu excess and Fe limitation, suggesting that *At*YSL2 play a role in the preservation of homeostasis for both metals [95]. In plants and fungi, OPTs are also able to transport glutathione, which is playing a role against heavy metal toxicity [22,98].

In bacteria, the major function of Opp seems to be the transport of peptides, used as nitrogen and carbon source [99]. In *Bacillus subtilis* and *Enterococcus faecalis*, Opp transports signalling peptide into the cell, the Phr peptides, which are regulating the activity of an aspartyl-phosphate phosphatase protein, and mating pheromones, being part of quorum sensing process [99]. In *Rhizobium etli*, a Gram-negative bacterium living in the soil and able to be in symbiosis with its host, *Phaseolus vulgaris*, an *opt* mutant was identified with a lower nitrogen fixation capacity [93]. The *optA* and *optB* mutants present growth defects when oligopeptides are used as the sole nitrogen source confirming that Opt system is involved in peptides import and illustrating its importance during symbiosis. The *opt* mutants also present resistance to bacitracin, a cyclic oligopeptide antibiotic. It is possible that the resistance to this antibiotic is due to the absence of its uptake through the Opt system [93]. In *E. coli*, Opp is involved in cell wall turnover process [100]. In *S. aureus*, the four Opp systems present several roles such as nutritional function or virulence [96]. *Chlamydia. trachomatis* is using Opp to import the amino acids that it is not able to synthesize, including histidine. Moreover, this bacterium possesses two additional genes encoding *oppA* [101]. Another function of Opp is peptidoglycan recycling in *C. trachomatis, E. coli, Listeria monocytogenes* and *Neisseria gonorrhoeae* [100,101]. Peptidoglycan recycling can be strategic for survival inside the host for pathogens. Firstly, the precursors of peptidoglycans are not found in the host and therefore it conserves the energy related to its endogenous production. Secondly, it limits the release of immunogenic fragments that would stimulate the host immune system, so it can be characterized as a pathoadaptation [101]. The operon expression can be modulated by environmental conditions, for example, in *E. coli* and in *Lactococcus lactis*, *oppA* expression is regulated by alanine and leucine and by branched-chain amino acid respectively [96,97]. In the

genome of *B. abortus* there are at least eight *opp* operons, illustrating the strong redundancy in *Brucella*. It is striking that only one *opp* operon has been affected by the mutations found in the suppressors, indicating its specific importance in Cu tolerance.

As all the studies reported, Opp is involved in a huge diversity of mechanisms: quorum sensing, symbiosis, nutrition, metals homeostasis, cell wall recycling [93,95,96,98,99,101]. First and foremost, it is imperative to confirm the suppressor phenotype in order to prove that all mutations appearing in the *opp* operon are linked to Cu pressure on bacteria. Growth experiments such as those achieved with *his* mutants could be performed to verify if indeed our suppressors are able to tolerate Cu compared to *his* mutants. To go further in confirming the suppressor phenotype, the different mutations could be incorporated in our *his* mutants and verify that the tolerance of Cu is enhanced resulting in growth raised on solid and liquid media. With all these described functions and the results obtained in this work, several hypotheses can be formulated.

First, $oppA_1$ and $oppA_2$ mRNA abundance seemed to be upregulated, at least in one of our suppressors (C6,Figure 24). This overexpression could lead to an indirect increase in the transport of peptides containing histidine residues. Consistent with the hypothesis of His buffer for intracellular Cu, peptides transport would be improved and the histidine residues contained in these peptides would allow counteracting the toxicity of Cu. To confirm that it is indeed $OppA_1$ and $OppA_2$ that are involved in this suppressor phenotype, different mutants in our suppressors should be constructed. A mutant in which $OppA_1$ is deleted and another in which $OppA_2$ is deleted would allow the identification whether the overexpression of both is necessary for Cu tolerance or whether only one of the two enzymes plays this suppressive role observed in the suppressors. Then Cu sensitivity should enhance when the suppressor phenotype is suppressed. Another possibility is to introduced either the two OppA proteins or the second part of the *opp* operon in a multicopy plasmid and incorporated this plasmid within the *his* mutants and observe if a function gain effect occur or not. That way it can be determined whether the suppressor phenotype is due to the first two proteins of the operon or to the remaining proteins of the operon.

Secondly, the deletion of the complete *opp* operon is not increasing Cu sensitivity as might be expected with the model where one of the OppA proteins is helping to Cu tolerance in our suppressors (Figure 25-26). However, it is possible that $OppA_{1\text{-}2}$ may only be beneficial for Cu tolerance in bacteria that are already experiencing difficulties. The relatively Cu tolerance in *Δopp* may also be due to the fact that the histidine synthesis pathway is intact. Therefore, as long as histidine is present and putatively playing its protective role against Cu, modulating the expression of *oppA* genes is not necessary for the bacteria. In order to confirm or refute this hypothesis, a double *Δhis Δopp* mutant would be necessary in order to observe whether the presence of the two mutations induces an increase of Cu sensitivity.

Thirdly, one of the mutations identified in the suppressors (B10) is leading to a stop codon in the $oppA_1$ gene (Table3), inducing an early stop of its translation. In the hypothesis where the two OppA proteins do not have the same substrate-binding properties, it is possible that one may be more beneficial than the other for Cu tolerance. Given that the stop mutation appeared in $OppA_1$, $OppA_1$ could have a negative impact on Cu tolerance unlike $OppA_2$ which could be more advantageous for bacteria. It is possible to imagine that $OppA_2$ could be beneficial by importing only naked peptides, containing histidine residues while $OppA_1$ would import chelated Cu. Indeed, it was demonstrated that NikA from *E. coli*, binding Ni-chelator complex shared 35% of homology with OppA in the structure [96]. However, this remains a speculation. The structure of the two OppA proteins as well as the location of the mutations in their

structure should be analysed in order to better understand how the mutations are giving an advantage to face Cu toxicity. Then, *in silico* analysis of the OppA structures needs to be carried out and identify the position where the mutations occurred in the different suppressors, in order to potentially identify specific parts touched by the mutations such as the binding domain of the substrate.

CONCLUSION

The present work focused on the ability of *B. abortus* to tolerate Cu and the potential mechanisms put in place, all in a context where histidine biosynthesis is defective. Our bioinformatic analysis confirmed that a link between histidine and metals exists. The various experiments carried out during this work supported this link by highlighting a Cu sensitivity when histidine biosynthesis pathway is incomplete, as in our *his* mutants. However, the results suggest that *B. abortus*, unlike other bacteria, does not seem to use the usual Cu detoxification systems leading to the hypothesis where histidine could be a first-line to tolerate Cu toxicity in the bacteria. Most interestingly, the suppressors obtained demonstrated that the *opp* operon also has a role in the response to Cu toxicity. Indeed, it could be a way for the bacteria to escape the toxicity when histidine is not produced. In the future, it would be interesting to confirm the role of histidine in Cu homeostasis and to further characterize the mechanisms used by *B. abortus* to deal with Cu. Overall, it would provide a better understanding of the physiology of *B. abortus* but also of its response to the environment.

MATERIALS AND METHODS

Bacterial strains and growth conditions

All *Escherichia coli* strains used during the thesis were grown in Luria-Bertani (LB) medium. Two different strains were used: DH10B *E. coli* for plasmid constructions and S17-1 *E .coli*, a conjugative strain, for the mating with *Brucella.* The strain of *Brucella* used in our experiment is *B. abortus* 544 and was cultivated in Tryptic Soy Broth (TSB) rich medium.

Depending on the plasmid used for constructions, different antibiotics were used at the following concentrations: ampicillin (100 µg/ml), chloramphenicol (20 µg/ml), kanamycin (50 µg/ml), nalidixic acid (25 µg/ml).

Plasmids and constructions

Primers sequences used are detailed in Table 4.

Table 4. **Primers used in this work.**

Name	**5'-3' Sequence**
F-znuACB-Sma1	TCCCCCGGGCGTCGAAAACCAGCGTCTG
R-znuACB-Xba1	CTAGTCTAGACCACGGAAAGGGAGCAAGAG
F1-copA-bis	CCCTATCGGTGATTGGGTC
R1-copA-bis	GCTCAGAACGCATGGCAATCCCTTTCGTG
F2-copA-bis	GATTGCCATGCGTTCTGAGCAATGCCTTG
R2-copA	GAAGCGAACAGGTCGAAC
F1-cueO	GTGAAAGGGGGCTTTCTC
R1-cueO	AAACGGTCACGGCGGGTAATTCCAGTCATG
F2-cueO	ATTACCCGCCGTGACCGTTTGAGAGCAAGG
R2-cueO	AAGAGCCGGTACGATCTTGC
F1-hutT-new	TTTACCCAGACCGGCTTCG
R1-hutT-new	CGGGCTTCATGCAAGCGCCTCTTATGTTGG
F2-hutT-new	AGGCGCTTGCATGAAGCCCGCCATTTGG
R2-hutT-new	CGATACGGCATCGGATTGC
F-hutH-XhoI	CCGCTCGAGTAACCGCACGTCCGAATGG
R-hutH-XbaI	CTAGTCTAGATTTCCCTGGCGGGTTTCAACG
F-check-LysK	TGACGGATAGTGGTTGCCG
R-check-LysK	CTGAGCCCCTTTCAGTTCC
F-check-LysR21	AGCCTTCCGGCAAAAGTGC
R-check-LysR21	AGGCTGCCTTCAAAACCGGC
F-check-amont-BAB2_0699	CGCCGCTTCACGATATAGC

R-check-BAB2_0699	**TGGGATCATCGTACCCTGC**
F-check-BAB2_0699-0700	GATTTCCTCGCCGATCAG
R-check-aval-BAB2_0700	ATCTTCGGAGCGTGTAGC
F-start-BAB2_0699	CTGATGGGCGTGTGTCTTCT
R-start-BAB2_0699	CGGTGGACGTGTGATGATGA
F-start-BAB2_0700	CGACACTGGATCAGCACCAT
R-start-BAB2_0700	ACCTTGCCGTCTTCCGAAAT

Table 5. **Strains used in this work.**

Name	**Strains**	**Antibiotic resistance**
pBBRMCS1-znuACB	DH10B	Cm
pNPTS-copA	DH10B	Kan
pNPTS-cueO	DH10B	Kan
pNPTS-hutT	DH10B	Kan
pBBRMCS1-hutH	DH10B	Cm
pBBRMCS1-znuACB	S17	Cm
pNPTS-copA	S17	Kan
pNPTS-cueO	S17	Kan
pNPTS-hutT	S17	Kan
pBBRMCS1-hutH	S17	Cm
ΔhisA	*B. abortus* 544	
ΔhisB	*B. abortus* 544	
hisBE17Q	*B. abortus* 544	
ΔhisC	*B. abortus* 544	
ΔhisD	*B. abortus* 544	
ΔhutH	*B. abortus* 544	
ΔhisA-pMR10-hisA	*B. abortus* 544	Kan
ΔhisB-pMR10-hisB	*B. abortus* 544	Kan
ΔhisC-pMR10-hisC	*B. abortus* 544	Kan
ΔhisD-pMR10-hisD	*B. abortus* 544	Kan
pBBRMCS1-znuACB	*B. abortus* 544	Cm
pBBRMCS1-znuACB	*B. abortus* 544 *ΔhisB*	Cm
ΔcopA	*B. abortus* 544	
ΔcueO	*B. abortus* 544	
ΔhutT	*B. abortus* 544	
pBBRMCS1-hutH	*B. abortus* 544	Cm
pBBRMCS1-hutH	*B. abortus* 544 *ΔhisB*	Cm
Δopp	*B. abortus* 544	

For Δ*copA*, Δ*cueO* and Δ*hutT* mutants, the whole gene was removed by homologous recombination. In order to do that, a joined PCR was applied. Two regions (one upstream and

one downstream of the target gene) of 500 – 600 base pairs were amplified using primer couple; F1/R1 for the upstream region and F2/R2 for the downstream region and this for each

deletion mutant. After, these two amplified fragments were fused together through a complementary region designed in the primers used and the 1000 base pairs region was amplified by PCR using F1and R2 primers. Afterwards, it was inserted in an *Eco*RV-linearized pNPTS plasmid and was cloned in DH10B *E. coli*. Then, the plasmid was purified and checked by sequencing thereafter. To perform an integrative conjugation, the plasmid was inserted in S17 *E. coli* and thus in *B. abortus* 544 WT by mating (see *Conjugaison*). Colonies obtained after the conjugaison were streaked on TSB plate containing Kan. From on streak, a bacterial culture was launched in liquid TSB and incubated at 37°C (without antibiotic allowing the loss of the plasmid). Then 100 µl of this culture were spread on TSB agar containing sucrose (5%) (allowing selection of bacteria which had excised the plasmid and lost selection marker). After 5 days of incubation, colonies formed were spread on two plates containing respectively kan and sucrose. To check the presence of insert, only bacteria which had grown on sucrose and not on antibiotic were selected and inactivated. The gene deletion was then controlled by PCR.

To construct *znuACB* and *hutH* overexpression mutants, the gene was amplified by regular PCR. For *znuACB* construction, the designed primers included restriction sites for *SmaI* and *XbaI* restriction enzymes. PCR product was purified and inserted by ligation into a pBBRMCS1 previously digest by *SmaI* and *XbaI*. The gene expression was under P_{lac} control. The final construction was transformed in DH10B *E. coli* before being inserted into S17 *E. coli*. Then, this overexpression plasmid was transferred into *B. abortus* 544 WT and *B. abortus ΔhisB* by mating. Concerning *hutH* overexpression, the same procedure was applied but restriction enzymes used were *XhoI* and *XbaI* in this case.

The different strains used in this work are summarized in Table 5.

Transformation in competent strains

The competent strains used during the thesis were *E. coli* DH10B and *E. coli* S17. The transformation is here a temperature shock transformation. The defined volume of DNA was added into 50 µl of bacterial culture. Bacteria were incubated on ice during 20 minutes and followed by a heat shock at 42°C during 1 minute, then, bacteria were putted back on ice during 2 minutes. After, 900 µl of LB medium were added in the culture and bacteria were putted at 37°C with agitation during at least 45 minutes. After the bacterial incubation, 100 µl of the supernatant were plated on LB agar petri dish containing the right antibiotic, IPTG and X-gal for blue screen. The rest of culture was centrifuged at 5,000 rpm for 3 minutes. 700 µl of supernatant was removed. The pellet was resuspended with the rest of supernatant (about 100µl) then plated on a second LB agar petri dish. Both plates were placed in incubator at 37°C overnight.

Conjugation

To perform the conjugation, overnight cultures of the conjugative *E. coli* S17-1 carrying the plasmid of interest and *B. abortus* 544 were grown at 37°C overnight. 50 µl of *E. coli* culture was added to 1 ml of *B. abortus* culture. The mix culture was then centrifuged at 7,000 rpm during 2,5 minutes. Supernatant was removed and 1ml of freshTSB medium was added to resuspend the bacterial pellet. Then, a second centrifugation was performed. After, the supernatant was partially removed; the pellet was resuspended with 100µl supernatant left and spotted on TSB-agar (without being too spread to increase conjugation likelihood). For a

replicative plasmid, such as pBBRMCS1, the conjugation drop was incubated at 37°C during 4 hours. For an integrative plasmid, such as pNPTS, the drop was incubated at for 24 hours. After the incubation period, bacteria were resuspended in 300 µl of TSB. 100 µl of the bacteria culture was spread on TSB agar supplemented with nalidixic acid (1 µg/ml) and kanamycin (10 µg/ml) or chloramphenicol (20 µg/ml) and incubated for 3 to 4 days at 37°C. Clones which integrated the plasmid containing the antibiotic resistance gene through homologous recombination were selected. Then, colonies formed were streaked on TSB agar with the appropriate antibiotic but without nalidixic acid.

Bioinformatic analysis

Proteome fasta file was downloaded from NCBI and submitted by Oak Ridge National Laboratory. The bioinformatic programme used was made by Damien Devos (CABD, Sevilla, Spain). It reads the fasta file and, for each protein sequence, counts the number of the amino acid histidine (represented by an H in the sequence). It also calculates the percentage of histidine in the sequence in order to illustrate the enrichment of proteins in histidine. An arbitrary threshold value of 5 % was established and proteins with a percentage equal to or greater than 5 are found in the table 2. Only 85 out of 2941 predicted proteins (thus 2.9%) have a proportion of His residues >5%.

Metal sensitivity experiments

Bioscreen

All *B. abortus* strains were grown in TSB at 37°C overnight. The next morning, OD of the bacterial culture was measured and cultures were diluted to obtain an optical density of 0.1 at 600 nm. Each well in 96-well plate contains a total volume of 200µl. According to programs used, bacterial growth was measured by reading OD_{600} every 10 minutes during 24h or every 30 minutes during 48 h (Bioscreen C MBR).

Spotting assays

For 10-fold serial dilutions, the different *B. abortus* strains used were grown in TSB at 37°C overnight. The next day, OD of cultures was measured and dilutions were carried out as to obtain an OD of 0.1 at 600 nm. 10-fold dilutions (from 10^{-1} to 10^{-8} in PBS) were prepared in a 96-well plate. A 20 µl drop of each dilution of the samples was spotted on TSB agar plate containing TPEN, EDTA, $ZnSO_4$, $FeSO_4$, $MnSO_4$, $MgSO_4$ or $CuSO_4$ at different concentrations. Plates were incubated at 37°C for 4 days and pictures were taken.

Solid medium

All *B. abortus* strains were grown in TSB at 37°C overnight. The next day, OD of the cultures was measured and dilutions were carried out as to obtain a DO of 0.1. TSB agar petri dish containing $CuSO_4$ at final concentration of 1.6 or 2 mM was divided by strains number. A volume of 20 µl for each bacterial culture was plated on copper plate. Afterwards, plates were placed in the incubator at 37°C for 4 days.

Disk diffusion assay

Brucella strains were grown in TSB medium at 37°C overnight. The day following, bacterial OD was measured and dilutions were achieved to normalize the OD at 0.1. 100µl of this culture was spread on TSB agar plates, and after cultures had dried, a sterile Whatman disk was placed in the center of the plate. Each disk was previously soaked with 2 or 4 M solution of $CuCl_2$ for one hour, and the plates were incubated at 37°C for 4 days. The diameter of the

inhibition zones around each disk was measured in three different ways and the mean was indicated in centimeters.

Suppressors

For all *Δhis* mutants, isolated colonies formed on 1.6 or 2 mM $CuSO_4$ plates after 4 to 5 days were restreacked on new TSB agar 1.6 and 2 mM $CuSO_4$ plates to confirm colonies formation and putative suppressive mutations leading to a suppressor's phenotype. A liquid culture for each suppressor was also launched at 37°C overnight. From these liquid cultures, a -80°C storage was carried out for each suppressors. In order to extract genomic DNA (gDNA), bacterial inactivation needed to be achieved first. In order to do that, bacterial cultures were centrifugated at 7,000 rpm for 5 minutes. After, supernatant were removed and bacterial pellets were resuspended in 300 µl of PBS. Then, bacteria were inactivated at 80°C during at least 1 hour. Afterwards, 100 µl of SDS 10% were added. The gDNA extraction was achieved following manufactural instructions of the Macherey-Nagel™ NucleoSpin™ Tissue Kit. Bacterial SNP sequencing was performed by BIO, part of Pathology and Genetics Institut (http://www.bio-be.be/biopharma-croservices/). SNP sequencing analysis was carried out on Galaxy.org (https://usegalaxy.org/) with Snippy tool.

Reverse transcription followed by quantitative PCR

Bacterial cultures (10 ml) were grown in TSB medium overnight at 37°C to reach exponential phase (OD 0.5- 0.8). Bacterial pellet was obtained by centrifugation and washed twice in sterile PBS, and lysed with 100µl of SDS 10% and 10 µl of Proteinase K. The resuspended pellet was placed in the incubator for 1 h at 37°C under agitation. RNA was extracted using TriPure isolation reagent according to the lab's protocol. RNA (2 µg) sample was treated with DNase I for 45 min at 37°C. DNase I was inactivated with EDTA 50 mM for 10 min at 65 °C. Then RNA was reverse transcribed with reverse transcriptase, haxamer random primers 10X, RT Buffer 10X and dNTPs 25X. In parallel a negative control was conducted without reverse transcriptase. cDNAs were amplified with specific primers (couple F/R-start, Table 3) and SybrGreen on a LightCycler 96 Instrument. Primer specificity was assessed with melting curves. mRNA fold change was calculated with $2^{-\Delta\Delta Ct}$ and GAPDH was used to normalized the results.

ANNEX

Table S1. **Histidine enrichment in *Brucella abortus* strain 2308 proteome.**

Tag	%[a,b]	Name	Functions
BAB1_0301	14.04	UreE	Nickel donor during urease metallocenter assembly
BAB1_1974	10.74	QueD	7-cyano-7-deazaguanine biosynthesis and purine metabolism
BAB_RS33715	10.53	Uncharacterized protein	Unknown
BAB_RS22295	9.68	CbtB	Cobalt transporter subunit
BAB2_0432	9.09	NikR	Transcriptional repressor of the nikABCDE operon
BAB_RS32835	9.09	Uncharacterized protein	Unknow
BAB2_0246	8.44	GTP-binding protein	Cobalamin synthesis
BAB2_1080	7.72	ZnuC	Energy coupling in ZnuABC zinc uptake transport system
BAB1_2027	7.69	BolA-like protein	DNA-binding regulator Stress-induced morphogen
BAB1_1818	7.37	Usg protein	Unknown
BAB2_0964	7.32	GAF/GGDEF domain protein	Diguanylate cyclase
BAB_RS33725	7.29	Uncharacterized protein	Unknown
BAB1_1173	7.19	LpxA	Lipid A biosynthesis
BAB1_0771	7.14	Zinc finger domain	Unknown
BAB1_0174	7.06	Lactoylglutathione lyase	Methylglyoxal detoxification
BAB2_0545	6.96	RibH2	Riboflavin biosynthesis
BAB1_1743	6.94	Uncharacterized protein	Unknown
BAB1_2036	6.92	GTP-binding protein	Cobalamin synthesis protein
BAB1_2175	6.90	Irr	Ferriv uptake regulation
BAB_RS25890	6.90	Uncharacterized protein	Unknown
BAB_RS21185	6.78	Uncharacterized protein	Unknown
BAB1_1754	6.78	YdcH family protein	Unknown

BAB1_1347	6.73	Serine hydrolase (ydeN)	Esterase activity
BAB_RS17660	6.56	Superoxyde dismutase	Superoxyde dismutase activity
BAB_RS22375	6.52	Serine hydrolase family protein	Esterase activity
BAB1_1991	6.45	Gamma-glutamylcyclotransferase	Glutathione catabolic process
BAB_RS17240	6.41	Uncharacterized protein	Unknown
BAB1_1668	6.38	Fur	Ferric uptake negative regulation
BAB1_1476	6.37	Alpha.beta hydrolase	Lipid transport and metabolism
BAB2_0535	6.36	SodC	Superoxide dismutase activity: radicals elimination
BAB2_1079	6.29	ZnuA	ZnuABC zinc uptake transport system
BAB_RS32250	6.25	Uncharacterized protein	Unknown
BAB2_1082	6.21	Zur	Fe2+ or Zn2+ uptake regulation
BAB1_0161	6.17	DUF1150 family protein	Unknown
BAB1_0497	6.16	CoxC Cytochrome c oxydase III	Aerobic electron transport chain
BAB1_0751	6.15	Uncharacterized protein	Unknown
BAB2_0644	5.91	Metal-dependant hydrolase	Hydrolase activity
BAB1_0714	5.88	Damage-inducible protein DinB	Unknown
BAB1_0518	5.85	MutY adenine glycosylase	Adenine glycosylase active on G-A mispairs
BAB1_0556	5.83	Uncharacterized protein	Unknown
BAB1_0042	5.79	Cytochrome o ubiquinol oxidase subunit IV	Electron transport
BAB1_1716	5.78	RuvC	Nuclease activity; Holliday junction intermediates resolution
BAB1_0456	5.70	Histone deacetylase family	Deacetylase activity
BAB1_1899	5.69	VOC family protein	Glyoxalase/Bleomycin resistance protein/dioxygenase
BAB1_1689	5.63	Uncharacterized protein	Unknown
BAB1_1732	5.63	2Fe-2S ferredoxins, iron-sulfur binding protein	Unknown
BAB1_1828	5.63	Uncharacterized protein	Unknown
BAB1_1189	5.57	Uncharacterized protein	Unknown
BAB2_0495	5.56	Uncharacterized protein	Unknown

BAB_RS22085	5.52	Uncharacterized protein	Unknown
BAB1_1001	5.48	Uncharacterized protein	Unknown
BAB1_1755	5.48	Uncharacterized protein	Unknown
BAB2_1068	5.48	Class II aldolase/adducin, N-terminal:ATP/GTP-binding site	Carbohydrate transport and metabolism
BAB2_1145	5.45	Sulfatase	Sulfuric ester hydrolase activity
BAB2_0505	5.44	Lectin-like protein BA14k	Immunoglobulin-binding and hemagglutination properties Virulence (LPS biosynthesis)
BAB2_0534	5.43	CueO	Copper oxidation
BAB2_1016	5.41	Universal stress protein (Usp)	Stress survival
BAB1_0814	5.38	Uncharacterized protein	Unknown
BAB1_0135	5.36	Uncharacterized protein	Unknown
BAB1_1617	5.35	Gfo/Idh/MocA family oxidoreductase	Dehydrogenase activity
BAB1_1581	5.33	Metallo-phosphoesterase	Hydrolase activity
BAB1_1297	5.32	DUF2218 domain-containing protein	Unknown
BAB1_1495	5.26	Antifreeze protein, type I	Subzero environments survival
BAB1_1904	5.26	GCN5-related N-acetyltransferase	Acetyltransferase activity
BAB1_0041	5.26	Cytochrome c oxidase, subunit III	Aerobic electron transport chain
BAB1_1568	5.26	Aspartyl/asparaginyl beta-hydroxylase	Unknown
BAB1_0573	5.23	Helix-turn-helix transcriptional regulator	Transcriptional regulator
BAB1_0856	5.19	BolA-like protein	DNA-binding regulator Stress-induced morphogen
BAB1_1666	5.19	Pseudouridine synthase	Pseudourine synthesis from uracil
BAB1_1284	5.18	Cold-shock DNA-binding domain	DNA binding in low temperature
BAB1_1277	5.16	PAS domain-containing protein	Unknown
BAB1_1219	5.15	DJ-1/PfpI family protein	Peptidase activity
BAB1_2161	5.15	TrmB	N(7)-methylguanine-tRNA biosynthesis
BAB1_1632	5.13	Uncharacterized protein	Unknown
BAB1_0085	5.13	YncA	Amino acid transport and metabolism

BAB2_0777	5.11	GntR family	DNA-binding transcriptional regulator
BAB2_0326	5.10	PurU	IMP biosynthesis via de novo pathway
BAB1_0926	5.10	AroQ	Chorismate biosynthesis
BAB1_0051	5.09	DUF1775 domain-containing protein	Unknown
BAB_RS33345	5.08	Uncharacterized protein	Unknown
BAB2_0897	5.08	Gfo/Idh/MocA family oxidoreductase	Dehydrogenase activity
BAB2_0170	5.06	YdcH family protein	Unknown
BAB1_1355	5.03	CREC-EF hand family protein	Calcium binding
BAB1_0961	5.00	Uncharacterized protein	Unknown
BAB2_0802	5.00	PIG-L family deacetylase	Deacetylase activity

Proteome fasta file was downloaded from NCBI and submitted by Oak Ridge National Laboratory. The bioinformatic programme used was made by Damien Devos (CABD, Sevilla, Spain). It reads the fasta file and, for each protein sequence, counts the number of the amino acid histidine (represented by an H in the sequence). It also calculates the percentage of histidine in the sequence in order to illustrate the enrichment of proteins in histidine.

[a] % indicates the percentage of histidine in the amino acid sequence of the protein.

[b] We have established an arbitrary threshold value of 5 %, proteins with a percentage equal to or greater than 5 are found in the table above. A minority of the protein has enrichment above 5 % and these proteins could be more strongly impacted by histidine starvation caused by mutations in the biosynthetic pathway. Only 85 out of 2941 predicted proteins (thus 2.9%) have a proportion of His residues >5%.

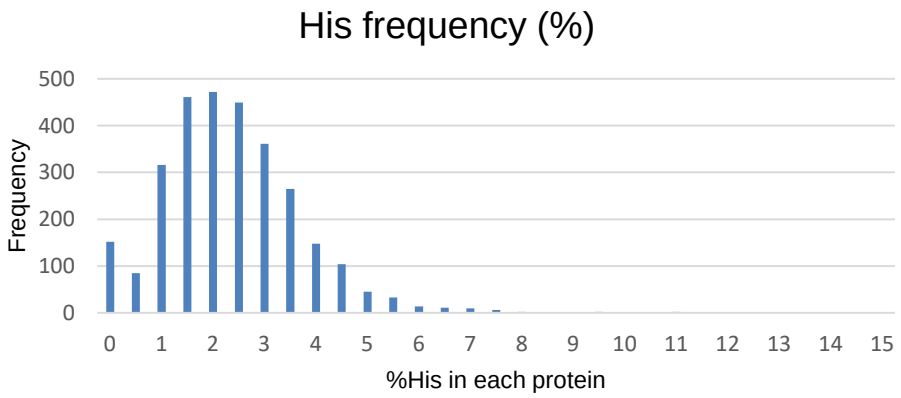

Figure S1. **Histidine frequency in the proteome of *B. abortus* 2308.** Histidine frequency in each protein in the *B. abortus* 2308 proteome was computed *via* a bioinformatic programme made by Damien Devos (CABD, Sevilla, Spain). For each protein sequence, it counts the number of the amino acid histidine (represented by an H in the sequence) and calculates the percentage of histidine in the sequence in order to illustrate the enrichment of proteins in histidine. An arbitrary threshold value of 5 % was established. Only 85 out of 2941 predicted proteins (thus 2.9%) have a proportion of His residues >5%.

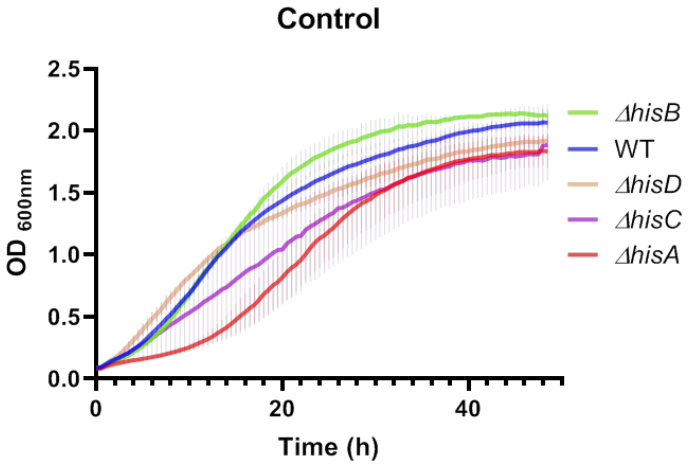

Figure S2. **Growth curves of *B. abortus* 544 in TSB medium.** WT and *his* mutants were grown in TSB medium. Overnight cultures of strains grown in TSB were diluted to optical density (OD) of 0.1. During growth, OD at 600 nm was measured every 30 minutes for 48 hours. Data are representative of results of biological triplicates.

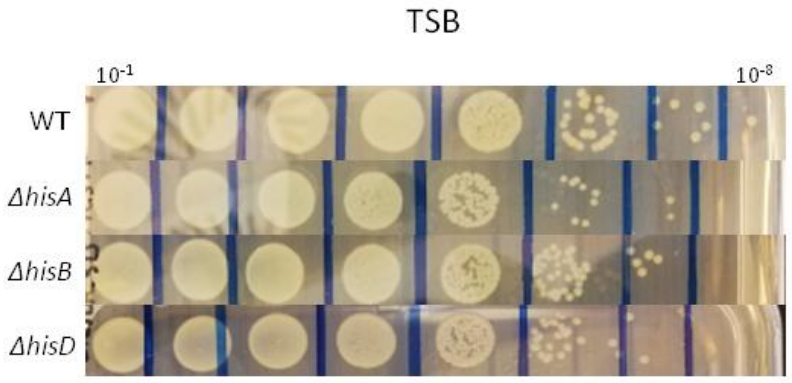

Figure S3. **Growth of *B. abortus* 544 in TSB medium.** Overnight liquid cultures of *B. abortus* 544, Δ*hisA*, Δ*hisB* and Δ*hisD* were normalized at OD 0.1 and serially diluted and spotted on TSB agar plate. The pictures were taken after 4-5 days at 37°C.

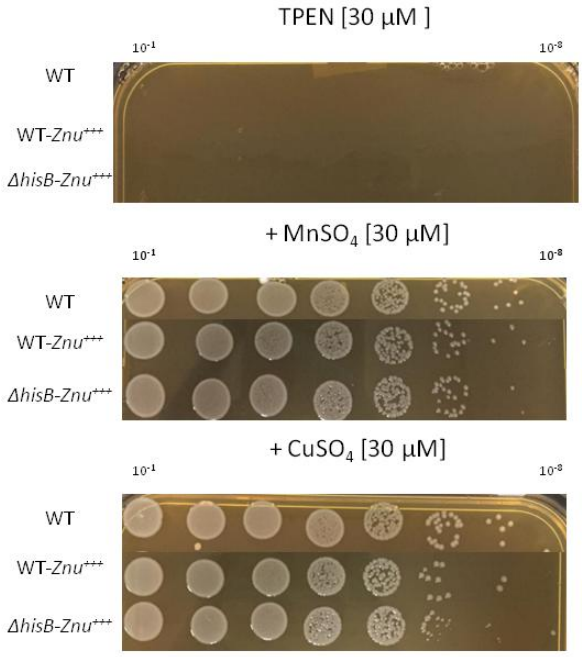

Figure S4. **TPEN at a final concentration of 30 µM inhibits WT-*Znu*$^{+++}$, Δ*hisB-Znu*$^{+++}$ and WT growth and metals repletion restores bacterial growth.** Overnight liquid cultures were normalized at OD 0.1 and serially diluted and spotted on TSB agar plate containing 30 µM TPEN (top). Different metals at 30 µM were added; $MnSO_4$ (middle) and $CuSO_4$ (bottom). The pictures were taken after 4-5 days at 37°C.

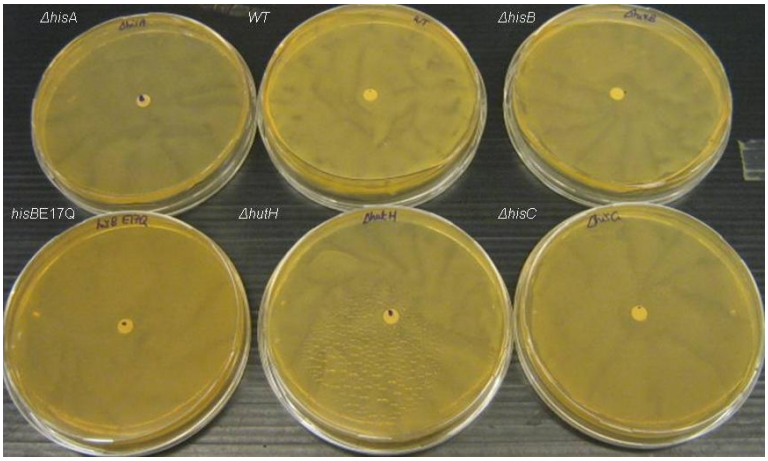

Figure S5. **Cu sensitivity of WT, *ΔhisA, ΔhisB, hisE17Q* and *ΔhisC, ΔhutH* strains**. 100 µl of an overnight culture of each *B. abortus* strain was spread out on TSB plates where a disc was placed in the middle on which 10 µl of 37.3 mM $CuCl_2$ solution were deposited. On top: *ΔhisA*, WT and *ΔhisB*. Bottom: *his*BE17Q, *ΔhutH* and *ΔhisD*. The pictures were taken after 4-5 days at 37°C. No inhibition zones could be observed.

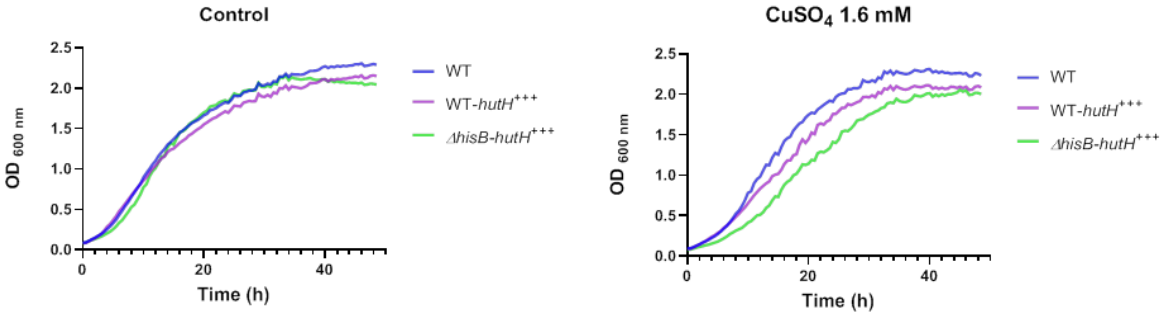

Figure S6. **Effect of *hutH* overexpression on the growth curves of *B. abortus* 544 in the presence of Cu.** WT, WT-*hutH*$^{+++}$ and *ΔhisB-hutH* $^{+++}$ strains were grown in TSB medium (left) and TSB medium containing 1.6 mM of $CuSO_4$ (right). Overnight cultures of strains grown in TSB were diluted to optical density (OD) of 0.1. During growth, OD at 600 nm was measured every 30 minutes for 48 hours. Data are not representative of results of biological triplicates.

REFERENCES

1. Alifano, P., Fani, R., Liò, P., Lazcano, A., Bazzicalupo, M., Carlomagno, M. S. & Bruni, C. B. Histidine Biosynthetic Pathway and Genes : Structure , Regulation , and Evolution. *Microbiol. Rev.* **60**, 44–69 (1996).

2. Itoh, Y., Nishijyo, T. & Nakada, Y. Histidine catabolism and catabolite regulation. in *Pseudomonas* 371–395 (2007).

3. Brenner, M. & Ames, B. N. The Histidine Operon and Its Regulation. in *Metabolic Regulation: Metabolic Pathways* 349–387 (ACADEMIC PRESS, INC., 1971). doi:10.1016/B978-0-12-299255-1.50018-3.

4. Carlomagno, M. S., Chiariotti, L., Alifano, P., Nappo, A. G. & Bruni, C. B. Structure and Function of the *Salmonella* Typhimurium and Escherichia coli K-12 Histidine Operons. *J. Mol. Biol.* 585–606 (1988).

5. Frandsen, N. & D'Ari, R. Excess histidine enzymes cause AICAR-independent filamentation in *Escherichia coli*. *Mol. Gen. Genet.* 348–354 (1993).

6. Moyed, H. S. & Magasanik, B. The Biosynthesis of the Imidazole Ring of Histidine. *J. Biol. Chem.* **235**, 149–154 (1960).

7. Umbarger, H. E. Amino acid biosynthesis and its regulation. *Annu. Rev. Biochem.* **47**, 533–606 (1978).

8. Bender, R. A. Regulation of the Histidine Utilization (Hut) System in Bacteria. *Microbiol. Mol. Biol. Rev.* **76**, 565–584 (2012).

9. Tabor, H., Mehler, A. H., Hayaishi, O. & White, J. Urocanic acid as an intermediate in the enzymatic conversion of histidine to glutamic and acids. *J. Biol. Chem.* **196**, 121–128 (1952).

10. Taylor, R. G., Lambert, M. A., Sexsmith, E., Sadler, S. J., Ray, P. N., Mahuran, D. J. & McInness, R. R. Cloning and Expression of Rat Histidase. *J. Biol. Chem.* **265**, 18192–18199 (1990).

11. Chasin, L. A. & Magasanik, B. Induction and Repression of the Histidine-degrading Enzymes of *Bacillus subtilis*. *J. Biol. Chem.* **243**, 5165–5178 (1968).

12. Lessie, T. G. & Neidhardt, F. C. Formationi anid Operation of the Histidine-degrading Pathwvay in *Pseutdomonas aeruginosa. J. Bacteriol.* **3**, 1800–1810 (1967).

13. Schlesinger, S., Scotto, P. & Magasanik, B. Exogenous and Endogenous Induction of the Enzymes in *Aerobacter aerogenes*. *J. Biol. Chem.* **240**, 4331–4337 (1965).

14. Smith, G. R. & Magasanik, B. The Two Operons of the Histidine in *Salmonella* Typhimurium. *J. Biol. Chem.* **6**, 3330–3341 (1971).

15. Ames, G. F. Uptake of Amino Acids by *Salmonella* Typhimurium. *Arch. Biochem. Biophys.* **8**, 1–18 (1964).

16. Zhang, X., George, A., Bailey, M. J. & Rainey, P. B. The histidine utilization (hut) genes of *Pseudomonas fluorescens* SBW25 are active on plant surfaces , but are not required for competitive colonization of sugar beet seedlings. *Microbiology* **152**, 1867–1875 (2006).

17. Hood, M. I. & Skaar, E. P. Nutritional immunity : transition metals at the pathogen-host interface. *Nat. Rev. Microbiol.* **10**, 525–537 (2012).

18. Sundberg, R. J. & Martin, R. B. Interactions of Histidine and Other Imidazole Derivatives with Transition Metal Ions in Chemical and Biological Systems. *Chem. Rev.* **74**, 471–517 (1974).

19. Perrin, D. D. & Sharna, V. S. Histidine Complexes with some Bivalent Cations. *J. Chem. Soc.* 724–728 (1967).

20. Hemdan, E. S., Zhao, Y.-J., Sulkowski, E. & Porath, J. Surface topography of histidine residues : A facile probe by immobilized metal ion affinity chromatography. *PNAS* **86**, 1811–1815 (1989).

21. Dietl, A., Amich, J., Leal, S., Beckmann, N., Binder, U., Beilhack, A. & Pearlman, E. Histidine biosynthesis plays a crucial role in metal homeostasis and virulence of *Aspergillus fumigatus*. *Virulence* **7**, 465–476 (2016).

22. Solioz, M. *Copper and Bacteria. Evolution, Homeostasis and Toxicity*. (2018).

23. Kim, B.-E., Nevitt, T. & Thiele, D. J. Mechanisms for copper acquisition , distribution and regulation. *Nat. Chem. Biol.* **4**, 176–185 (2008).

24. Rensing, C. & Grass, G. *Escherichia coli* mechanisms of copper homeostasis in a changing environment. *FEMS Microbiol. Lett.* **27**, 197–203 (2003).

25. Ridge, P. G., Zhang, Y. & Gladyshev, V. N. Comparative Genomic Analyses of Copper Transporters and Cuproproteomes Reveal Evolutionary Dynamics of Copper Utilization and Its Link to Oxygen. *PLoS One* 1–9 (2008) doi:10.1371/journal.pone.0001378.

26. Giachino, A. & Waldron, K. J. Copper tolerance in bacteria requires the activation of multiple accessory pathways. *Mol. Gen. Genet.* 1–14 (2020) doi:10.1111/mmi.14522.

27. Lemire, J. A., Harrison, J. J. & Turner, R. J. Antimicrobial activity of metals: mechanisms, molecular targets and applications. *Nat. Rev. Microbiol.* **11**, 371–384 (2013).

28. Macomber, L. & Imlay, J. A. The iron-sulfur clusters of dehydratases are primary intracellular targets of copper toxicity. *PNAS* **106**, 8344–8349 (2009).

29. Macomber, L., Rensing, C. & Imlay, J. A. Intracellular Copper Does Not Catalyze the Formation of Oxidative DNA Damage in Escherichia coli. *J. ba* **189**, 1616–1626 (2007).

30. Andreini, C., Banci, L., Bertini, I. & Rosato, A. Occurrence of Copper Proteins through the Three Domains of Life : A Bioinformatic Approach. *J. Proteome Res.* **7**, 209–216 (2008).

31. Merchant, S. S. & Helmann, J. D. Elemental Economy : Microbial Strategies for Optimizing Growth in the Face of Nutrient Limitation. *Advances in Microbial Physiology* vol. 60 (Elsevier Ltd., 2012).

32. Chandrangsu, P., Rensing, C. & Helmann, J. D. Metal homeostasis and resistance in bacteria. *Nat. Rev. Microbiol.* **15**, 338–350 (2017).

33. Outten, F. W., Huffman, D. L., Hale, J. A. & O'Halloran, T. V. The Independent cue and cus Systems Confer Copper Tolerance during Aerobic and Anaerobic Growth in *Escherichia coli*. *J. pf Biol. Chem.* **276**, 30670–30677 (2001).

34. Outten, F. W., Outten, C. E., Hale, J. & O'Halloran, T. V. Transcriptional Activation of an *Escherichia coli* Copper Efflux Regulon by the Chromosomal MerR Homologue , CueR. *J. Biol. Chem.* **275**, 31024–31029 (2000).

35. Osman, D., Waldron, K. J., Denton, H., Taylor, C. M., Grant, A. J., Mastroeni, P., Robinson, N. J. & Cavet, J. S. Copper Homeostasis in Salmonella Is Atypical and Copper-CueP Is a Major Periplasmic Metal Complex. *J. Biol. Chem.* **285**, 25259–25268 (2010).

36. Achard, M. E. S., Tree, J. J., Holden, J. A., Simpfendorfer, K. R., Wijburg, O. L. C., Strugnell, R. A., Schembri, M. A., Sweet, M. J., Jennings, M. P. & McEwan, A. G. The multi-copper-ion oxidase cueO of *Salmonella enterica* Serovar Typhimurium is required for systemic virulence. *Infect. Immun.* **78**, 2312–2319 (2010).

37. Neyrolles, O., Wolschendorf, F., Mitra, A. & Niederweis, M. Mycobacteria , metals , and the macrophage. *Immunol. Rev.* **264**, 249–263 (2015).

38. Kehl-Fie, T. E. & Skaar, E. P. Nutritional immunity beyond iron: a role for manganese and zinc. *Curr. Opin. Chem. Biol.* **14**, 218–224 (2010).

39. Botella, H., Stadthagen, G., Lugo-villarino, G., De Chastellier, C. & Neyrolles, O. Metallobiology of host – pathogen interactions : an intoxicating new insight. *Trends Microbiol.* **20**, 106–112 (2012).

40. Andreini, C., Banci, L., Bertini, I. & Rosato, A. Zinc through the Three Domains of Life. *J. Proteome Res.* **5**, 3173–3178 (2006).

41. Djoko, K. Y., Ong, C. Y., Walker, M. J. & Mcewan, A. G. The Role of Copper and Zinc Toxicity in Innate Immune Defense against Bacterial Pathogens. *J. Biol. Chem.* **290**, 18954–18961 (2015).

42. Wagner, D., Maser, J., Lai, B., Cai, Z., Barry III, C. E., zu Bentrup, K. H., Russell, D. G. & Bermudez, L. E. Elemental Analysis of *Mycobacterium avium*-, *Mycobacterium tuberculosis*-, and *Mycobacterium smegmatis*-Containing Phagosomes Indicates Pathogen-Induced Microenvironments within the Host Cell's Endosomal System. *J. Immunol.* **174**, 1491–1500 (2005).

43. Botella, H. *et al.* Mycobacterial P 1 -Type ATPases Mediate Resistance to Zinc Poisoning in Human Macrophages. *Cell Host Microbe* **10**, 248–259 (2011).

44. White, C., Lee, J., Kambe, T., Fritsche, K. & Petris, M. J. A Role for the ATP7A Copper-transporting ATPase in Macrophage Bactericidal Activity. *J. Biol. Chem.* **284**, 33949–33956 (2009).

45. Von Bargen, K., Gorvel, J. & Salcedo, S. P. Internal affairs : investigating the *Brucella* intracellular lifestyle. *FEMS Microbiol. Rev.* **36**, 533_562 (2012).

46. Corbel, M. Brucellosis : an Overview. *Emerg. Infect. Dis.* **3**, 213–221 (1997).

47. Evans, A. C. Further Studies on Bacterium Abortus and Related Bacteria : II . A Comparison of Bacterium Abortus with Bacterium Bronchisepticus and with the Organism Which Causes Malta. *J. Infect. Dis.* **22**, 580–593 (1918).

48. Moreno, E. & Moriyó, I. The Genus *Brucella*. in *Prokaryotes* 315–456 (2006).

49. Moreno, E., Stackebrandt, E., Dorsch, M., Wolters, J., Busch, M. & Mayer, H. *Brucella abortus* 16S rRNA and Lipid A Reveal a Phylogenetic Relationship with Members of the Alpha-2 Subdivision of the Class Proteobacteria. *J. Bacteriol.* **172**, 3569–3576 (1990).

50. López-goñi, I. & Moriyón, I. *Brucella : Molecular and Cellular Biology*. (2004).

51. Michaux-Charachon, S., Bourg, G., Jumas-Bilak, E., Guigue-Talet, P., Allardet-Servent, A., O'Callaghan, D. & Ramuz, M. Genome Structure and Phylogeny in the Genus *Brucella*. *J. Bacteriol.* **179**, 3244–3249 (1997).

52. Van Der Henst, C., Barsy, M. De, Zorreguieta, A., Letesson, J. & De Bolle, X. The *Brucella* pathogens are polarized bacteria. *Microbes Infect.* **15**, 998–1004 (2013).

53. Roop II, R. M. & Caswell, C. C. *Metals and the Biology and Virulence of Brucella*. (Springer International Publishing, 2017).

54. Verger, J., Grimont, F., Grimont, P. A. D. & Grayon, M. *Brucella* , a Monospecific Genus as Shown by Deoxyribonucleic Acid Hybridization. *Int. J. Syst. Bacteriol.* 292–295 (1985).

55. Young, E. J. & Corbel, M. J. *Brucellosis : Clinical and Laboratory Aspects*. (CRC Press, 1989).

56. Moreno, E. & Moriyo, I. *Brucella melitensis* : A nasty bug with hidden credentials for virulence. *PNAS* **99**, 1–3 (2002).

57. Archambaud, C., Salcedo, S. P., Lelouard, H., Devilard, E., de Bovis, B., Van Rooijen, N., Gorvel, J. & Malissen, B. Contrasting roles of macrophages and dendritic cells in controlling initial pulmonary *Brucella* infection. *Eur. J. Biochem.* **40**, 3458–3471 (2010).

58. Roop II, R. M., Gaines, J. M., Anderson, E. S., Caswell, C. C. & Martin, D. W. Survival of the fittest : how *Brucella* strains adapt to their intracellular niche in the host. *Med. Microbiol. Immunol.* **1998**, 221–238 (2009).

59. Samartino, L. E. & Enright, F. PATHOGENESIS OF ABORTION OF BOVINE BRUCELLOSIS. *Comp. Immunol. Microbiol. Infect. Dis.* **16**, 95–101 (1993).

60. Porte, F., Naroeni, A., Ouahrani-bettache, S. & Liautard, J. Role of the *Brucella suis* Lipopolysaccharide O Antigen in Phagosomal Genesis and in Inhibition of Phagosome-Lysosome Fusion in Murine Macrophages. *Infect. Immun.* **71**, 1481–1490 (2003).

61. Kim, S., Watarai, M., Suzuki, H., Makino, S., Kodama, T. & Shirahata, T. Lipid raft microdomains mediate class A scavenger receptor-dependent infection of *Brucella abortus*. *Microb. Pathog.* **37**, 11–19 (2004).

62. Celli, J. The changing nature of the *Brucella* -containing vacuole. *Cell. Microbiol.* **17**, 951–958 (2015).

63. Starr, T., Ng, T. W., Wehrly, T. D., Knodler, L. A. & Celli, J. *Brucella* Intracellular Replication Requires Trafficking Through the Late Endosomal / Lysosomal Compartment. *Traffic* **9**, 678–694 (2008).

64. Arenas, G. N., Staskevich, A. S., Aballay, A. & Mayorga, L. S. Intracellular Trafficking of *Brucella abortus* in J774 Macrophages. *Infect. Immun.* **68**, 4255–4263 (2000).

65. Celli, J., Chastellier, C. De, Franchini, D., Pizarro-cerda, J., Moreno, E. & Gorvel, J. *Brucella* Evades Macrophage Killing via VirB-dependent Sustained Interactions with the Endoplasmic Reticulum. *J. Eperimental Med.* **198**, 545–556 (2003).

66. Sternon, J.-F., Godessart, P., Gonçalves de Freitas, R., Van der Henst, M., Poncin, K., Francis, N., Willemart, K., Christen, B., Letesson, J.-J. & De Bo. Transposon Sequencing of *Brucella abortus* Uncovers Essential Genes for Growth In Vitro and Inside Macrophages. *Infect. Immun.* **86**, 1–20 (2018).

67. Wu, T., Wang, S., Wang, Z., Peng, X., Lu, Y. & Wu, Q. A multicopper oxidase contributes to the copper tolerance of *Brucella melitensis* 16M. *FEMS Microbiol. Lett.* **362**, 1–7 (2015).

68. Bucheder, F. & Broda, E. Energy-Dependent Zinc Transport by *Escherichia coli*. *Eur. J. Biochem.* **45**, 556–559 (1974).

69. Hantke, K. Bacterial zinc transporters and regulators. *BioMetals* 239–249 (2001).

70. Patzer, S. I. & Hantke, K. The Zinc-responsive Regulator Zur and Its Control of the znu Gene Cluster Encoding the ZnuABC Zinc Uptake System in *Escherichia coli* response to the intracellular zinc concentration by the. *J. Biol. Chem.* **275**, 24321–24332 (2000).

71. Patzer, S. I. & Hantke, K. The ZnuABC high-affinity zinc uptake system and its regulator Zur in *Escherichia coli*. *Mol. Microbiol.* **28**, 1199–1210 (1998).

72. Roop II, R. M. Metal acquisition and virulence in *Brucella*. *Anim. Heal. Res. Rev.* **13**, 1–19 (2013).

73. Gaballa, A. & Helmann, J. D. Identification of a Zinc-Specific Metalloregulatory Protein , Zur , Controlling Zinc Transport Operons in Bacillus subtilis. *J. Bacteriol.* **180**, 5815–5821 (1998).

74. Kim, S., Watanabe, K., Shirahata, T. & Watarai, M. Zinc uptake system (znuA locus) of *Brucella abortus* is essential for intracellular survival and virulence in mice. *J. Vet. Med. Sci.* **66**, 4–8 (2004).

75. Sheehan, L. M., Budnick, J. A., Roop II, M. R. & Caswell, C. Coordinated zinc homeostasis is essential for the wild-type virulence of *Brucella abortus*. *J. Bacteriol.*

197, 1582–1591 (2015).

76. Rhee, K. Y., Sorio De Carvalho, L. P., Bryk, R., Ehrt, S., Marrero, J., Park, S. W., Schnappinger, D., Venugopal, A. & Nathan, C. Central carbon metabolism in *Mycobacterium tuberculosis* : an unexpected frontier. *Trends Microbiol.* **19**, 307–314 (2011).

77. Murphy, J. T., Bruinsma, J. J., Schneider, D. L., Collier, S., Guthrie, J., Robertson, J. D., Mardis, E. R. & Kornfeld, K. Histidine Protects Against Zinc and Nickel Toxicity in *Caenorhabditis elegans*. *PLoS Genet.* **7**, 1–12 (2011).

78. Fung, D. K. chun, Lau, W. Y., Chan, W. T. & Yan, A. Copper Efflux Is Induced during Anaerobic Amino Acid Limitation in *Escherichia coli* To Protect Iron-Sulfur Cluster Enzymes and. *J. Bacteriol.* **195**, 4556–4568 (2013).

79. Lebrette, H., Borezée-Durant, E., Martin, L., Richaud, P., Boeri Erba, E. & Cavazza, C. Novel insights into nickel import in *Staphylococcus aureus*: The positive role of free histidine and structural characterization of a new thiazolidine-type nickel chelator. *Metallomics* **7**, 613–621 (2015).

80. Lebrette, H., Brochier-Armanet, C., Zambelli, B., De Reuse, H., Borezée-Durant, E., Ciurli, S. & Cavazza, C. Promiscuous nickel import in human pathogens: Structure, thermodynamics, and evolution of extracytoplasmic nickel-binding proteins. *Structure* **22**, 1421–1432 (2014).

81. Li, Y. & Zamble, D. B. Nickel Homeostasis and Nickel Regulation : An Overview. *Chem. Rev.* **109**, 4617–4643 (2009).

82. Chivers, P. T., Benanti, E. L., Heil-chapdelaine, V., Iwig, J. S. & Rowe, J. L. Metallomics Identification of Ni- (L -His) 2 as a substrate for NikABCDE-dependent nickel uptake in *Escherichia coli*. *Metallomics* **4**, 1043–1050 (2012).

83. Lebrette, H., Iannello, M., Fontecilla-camps, J. C. & Cavazza, C. The binding mode of Ni- (L -His) 2 in NikA revealed by X-ray crystallography. *J. Inorg. Biochem.* **121**, 16–18 (2013).

84. Shaik, M. M., Cendron, L., Salamina, M., Ruzzene, M. & Zanotti, G. *Helicobacter pylori* periplasmic receptor CeuE (HP1561) modulates its nickel affinity via organic metallophores. *Mol. Microbiol.* **91**, 724–735 (2014).

85. Milagres, A. M. F., Machuca, A. & Napoleão, D. Methods Detection of siderophore production from several fungi and bacteria by a modification of chrome azurol S (CAS) agar plate assay. *J. Microbiol. Methods* **37**, 1–6 (1999).

86. Yang, X., Becker, T., Walters, N. & Pascual, D. W. Deletion of znuA virulence factor attenuates *Brucella abortus* and confers protection against wild-type challenge. *Infect. Immun.* **74**, 3874–3879 (2006).

87. Hood, M. I., Mortensen, B. L., Moore, J. L., Zhang, Y., Kehl-Fie, T. E., Sugitani, N., Chazin, W. J., Caprioli, R. M. & Skaar, E. P. Identification of an *Acinetobacter baumannii* Zinc Acquisition System that Facilitates Resistance to Calprotectin-mediated Zinc Sequestration. *PLoS Pathog.* **8**, 20–24 (2012).

88. Garnacho-Montero, J., Ortiz-Leyba, C., Jiménez-Jiménez, F. J., Barrero-Almodóvar, A.

E., García-Garmendia, J. L., Bernabeu-Wittell, M., Gallego-Lara, S. L. & Madrazo-Osuna, J. Treatment of multidrug-resistant *Acinetobacter baumannii* ventilator-associated pneumonia (VAP) with intravenous colistin: A comparison with imipenem-susceptible VAP. *Clin. Infect. Dis.* **36**, 1111–1118 (2003).

89. Mortensen, B. L., Rathi, S., Chazin, W. J. & Skaar, P. *Acinetobacter baumannii* Response to Host-Mediated Zinc Limitation Requires the Transcriptional Regulator Zur. *J. Bacteriol.* **196**, 2616–2626 (2014).

90. Nairn, B. L., Lonergan, Z. R., Wang, J., Braymer, J. J., Zhang, Y., Calcutt, M. W., Lisher, J. P., Gilston, B. A., Chazin, W. J., De Crécy-Lagard, V., Giedroc, D. P. & Skaar, E. P. The Response of *Acinetobacter baumannii* to Zinc Starvation. *Cell Host Microbe* **19**, 826–836 (2016).

91. Kim, S., Watanabe, K., Shirahata, T. & Watarai, M. Zinc uptake system (znuA locus) of *Brucella abortus* is essential for intracellular survival and virulence in mice. *J. Vet. Med. Sci.* **66**, 1059–1063 (2004).

92. Samanovic, M. I., Ding, C., Thiele, D. J. & Darwin, K. H. Copper in Microbial Pathogenesis : Meddling with the Metal. *Cell Host Microbe Rev.* **11**, 106–115 (2012).

93. Vos, K., Braeken, K., Fauvart, M., Ndayizeye, M., Verhaert, J., Zachurzok, S., Lambrichts, I. & Michiels, J. The *Rhizobium etli* opt operon is required for symbiosis and stress resistance. *Environ. Microbiol.* **9**, 1665–1674 (2007).

94. Schmitt, L. & Tampé, R. Structure and mechanism of ABC transporters. *Curr. Opin. Struct. Biol.* **14**, 426–431 (2004).

95. Lubkowitz, M. The OPT Family Functions in Lon-Distance Peptide tand Metal Transport in Plants. *Genet. Eng. (N. Y).* **27**, 35–55 (2006).

96. Hiron, A., Borezée-Durant, E., Piard, J. C. & Juillard, V. Only one of four oligopeptide transport systems mediates nitrogen nutrition in *Staphylococcus aureus*. *J. Bacteriol.* **189**, 5119–5129 (2007).

97. Andrews, J. C. & Short, S. A. opp-lac Operon fusions and transcriptional regulation of the *Escherichia coli* trp-linked oligopeptide permease. *J. Bacteriol.* **165**, 434–442 (1986).

98. Lubkowitz, M. The oligopeptide transporters: A small gene family with a diverse group of substrates and functions? *Mol. Plant* **4**, 407–415 (2011).

99. Lazazzera, B. A. The intracellular function of extracellular signaling peptides. *Peptides* **22**, 1519–1527 (2001).

100. Park, J. T., Raychaudhuri, D., Li, H., Normark, S. & Mengin-Lecreulx, D. MppA, a periplasmic binding protein essential for import of the bacterial cell wall peptide L-alanyl-γ-D-glutamyl-meso-diaminopimelate. *J. Bacteriol.* **180**, 1215–1223 (1998).

101. Singh, R., Liechti, G., Slade, J. A. & Maurelli, A. T. *Chlamydia trachomatis* oligopeptide transporter performs dual functions of oligopeptide transport and peptidoglycan recycling. *Infect. Immun.* **88**, (2020).